



Calhoun: The NPS Institutional Archive
DSpace Repository

Theses and Dissertations

1. Thesis and Dissertation Collection, all items

2008

Performance analysis of decode-and-forward
with cooperative diversity and Alamouti
cooperative space-time coding in clustered
multihop wireless networks

Alexopoulos, Konstantinos

Monterey California. Naval Postgraduate School

Downloaded from NPS Archive: Calhoun



Calhoun is the Naval Postgraduate School's public access digital repository for research materials and institutional publications created by the NPS community. Calhoun is named for Professor of Mathematics Guy K. Calhoun, NPS's first appointed -- and published -- scholarly author.

Dudley Knox Library / Naval Postgraduate School
411 Dyer Road / 1 University Circle
Monterey, California USA 93943

<http://www.nps.edu/library>



NAVAL POSTGRADUATE SCHOOL

MONTEREY, CALIFORNIA

THESIS

**PERFORMANCE ANALYSIS OF DECODE-AND-FORWARD WITH
COOPERATIVE DIVERSITY AND ALAMOUTI COOPERATIVE
SPACE-TIME CODING IN CLUSTERED MULTIHOP WIRELESS
NETWORKS**

by

Konstantinos Alexopoulos

September 2008

Thesis Advisor:

Thesis Co-Advisor:

Murali Tummala

John C. McEachen

Approved for public release; distribution is unlimited

THIS PAGE INTENTIONALLY LEFT BLANK

REPORT DOCUMENTATION PAGE			<i>Form Approved OMB No. 0704-0188</i>	
Public reporting burden for this collection of information is estimated to average 1 hour per response, including the time for reviewing instruction, searching existing data sources, gathering and maintaining the data needed, and completing and reviewing the collection of information. Send comments regarding this burden estimate or any other aspect of this collection of information, including suggestions for reducing this burden, to Washington headquarters Services, Directorate for Information Operations and Reports, 1215 Jefferson Davis Highway, Suite 1204, Arlington, VA 22202-4302, and to the Office of Management and Budget, Paperwork Reduction Project (0704-0188) Washington DC 20503.				
1. AGENCY USE ONLY (Leave blank)		2. REPORT DATE September 2008	3. REPORT TYPE AND DATES COVERED Master's Thesis	
4. TITLE AND SUBTITLE Performance Analysis of Decode-and-Forward with Cooperative Diversity and Alamouti Cooperative Space-Time Coding in Clustered Multihop Wireless Networks			5. FUNDING NUMBERS	
6. AUTHOR Konstantinos Alexopoulos				
7. PERFORMING ORGANIZATION NAME(S) AND ADDRESS(ES) Naval Postgraduate School Monterey, CA 93943-5000			8. PERFORMING ORGANIZATION REPORT NUMBER	
9. SPONSORING /MONITORING AGENCY NAME(S) AND ADDRESS(ES) N/A			10. SPONSORING/MONITORING AGENCY REPORT NUMBER	
11. SUPPLEMENTARY NOTES The views expressed in this thesis are those of the author and do not reflect the official policy or position of the Department of Defense or the U.S. Government.				
12a. DISTRIBUTION / AVAILABILITY STATEMENT Approved for public release; distribution is unlimited			12b. DISTRIBUTION CODE A	
13. ABSTRACT <p>Space-time coding and spatial diversity schemes enhance the performance of energy constrained multihop clustered relay networks. The purpose of this thesis is to evaluate the performance of techniques such as the decode-and-forward with cooperative diversity and the Alamouti space-time coding, which were primarily used in relay multiple-input multiple-output communications, in distributed clustered two-hop and multihop relaying networks consisting of single-antenna terminals.</p> <p>Simulation results, in single carrier Rayleigh and Stanford University Interim channels for phase shift keyed and quadrature amplitude modulation, show that the use of the decode-and-forward with cooperative diversity and the Alamouti cooperative space-time coding schemes improve the error probability performance in a power constrained, clustered multihop relaying network operating in a multipath fading environment.</p>				
14. SUBJECT TERMS Cooperative Diversity, Spatial Diversity, Alamouti Cooperative Space-time Coding, Decode-and-forward, Cooperative Multiplexing, Amplify-and-forward, Clustered Relay Network, Single-antenna Terminal			15. NUMBER OF PAGES 121	
			16. PRICE CODE	
17. SECURITY CLASSIFICATION OF REPORT Unclassified	18. SECURITY CLASSIFICATION OF THIS PAGE Unclassified	19. SECURITY CLASSIFICATION OF ABSTRACT Unclassified	20. LIMITATION OF ABSTRACT UU	

NSN 7540-01-280-5500

Standard Form 298 (Rev. 2-89)
Prescribed by ANSI Std. Z39-18

THIS PAGE INTENTIONALLY LEFT BLANK

Approved for public release; distribution is unlimited

**PERFORMANCE ANALYSIS OF DECODE-AND-FORWARD WITH
COOPERATIVE DIVERSITY AND ALAMOUTI COOPERATIVE SPACE-TIME
CODING IN CLUSTERED MULTIHOP WIRELESS NETWORKS**

Konstantinos Alexopoulos
Lieutenant Junior Grade, Hellenic Navy
B.S., Hellenic Naval Academy, Piraeus, 2001

Submitted in partial fulfillment of the
requirements for the degree of

MASTER OF SCIENCE IN ELECTRICAL ENGINEERING

from the

**NAVAL POSTGRADUATE SCHOOL
September 2008**

Author: Konstantinos Alexopoulos

Approved by: Murali Tummala
Thesis Advisor

John C. McEachen
Co-Advisor

Jeffrey B. Knorr
Chairman, Department of Electrical and Computer Engineering

THIS PAGE INTENTIONALLY LEFT BLANK

ABSTRACT

Space-time coding and spatial diversity schemes enhance the performance of energy constrained multihop clustered relay networks. The purpose of this thesis is to evaluate the performance of techniques such as the decode-and-forward with cooperative diversity and the Alamouti space-time coding, which were primarily used in relay multiple-input multiple-output communications, in distributed clustered two-hop and multihop relaying networks consisting of single-antenna terminals.

Simulation results, for phase shift keyed and quadrature amplitude modulation signals in single carrier Rayleigh and Stanford University Interim channels, show that the use of the decode-and-forward with cooperative diversity and the Alamouti cooperative space-time coding schemes improve the error probability performance in a power constrained, clustered multihop relaying network operating in a multipath fading environment.

THIS PAGE INTENTIONALLY LEFT BLANK

TABLE OF CONTENTS

I.	INTRODUCTION.....	1
A.	THESIS OBJECTIVE	2
B.	RELATED WORK IN COOPERATIVE SPACE-TIME CODING, COOPERATIVE DIVERSITY AND SPATIAL MULTIPLEXING.....	2
C.	THESIS OUTLINE.....	3
II.	DISTRIBUTED IMPLEMENTATION OF MIMO TECHNIQUES	5
A.	MIMO COMMUNICATIONS	5
B.	SPATIAL DIVERSITY, SPATIAL MULTIPLEXING AND SPACE- TIME CODING	6
1.	Spatial Diversity	6
2.	Spatial Multiplexing	7
3.	Space-time Coding	8
a.	<i>2×1 Alamouti Space-time Coding Scheme.....</i>	9
b.	<i>2×2 Alamouti Space-time Coding Scheme.....</i>	12
C.	COOPERATIVE COMMUNICATIONS.....	14
1.	Distributed Networks.....	15
a.	<i>Ad hoc Networks</i>	15
b.	<i>Sensor Networks.....</i>	16
2.	Cooperative Networks	16
a.	<i>Clusters and Virtual Antenna Arrays.....</i>	16
b.	<i>Cooperative Diversity</i>	18
c.	<i>Three Terminals Relay Network.....</i>	18
d.	<i>Traditional Relaying Protocols.....</i>	19
e.	<i>Cooperative Spatial Multiplexing.....</i>	20
f.	<i>Cooperative Space-Time Coding</i>	21
D.	SUMMARY	21
III.	PERFORMANCE ANALYSIS OF COOPERATIVE TECHNIQUES IN MULTI-RELAY CHANNELS	23
A.	COOPERATIVE COMMUNICATION MODEL.....	23
B.	ANALYSIS OF THE RELAYING TECHNIQUES	26
1.	Non-cooperative Multi-hop Scheme.....	26
a.	<i>Decode-and-Forward</i>	27
b.	<i>Bit Error Probability for Decode-and-forward.....</i>	28
c.	<i>Amplify-and-Forward</i>	29
d.	<i>Bit Error Probability for Amplify-and-forward</i>	30
2.	Decode-and-Forward with Cooperative Diversity Scheme.....	31
a.	<i>Decode-and-Forward with Cooperative Diversity Scheme in Flat Fading Channel.....</i>	31
b.	<i>Bit Error Probability for Decode-and-forward with Cooperative Diversity</i>	34

c.	<i>Performance Evaluation of Decode-and-Forward with Cooperative Diversity in Rayleigh Fading Channel.....</i>	<i>36</i>
d.	<i>Decode-and-Forward with Cooperative Diversity in Frequency Selective Channel with ISI.....</i>	<i>38</i>
3.	Alamouti Cooperative Space-time Coding	40
a.	<i>Alamouti Cooperative Space-time Coding Scheme in Flat Fading Channel</i>	<i>41</i>
b.	<i>Bit Error Probability of Alamouti Cooperative Space-time Coding Scheme.....</i>	<i>44</i>
c.	<i>Alamouti Cooperative Space-time Coding Scheme in Frequency Selective Channel.....</i>	<i>46</i>
d.	<i>Performance Evaluation of Cooperative Alamouti Space-time Coding in Rayleigh Fading Channel</i>	<i>49</i>
C.	SUMMARY	50
IV.	SIMULATION RESULTS	51
A.	SIMULATION MODEL	51
B.	SIMULATION RESULTS FOR BPSK AND QPSK.....	53
1.	BPSK in Rayleigh Channel	53
2.	BPSK in SUI Channels	57
3.	QPSK in Rayleigh Channel.....	60
4.	QPSK in SUI Channels.....	61
5.	Multiple Hops in SUI1 Channel for BPSK and QPSK.....	64
C.	SIMULATION RESULTS FOR QAM.....	67
1.	16-QAM	67
2.	64-QAM	69
D.	SUMMARY	71
V.	CONCLUSIONS AND FUTURE WORK.....	73
A.	SUMMARY OF WORK.....	73
B.	SIGNIFICANT RESULTS.....	73
C.	SUGGESTIONS FOR FUTURE WORK.....	75
APPENDIX A.	STANFORD UNIVERSITY INTERIM MODELS	77
APPENDIX B.	MATLAB SOURCE CODE.....	79
LIST OF REFERENCES		95
INITIAL DISTRIBUTION LIST		99

LIST OF FIGURES

Figure 1.	Typical MIMO System with M Transmitting and N Receiving Antennas, which provides an $M \times N$ Spatial Diversity Order.	6
Figure 2.	Spatial Diversity Scheme with Quadruple Diversity Gain, since there are Four Independent Transmission Channels $h_{i,j}$).	7
Figure 3.	Spatial Diversity Scheme with Double Multiplexing Gain, since every two Consecutive Symbols are transmitted by Different Antennas.	8
Figure 4.	Alamouti 2×1 Scheme for Frequency Flat Slow Fading Channel.	9
Figure 5.	Alamouti 2×1 Scheme for a Frequency Selective Slow Fading Channel.	11
Figure 6.	Alamouti 2×2 Scheme for a Frequency Flat Slow Fading Channel.	12
Figure 7.	Alamouti 2×2 Scheme for a Frequency Selective Slow Fading Channel.	13
Figure 8.	Three Terminals Network with a Source (S), a Relay (R) and a Destination (D) Node.	15
Figure 9.	Distributed-MIMO Multi-terminal Relaying Network [After Ref. [32]].	17
Figure 10.	Decode-and-Forward Relaying Protocols in a Three-terminal Wireless Network.	19
Figure 11.	Amplify-and-Forward Relaying Protocols in a Three-terminal Wireless Network.	20
Figure 12.	The Coverage Areas of Mobile Terminals. Areas are indicated by the Dashed Circles.	24
Figure 13.	Multi-hop Relaying Topologies of Cooperative and Non-cooperative Schemes. (a) Non-cooperative Scheme and (b) Cooperative Dual-terminal Clustered Scheme.	24
Figure 14.	Cooperative Dual-relay Schemes. (a) Two-hop Scheme (b) Multi-hop Scheme.	26
Figure 15.	Two Parallel Single-terminal Relay Paths forming a Non-cooperative Multiple-hop Scheme with two sources to the left most side and a destination to the right most side.	27
Figure 16.	Cooperative Diversity Scheme in Multi-hop Frequency Flat Fading Channel.	32
Figure 17.	Performance of Two-hop C-DIV and Non-cooperative DF and AF Schemes for a SNR Difference between the Paths of 3 dB in Rayleigh Channel for BPSK.	37
Figure 18.	Cooperative Diversity Scheme in Multi-hop Frequency Selective Slow Fading Channel.	39
Figure 19.	Application of Two Parallel 2-by-1 Distributed Alamouti Space-time Schemes in Consecutive Hops Due to Non-cooperative Processing of Relays in Reception and Synchronization in Transmission.	41
Figure 20.	Alamouti Cooperative space-time coding Scheme in Multi-hop Frequency Flat Fading Channel.	42
Figure 21.	Calculated Performances of Alamouti Cooperative Space-time Coding, Decode-and-Forward with Cooperative Diversity, Decode-and-Forward	

	and Amplify-and-Forward Schemes in AWGN for BPSK in the Two-hop Relaying Network.	46
Figure 22.	Alamouti Cooperative space-time coding Relaying Scheme in Multi-hop Frequency Selective Fading Channel.	47
Figure 23.	Performance of Two-hop Cooperative C-STC and C-DIV and Non-cooperative DF and AF Schemes for a SNR Difference between the Paths of 3 dB in Rayleigh Channel for BPSK.	49
Figure 24.	Relay Schemes for Simulation. (a) Non-cooperative Two Hop (b) Cooperative Two Hop Scheme.	53
Figure 25.	Performance of Two-hop Cooperative C-STC, C-DIV and Non-cooperative DF Schemes for a SNR Difference between the Paths of 0 dB in Rayleigh Channel for BPSK.	55
Figure 26.	Performance of Two-hop Cooperative C-STC, C-DIV and Non-cooperative DF Schemes for a SNR Difference between the Paths of 5 dB in Rayleigh Channel for BPSK.	56
Figure 27.	Performance of Two-hop Cooperative C-STC, C-DIV and Non-cooperative DF Schemes for a SNR Difference between the Paths of 9 dB in Rayleigh Channel for BPSK.	57
Figure 28.	Performance of Two-hop Cooperative C-STC, C-DIV and Non-cooperative DF Schemes for a SNR Difference between the Paths of 3 dB in SUI1 Channel for BPSK.	58
Figure 29.	Performance of Two-hop Cooperative C-STC, C-DIV and Non-cooperative DF Schemes for a SNR Difference between the Paths of 3 dB in SUI3 Channel for BPSK.	59
Figure 30.	Performance of Two-hop Cooperative C-STC, C-DIV and Non-cooperative DF Schemes for a SNR Difference between the Paths of 3 dB in SUI6 Channel for BPSK.	60
Figure 31.	Performance of Two-hop Cooperative C-STC, C-DIV and Non-cooperative DF Schemes for a SNR Difference between the Paths of 3 dB in Rayleigh Channel for QPSK.	61
Figure 32.	Performance of Two-hop Cooperative C-STC, C-DIV and Non-cooperative DF Schemes for a SNR Difference between the Paths of 3 dB in SUI1 Channel for QPSK.	62
Figure 33.	Performance of Two-hop Cooperative C-STC, C-DIV and Non-cooperative DF Schemes for a SNR Difference between the Paths of 3 dB in SUI3 Channel for QPSK.	63
Figure 34.	Performance of Two-hop Cooperative C-STC, C-DIV and Non-cooperative DF Schemes for a SNR Difference between the Paths of 3 dB in SUI6 Channel for QPSK.	64
Figure 35.	Performance in Multiple Hops of C-STC, C-DIV and DF Schemes for BPSK in SUI1 Channel and an SNR Difference between the Paths of 3 dB in the Low SNR Region.	65
Figure 36.	Performance in Multiple Hops of C-STC, C-DIV and DF Schemes for QPSK in SUI1 Channel and an SNR Difference between the Paths of 3 dB in the Low SNR Region.	66

Figure 37.	Constellations used in the Simulation: (a) 16-QAM Rectangular and (b) 64-QAM Rectangular.....	67
Figure 38.	Performance of Two-hop Cooperative C-STC, C-DIV and Non-cooperative DF Schemes for a SNR Difference between the Paths of 3 dB in Rayleigh Channel for 16-QAM.	68
Figure 39.	Performance of Two-hop Cooperative C-STC, C-DIV and Non-cooperative DF Schemes for a SNR Difference between the Paths of 3 dB in SUI1 Channel for 16-QAM.	69
Figure 40.	Performance of Two-hop Cooperative C-STC, C-DIV and Non-cooperative DF Schemes for a SNR Difference between the Paths of 3 dB in Rayleigh Fading Conditions for 64-QAM.	70
Figure 41.	Performance of Two-hop Cooperative C-STC, C-DIV and Non-cooperative DF Schemes for a SNR Difference between the Paths of 3 dB in SUI1 Fading Conditions for 64-QAM.	71

THIS PAGE INTENTIONALLY LEFT BLANK

LIST OF TABLES

Table 1.	Transmission Sequence for the 2×1 Alamouti Scheme.	9
Table 2.	Transmission Sequence for the Dual-Antenna Distributed Alamouti Scheme.	42

THIS PAGE INTENTIONALLY LEFT BLANK

LIST OF ACRONYMS AND ABBREVIATIONS

AF	Amplify-and-Forward
AWGN	Additive White Gaussian Noise
BER	Bit Error Rate
BLAST	Bell Laboratories Layered Space-Time Architecture
CSI	Channel State Information
CSIR	Channel State Information at Receiver
C-DIV	Cooperative Diversity
C-STC	Cooperative Space-Time Coding
dB	Decibel
DC-STC	Dual-Antenna Cooperative Space-Time Coding
DF	Decode-and-Forward
ISI	Inter Symbol Interference
MIMO	Multiple Input Multiple Output
MRC	Maximal Ratio Combining
MT	Mobile Terminal
OFDM	Orthogonal Frequency Division Multiplexing
PSK	Phase Shift Keying
QAM	Quadrature Amplitude Modulation
SC	Single Carrier
SER	Symbol Error Rate
SM	Spatial Multiplexing
STC	Space-Time Coding
SUI	Stanford University Interim
VAA	Virtual Antenna Array

THIS PAGE INTENTIONALLY LEFT BLANK

EXECUTIVE SUMMARY

Space-time coding and cooperative diversity schemes were primarily used in multiple-input multiple-output communications, but can also be used to improve the bit error performance and the energy consumption in wireless, energy constrained multihop relay communication networks.

The objective of this research is evaluate the performance of the cooperative diversity and space-time transmission schemes, namely decode-and-forward with cooperative diversity and Alamouti cooperative space-time coding, in clustered multihop relay networks consisting of single-antenna elements. Decode-and-forward with cooperative diversity is the combination of decode-and-forward and multiple-input multiple-output techniques for single antenna terminals, which provides spatial diversity, is studied in this thesis. The Alamouti cooperative space-time coding algorithm is a combination of Alamouti space-time coding and decode-and-forward. These are compared to the non-cooperative relaying schemes of decode-and-forward and amplify-and-forward.

The wireless network topology used for the simulation is a network, which is formed by clusters that consist of two single-antenna terminals. There are two single-antenna source terminals that transmit under the same power limitation and one multi-antenna destination terminal. Simulation is initially conducted in a Rayleigh fading channel and Stanford university interim channel models. The performance measure is the error probability as a function of the signal to noise ratio or number of signal hops.

For phase shift keying and quadrature amplitude modulation signals, the obtained error probabilities are improved and the performance difference for the two users is significantly decreased compared to the non-cooperative schemes. The reduction of performance differences between the users in cooperative schemes shows that cooperation among terminals leads to sharing of the energy resources of the network, so that terminals can extend their lifetime or achieve greater coverage ranges. Decode-and-forward with cooperative diversity performed well in cases where the signal-to-noise difference between the paths was high and Alamouti cooperative space-time coding

performed better than other schemes in severe channel fading conditions. The cooperative schemes in multihop scenarios performed better than the non-cooperative schemes. We also noted that quadrature amplitude modulation suffered higher error probabilities in single carrier modulation; improvement was achieved compared to the non-cooperative schemes, but the use of orthogonal frequency division multiplexing is suggested in future research.

ACKNOWLEDGMENTS

I dedicate this work to my beloved mother Evaggelia Ordoumpozani, who always patiently stands by my side.

THIS PAGE INTENTIONALLY LEFT BLANK

I. INTRODUCTION

Cooperative wireless networks are a promising technology for future communication systems because cooperation in ad hoc networks can save limited network resources, including energy savings. In the last decade there has been a large ongoing research effort in this field. Cooperative techniques in wireless communication networks are the means to adopt the diversity, which is inherent in a wireless medium. The diversity achieved in a communication system, when such techniques are implemented, can be in code, frequency, space and time domains. The goal of cooperative diversity is to increase the reliability and the quality of service (QoS), coverage area range, and the data throughputs as well as improve the spectral efficiency of the wireless networks while prolonging the life of the nodes or user terminals by increasing energy efficiency. In a network consisting of independent users (ad hoc networks), achieving full diversity depends on the successful use of distributed coding and routing algorithms. Dynamic rather than static topologies and cooperation among heterogeneous networks further complicate the research efforts in this area.

Cooperative communications networks use techniques initially developed for multiple-input multiple-output (MIMO) communications. These techniques seek to achieve spatial diversity and/or spatial multiplexing gains. In [1], a decode-and-forward relaying scheme, was introduced. In [2] the BLAST algorithm was proposed to exploit spatial multiplexing gains in multiple-input multiple-output systems. The Alamouti space-time code was proposed in [3], based on the maximal ratio combining receive-diversity scheme as a fairly simple space-time coding technique for a two-antenna transmitter and a single or multi-antenna receiver. The Alamouti scheme can be extended to a system with $2n \times 2n$ antenna elements. Initially, it was introduced as a code which could achieve full diversity in a flat fading channel. Later in [4, 5] a modified version for multipath fading channels was proposed for the single-antenna receiver case. In [6], work done in [4, 5], was expanded to the two-antenna receiver case. This thesis will investigate the performance of the distributed form of decode-and-forward and of Alamouti space-time coding, which provide spatial diversity in clustered multihop relay networks.

A. THESIS OBJECTIVE

The objective of this research is to investigate the performance of the cooperative diversity and space-time transmission schemes, namely decode-and-forward with cooperative diversity and Alamouti cooperative space-time coding, in clustered multihop relay networks consisting of single-antenna elements. Their performance is compared to that of non-cooperative relaying schemes, namely non-cooperative decode-and-forward and amplify-and-forward.

Space-time coding was primarily studied for multiple-input multiple-output (MIMO) communications. Past work done [3-11] demonstrated that space-time coding benefits communications schemes with multiple-antenna elements. Currently, there is considerable research interest in extending MIMO communication techniques to wireless ad hoc networks to achieve improved performance. Spatial diversity is a common characteristic of MIMO communications and ad hoc networks. In this thesis, we implement the space-time codes in clustered multihop relay networks. Specifically, we implement the distributed forms of decode-and-forward scheme and of Alamouti space-time coding, which provide spatial diversity gains, in multihop relaying schemes of independent and power constrained terminals in order to evaluate their performance. Simulation results are obtained for BPSK, QPSK and QAM in Rayleigh and SUI fading channels.

B. RELATED WORK IN COOPERATIVE SPACE-TIME CODING, COOPERATIVE DIVERSITY AND SPATIAL MULTIPLEXING

Cooperative diversity for a simple three-terminal relay channel was first introduced in [12]. Later, in [1], several improvements were made in capacity bounds and cooperative schemes, such as decode-and-forward, were introduced. Modifications to amplify-and-forward scheme were proposed in [13-16]. Based on these, more relaying schemes were introduced in [17-24]. The performance and other characteristics of the aforementioned schemes in several environments were studied in [17-27]. Extensions to a multi-terminal, multihop network were made in [13-17], where a clustered model and ad hoc network architecture were studied and useful results for transmit and receive

diversity gains and relaying strategies were obtained. Although compared to MIMO full diversity gains are not achieved due to single antenna elements, data rate gains can be achieved compared to the non-cooperative cases [13]. Cooperative spatial multiplexing schemes are also studied in [9-10, 28-29]. The cooperative form of the decode-and-forward scheme for single antenna terminals, which provide spatial diversity, is studied in this thesis.

Cooperative space-time coding introduced numerous problems to be solved, such as the terminal localization, time synchronization and distributed processing between the cooperative terminals. Cooperative space-time coding for clustered networks is still under development. In [7] a short range link is proposed in each cluster to achieve synchronization and combined processing for Alamouti space-time coding. In [8] the performance of cooperative space-time coding is studied. Generally, cooperative space-time codes adopt both cooperative diversity schemes and cooperative spatial multiplexing schemes [11]. The success of a cooperative space-time coding scheme, among others, depends on the trade-off between spatial diversity gain and spatial multiplexing gain. In this thesis, the cooperative Alamouti space-time coding, which was developed for the three node network in [7], is extended to clustered multihop relay networks consisting of single-antenna terminals.

C. THESIS OUTLINE

This thesis is organized as follows. In Chapter II the fundamental concepts of MIMO communications and cooperative relaying networks is reviewed. Chapter III introduces the relaying schemes of non-cooperative amplify-and-forward and decode-and-forward, the cooperative decode-and-forward with cooperative diversity and the Alamouti cooperative space-time coding. Chapter IV presents simulation results on PSK and QAM. Chapter V presents the conclusions and the significant results that were obtained in this work and includes suggestions for future study. This thesis includes two appendices. Appendix A lists the six models of the Stanford University Interim (SUI) fading channels. In Appendix B, the Matlab code used for the simulation is included.

THIS PAGE INTENTIONALLY LEFT BLANK

II. DISTRIBUTED IMPLEMENTATION OF MIMO TECHNIQUES

In this chapter a brief review of multiple-input multiple-output (MIMO) communications, spatial diversity (SD), spatial multiplexing (SM) and space-time coding (STC) is presented. All the aforementioned topics are related to the research reported here and are required to comprehend the work done. The Alamouti space-time coding scheme for multiple-input multiple-output communications is also examined since its distributed form (presented in the next chapter) is the primary technique for relaying messages in wireless networks in this work. Also introduced are the relaying channels, the virtual antenna arrays and the wireless cooperative communications systems.

A. MIMO COMMUNICATIONS

Multiple-input multiple-output (MIMO) [2, 3, 30,31] systems were introduced in order to enhance the performance of the wireless communications systems to provide robustness, high data rates, and reliability by overcoming the channel fading with the use of multiple antennas. A MIMO system offers redundancy through the multiple independent channels, which are created between the transmitting and the receiving antennas of the system. Using multiple-input multiple output systems, significant improvements are made in the coverage ranges of the communication systems and the data throughput without the need for additional transmission power or bandwidth expansion. Figure 1 shows a schematic diagram of a typical MIMO system with M transmission antennas and N reception antennas. In such a system a signal can be carried through the $M \times N$ different independent channels that exist between the transmitter and the receiver. In Figure 1 $h_{i,j}(t,\tau)$ represents the fading channel between the i^{th} transmission antenna and the j^{th} reception antenna. Variable t is the time variable and τ denotes the signal delay variable when multipath fading occurs in the fading channel. When there is no multipath fading, then $\tau=0$. A MIMO system can provide both spatial diversity and spatial multiplexing gains. These concepts are defined in the next two paragraphs. It is

important to note that all the gains provided by this scheme may not be realized simultaneously. Instead, there is a trade-off occurring between them.

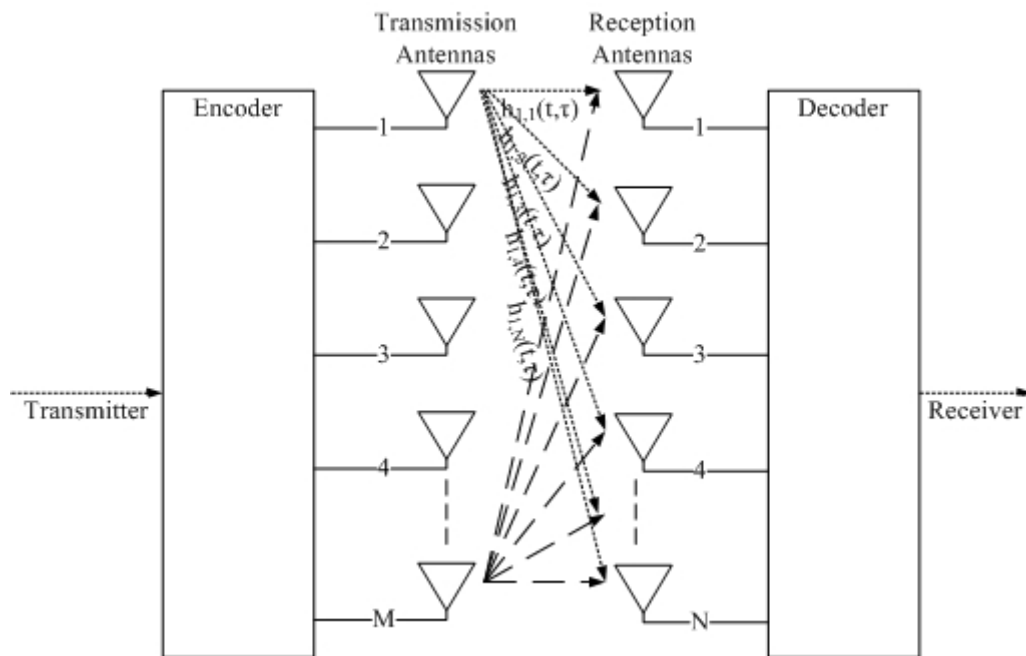


Figure 1. Typical MIMO System with M Transmitting and N Receiving Antennas, which provides an $M \times N$ Spatial Diversity Order.

B. SPATIAL DIVERSITY, SPATIAL MULTIPLEXING AND SPACE-TIME CODING

In the next two subsections, the two basic concepts of spatial diversity and spatial multiplexing in wireless communication are briefly described. Followed by that, space-time coding schemes are introduced.

1. Spatial Diversity

A signal is said to be spatially diverted when it is being carried to the destination not only by one wireless channel, but by multiple parallel independent channels. Hence in a spatial diversity scheme [1, 2, 3, 30] the information message is copied in a domain (space, time, frequency) several times and is transmitted through all the possible independent fading channels $h_{i,j}(t, \tau)$ between the i^{th} source and the j^{th} destination of the wireless medium that are between the transmitter and the receiver. These multiple copies

of the signal to the receiver provide the system with redundancy since the probability that all copies experience deep fading is highly reduced [30]. Thus, a system with multiple antennas for transmission and reception, like the one depicted in Figure 2, can achieve spatial diversity and enhance the quality of service (QoS) of one's communications. The system depicted in Figure 2 has two transmission antennas and two reception antennas and achieves spatial diversity order of four. Spatial diversity can be further divided into transmission diversity and reception diversity schemes when it occurs at the transmitter's or receiver's side, respectively. The system of Figure 2 has a transmission diversity order of two and a reception diversity order of two since it has two transmission and two reception antennas, respectively.

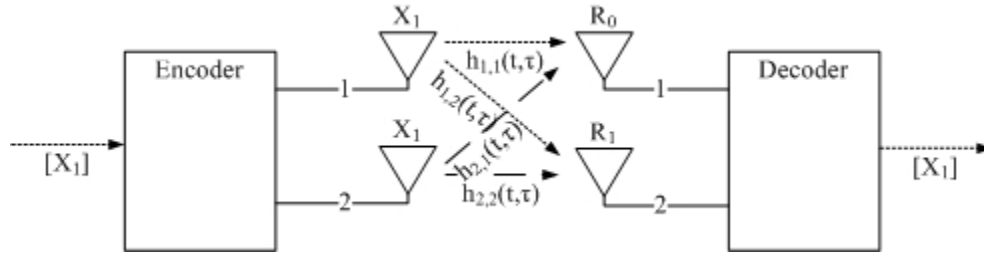


Figure 2. Spatial Diversity Scheme with Quadruple Diversity Gain, since there are Four Independent Transmission Channels $h_{i,j}$).

2. Spatial Multiplexing

Spatial multiplexing, on the other hand, is a technique used to increase data rates in wireless communications. This is achieved by dividing the data stream and transmitting it through multiple independent non-interfering channels. A signal is spatially multiplexed when different portions of the signal are being transmitted through different independent fading channels. Thus if a channel suffers fading in one of the sub-channels, then only a small portion of the information will be lost. Also the achieved transmission rate is increased by a factor equal to the number of independent channels used. A spatial multiplexing scheme is depicted in Figure 3, which divides the stream $[X_1 X_2]$ such that symbol X_1 is transmitted by transmission antenna 1 and symbol X_2 is transmitted by transmission antenna 2. Each symbol is transmitted through two independent fading channels $h_{i,j}$; symbol X_1 is transmitted through $h_{1,1}$ and $h_{1,2}$.

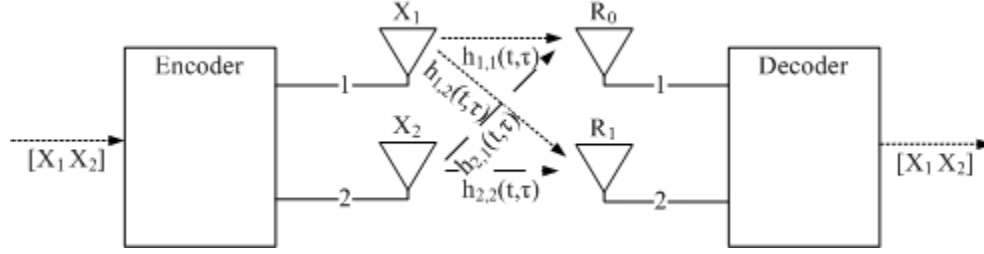


Figure 3. Spatial Diversity Scheme with Double Multiplexing Gain, since every two Consecutive Symbols are transmitted by Different Antennas.

Without reducing the quality of the signal, spatial multiplexing takes advantage of the multiple channels of the wireless medium. Achieved data rates, compared to a single-input single-output (SISO) system, can be increased by factor $d = \min\{N, M\}$, the number of the independent channels; for the system in Figure 3, $d=2$ [30].

Both spatial diversity and spatial multiplexing gains, which can be achieved, grow with the number of antennas, since more alternative independent channels are provided to the system.

3. Space-time Coding

Real-time voice and image transmissions over wireless networks demand high data rates and quality of service (QoS). Space-time coding was developed to increase both reliability and link capacity. There are two broad categories of space-time (ST) codes; those targeted to increase reliability/QoS of MIMO communications and those developed to offer higher data rates. Alamouti [3] is a scheme targeted to provide reliability and BLAST [2] is an architecture that offers higher rates by providing spatial multiplexing.

Alamouti proposed an algorithm that offers transmit diversity to increase reliability in a flat fading channel (Rician and Rayleigh) [3]. The technique is optimum for two transmission antennas and as many reception antennas as possible. The equations for a system with two transmission antennas and one reception antenna (2×1) and a 2×2 system were derived in [3]. The Alamouti space-time coding scheme can achieve full spatial diversity gain (a gain of two for the 2×1 scheme and a gain of four for the 2×2 scheme) without decreasing the achieved data rates since there is also a spatial

multiplexing gain of order two which doubles the achieved data rates. Thus the reduction of the achieved rate that occurs because of the retransmission of the symbols at the second time slots is offset by the simultaneous increase of the rates since at each time slot two symbols are transmitted.

a. 2×1 Alamouti Space-time Coding Scheme

The Alamouti space-time coding scheme, as proposed in [3], for the system with two transmission antennas and one reception antenna is shown in Figure 4. It is assumed that the complex channel coefficients $h_{i,j}$ are constant across two consecutive symbol periods and that it is a frequency flat fading (memoryless channel) environment for the allocated frequency bandwidth. The information symbols to be transmitted are X_1 and X_2 . The system during the first symbol period transmits $[X_1, X_2]$ and during the second symbol period transmits $[-X_2^*, X_1^*]$ as given in Table 1, where X_1^* denotes the complex conjugate of X_1 and T denotes the symbol transmission period.

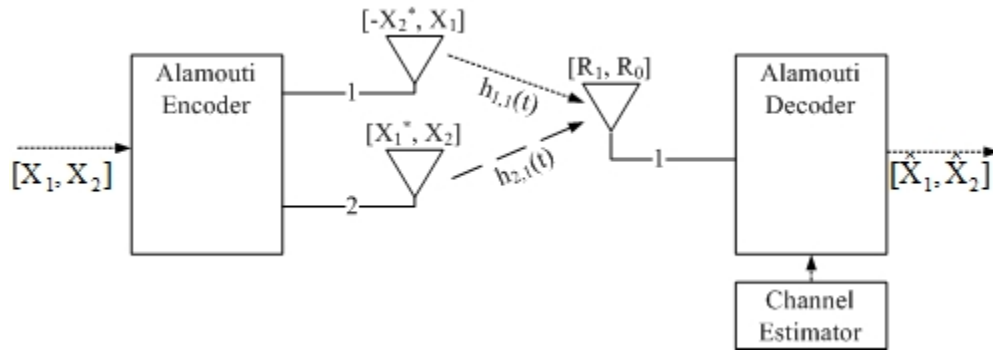


Figure 4. Alamouti 2×1 Scheme for Frequency Flat Slow Fading Channel.

	Antenna 1	Antenna 2
time t	X_1	X_2
time $t + T$	$-X_2^*$	X_1^*

Table 1. Transmission Sequence for the 2×1 Alamouti Scheme.

From [3], for frequency flat, slow fading channel conditions, the channel coefficients are assumed to be constant during two consecutive symbol periods,

$$h_{1,1}(t) = h_{1,1}(t+T)$$

and

$$h_{2,1}(t) = h_{2,1}(t+T),$$

(2.1)

the received signals at times t and $t+T$, respectively are [18]:

$$R_0(t) = R(t) = h_{1,1}(t)X_1(t) + h_{2,1}(t)X_2(t) + n_0(t)$$

and

(2.2)

$$R_1(t) = R(t+T) = -h_{1,1}(t)X_2^*(t) + h_{2,1}(t)X_1^*(t) + n_0(t+T)$$

where n_0 represent noise at the receiver. The estimates of the signals are calculated in the decoder/combiner as follows [3]:

$$\hat{X}_1(t) = h_{1,1}^*(t)R_0(t) + h_{2,1}(t)R_1^*(t)$$

and

(2.3)

$$\hat{X}_2(t) = h_{1,1}^*(t)R_0(t) - h_{2,1}(t)R_1^*(t).$$

The Alamouti 2×1 scheme for the single carrier (SC) case in a channel with multipath fading and inter symbol interference (ISI) is depicted in Figure 5 and has been studied in [4]. The channel has memory hence it is represented by its impulse response $h_{i,j}$ as a function of the unit delay operator q^{-1} [4]. The single channel impulse response $h_{i,j}$ is then represented as a discrete-time filter given by [5]

$$h_{i,j}(q^{-1}) = h_{i,j_0} + h_{i,j_1}q^{-1} + \dots + h_{i,j_P}q^{-P} \quad (2.4)$$

where h_{i,j_n} for $n=0,1,2,\dots,P$ are the discrete-time filter coefficients and P indicates the number of the paths. The Stanford University Interim (SUI) channel models are widely used in the literature to realize channels with memory [5]. The SUI channels are used in this work to simulate the frequency selective multipath fading with $P=2$.

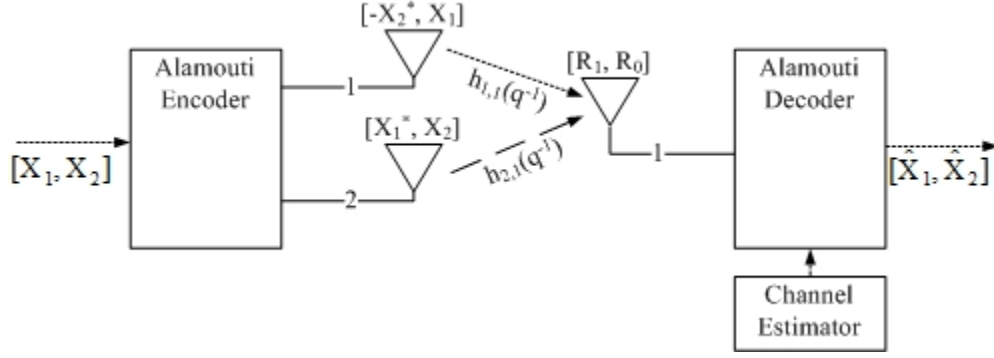


Figure 5. Alamouti 2×1 Scheme for a Frequency Selective Slow Fading Channel.

In a frequency selective channel with intersymbol interference, the space-time block coding technique [4, 5] is applied to demonstrate intersymbol interference. The symbols are transmitted in blocks of N consecutive symbols, given by

$$\begin{aligned} X_1 &= [X_1(1), X_1(2), \dots, X_1(t), \dots, X_1(N)], \\ X_2 &= [X_2(1), X_2(2), \dots, X_2(t), \dots, X_2(N)]. \end{aligned} \quad (2.5)$$

Typically $N > 1$ for channels with ISI. If $N = 1$, the channel is multipath with no ISI, which means that the maximum rms delay is smaller than the intersymbol guard period. From (2.2), for $P = 2$, assuming that channel fading coefficients remain constant during consecutive block transmissions, the received signals, R_0 and R_1 for the 2×1 Alamouti system are then expressed as

$$\begin{aligned} R_0(t) &= h_{1,1_0} X_1(t) + h_{1,1_1} X_1(t-1) + h_{1,1_2} X_1(t-2) \\ &\quad + h_{2,1_0} X_2(t) + h_{2,1_1} X_2(t-1) + h_{2,1_2} X_2(t-2) + n_0(t) \end{aligned}$$

and (2.6)

$$\begin{aligned} R_1(t) &= -h_{1,1_0} X_2^*(t) - h_{1,1_1} X_2^*(t-1) - h_{1,1_2} X_2^*(t-2) \\ &\quad + h_{2,1_0} X_1^*(t) + h_{2,1_1} X_1^*(t-1) + h_{2,1_2} X_1^*(t-2) + n_0(t+T). \end{aligned}$$

where T denotes the symbol transmission period.

Substituting (2.4) into (2.6) gives

$$R_0(t) = h_{1,1}(q^{-1})X_1(t) + h_{2,1}(q^{-1})X_2(t) + n_0(t)$$

(2.7)

and

$$R_1(t) = -h_{1,1}(q^{-1})X_2^*(t) + h_{2,1}(q^{-1})X_1^*(t) + n_0(t+T).$$

The decoder calculates the estimated signals as follows [18]:

$$\hat{X}_1(t) = h_{1,1}^*(q)R_0(t) + h_{2,1}(q^{-1})R_1^*(t),$$

(2.8)

$$\hat{X}_2(t) = h_{2,1}^*(q)R_0(t) - h_{1,1}(q^{-1})R_1^*(t).$$

where $h_{i,j}(q)$ [20] represents a non-causal realization of the channel filter $h_{i,j}(q^{-1})$.

b. 2×2 Alamouti Space-time Coding Scheme

The Alamouti space-time coding scheme for the system with two transmission antennas and two reception antennas in a memoryless channel, as proposed in [3], is shown in Figure 6. The transmission scheme is the same as with the 2×1 system case.

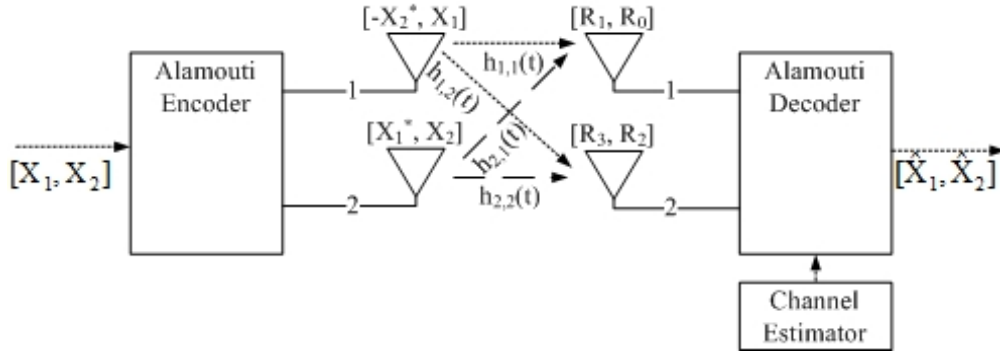


Figure 6. Alamouti 2×2 Scheme for a Frequency Flat Slow Fading Channel.

Received signals at receive antenna 1 are:

$$R_0(t) = h_{1,1}(t)X_1(t) + h_{2,1}(t)X_2(t) + n_0(t),$$

(2.9)

$$R_1(t) = -h_{1,1}(t)X_2^*(t) + h_{2,1}(t)X_1^*(t) + n_0(t+T)$$

where n_0 represents noise at receive antenna 1. At receive antenna 2 the received signals are:

$$R_2(t) = h_{1,2}(t)X_1(t) + h_{2,2}(t)X_2(t) + n_1(t) \quad (2.10)$$

and

$$R_3(t) = -h_{1,2}(t)X_2^*(t) + h_{2,2}(t)X_1^*(t) + n_1(t+T).$$

at time instances t and $t+T$, respectively, where n_1 represents noise at receive antenna 2. Again, the estimates of the signals in the decoder/combiner are given as [3]

$$\hat{X}_1(t) = h_{1,1}^*(t)R_0(t) + h_{2,1}(t)R_1^*(t) + h_{1,2}^*(t)R_2(t) + h_{2,2}(t)R_3^*(t), \quad (2.11)$$

$$\hat{X}_2(t) = h_{1,1}^*(t)R_0(t) - h_{2,1}(t)R_1^*(t) + h_{1,2}^*(t)R_2(t) - h_{2,2}(t)R_3^*(t).$$

The 2×2 scheme for frequency selective channel with ISI coefficients $h_{ij}(q^{-l})$ is shown in Figure 7. The transmission sequence is given by (2.5).

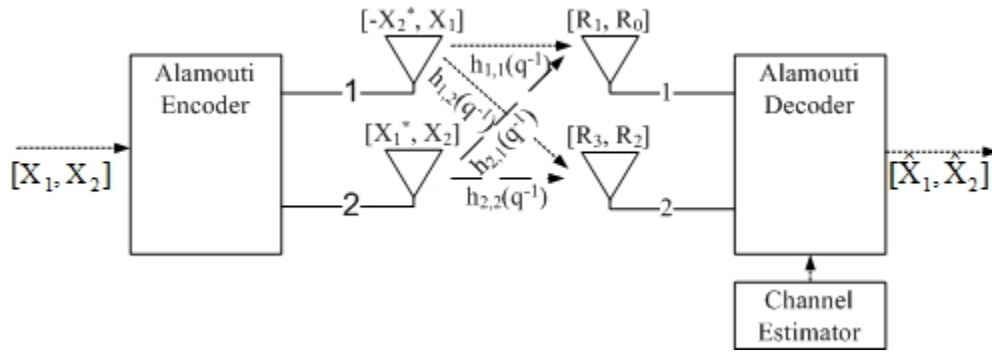


Figure 7. Alamouti 2×2 Scheme for a Frequency Selective Slow Fading Channel.

The received signals are [5]:

$$\begin{aligned} R_0(t) &= h_{1,1}(q^{-1})X_1(t) + h_{2,1}(q^{-1})X_2(t) + n_0(t), \\ R_1(t) &= R_0(t+T) = -h_{1,1}(q^{-1})X_2^*(t) + h_{2,1}(q^{-1})X_1^*(t) + n_0(t+T), \\ R_2(t) &= h_{1,2}(q^{-1})X_1(t) + h_{2,2}(q^{-1})X_2(t) + n_1(t), \\ R_3(t) &= R_2(t+T) = -h_{1,2}(q^{-1})X_2^*(t) + h_{2,2}(q^{-1})X_1^*(t) + n_1(t+T). \end{aligned} \quad (2.13)$$

Finally, the estimated symbol blocks as decoded by the decoder/combiner are:

$$\hat{X}_1(t) = h_{1,1}^*(q)R_0(t) + h_{2,1}(q^{-1})R_1^*(t) + h_{1,2}^*(q)R_2(t) + h_{2,2}(q^{-1})R_3^*(t)$$

(2.14)

and

$$\hat{X}_2(t) = h_{2,1}^*(q)R_0(t) - h_{1,1}(q^{-1})R_1^*(t) + h_{2,2}^*(q)R_2(t) - h_{1,2}(q^{-1})R_3^*(t)$$

where $h(q)$ represents a non-causal realization of the channel filter.

In each case the decoded symbol blocks are obtained using a maximum likelihood (ML) detector. A maximum likelihood detector maps the estimated symbols $\hat{X}_1(t)$ and $\hat{X}_2(t)$ to the most probable reference symbols from the phase shift keying modulation (PSK) or quadrature amplitude modulation (QAM) constellation being used. The measure used for mapping is the two dimensional distance between the estimated and the reference symbol on the constellation grid.

C. COOPERATIVE COMMUNICATIONS

The overall concept behind cooperation in wireless communications is to make the independent, and by nature non-cooperative, users of the network share their limited resources. Cooperation can be classified as implicit or explicit [31]. Implicit cooperation is a primitive form of cooperation and does not require any pre-established cooperative framework. A wireless communication protocol can be considered an implicit cooperation protocol if it applies rules for medium sharing among users (for example ALOHA).

On the other hand, explicit cooperation requires advanced cooperative protocols to be pre-established. In this type of cooperation, the elements of the system are directed to cooperate by these protocols [31]. Cooperation is also extended to the relaying procedures, which are targeted to extend the coverage range of the communication systems. The simplest topology where cooperative procedures occur in is a network which consists of three independent terminals/devices, as depicted in Figure 8. Of these

three terminals one acts as the source terminal (S) of the signal, the other acts as a relaying terminal (R), which conveys the signal, and the last is the destination terminal (D). This is the fundamental example of cooperation and is further described in this chapter as part of the cooperative communications systems.

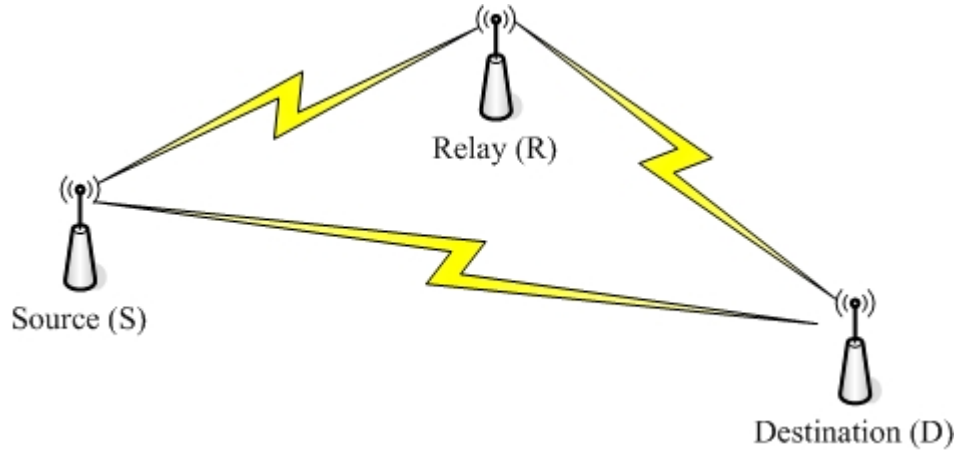


Figure 8. Three Terminals Network with a Source (S), a Relay (R) and a Destination (D) Node.

1. Distributed Networks

Distributed networks are networks that do not have a central controller to share the medium and control the communication. The two broad categories of distributed networks are the ad hoc networks and sensor networks.

a. *Ad hoc Networks*

Ad hoc translated from Latin is “for this,” and literally means “for this purpose only.” Thus, ad hoc networks are the networks which consist of terminals that move randomly and are brought together only for the temporary purposes of connectivity. These terminals are usually single antenna elements, independent, and connect on the volunteer basis only to help the wireless communications. An ad hoc network can consist of homogeneous or heterogeneous, portable or non-portable elements like mobile phones, computers, handhelds, wireless sensors, routers and other devices. These terminals are usually under temporary or permanent energy constraints. The portable nature of the majority of these devices indicates the dynamic topology and connectivity that

characterizes an ad hoc network. An ad hoc network can be established in a room, on an airplane or in open space and can use different short-range and long-range interfaces, such as ZigBee, Wi-Fi and WiMaX.

b. Sensor Networks

Sensor networks are distributed networks of small sensor terminals. These terminals may not be autonomous and have power and processing constraints. Yet, an operational requirement is to prolong their lifetime as long as possible while preserving reliability in data exchange and longer coverage ranges. Sensor networks, in contrast with ad hoc networks, are not dynamic and their traffic is usually periodic and of low intensity.

2. Cooperative Networks

Cooperation in wireless networks is proven to be an advantageous technique. In wireless communications cooperation is regarded as the sharing of the resources and the encoding and decoding capabilities of the network users. Distributed terminals cooperate to relay signals to distant terminals. For practical reasons not all terminals in a given area of interest are needed to cooperate. Typically terminals form clusters under the direction of specified protocols and selected terminals in the cluster participate in a cooperative communication scheme. Next we discuss how independent terminals form clusters to cooperate. Also, the concept of cooperative diversity is described along with decode-and-forward and amplify-and-forward schemes in the three terminal networks of Figure 8.

a. Clusters and Virtual Antenna Arrays

In a MIMO system antenna arrays are used to mitigate the fading. The terminals that form an ad hoc network are usually single antenna elements which cannot exploit spatial diversity gains to overcome fading. The deployment of antenna arrays on portable mobile terminals is impractical. Groups of distributed single antenna terminals can form virtual antenna arrays (VAA) and overcome this problem. Of course, communicating terminals can have more than one antenna, but this case is an expansion

of MIMO relaying and not cooperative relaying, which will be examined here. The virtual antenna array concept has been studied for sensor networks, ad hoc networks, cellular-type networks and WLAN-type networks [31]. From this point forward, devices that form virtual antenna arrays are referred to as mobile terminals (MT) [31]. Figure 9 depicts a distributed-MIMO clustered multi-relay network model. The terminals (MT) in each cluster can cooperate or they do not have to relay information. Several sub-MIMO systems are formed by the mobile terminals, which can cooperate through a short range link in each cluster [31, 32 and 7]. This link is depicted with a dash-dotted line in the vertical direction.

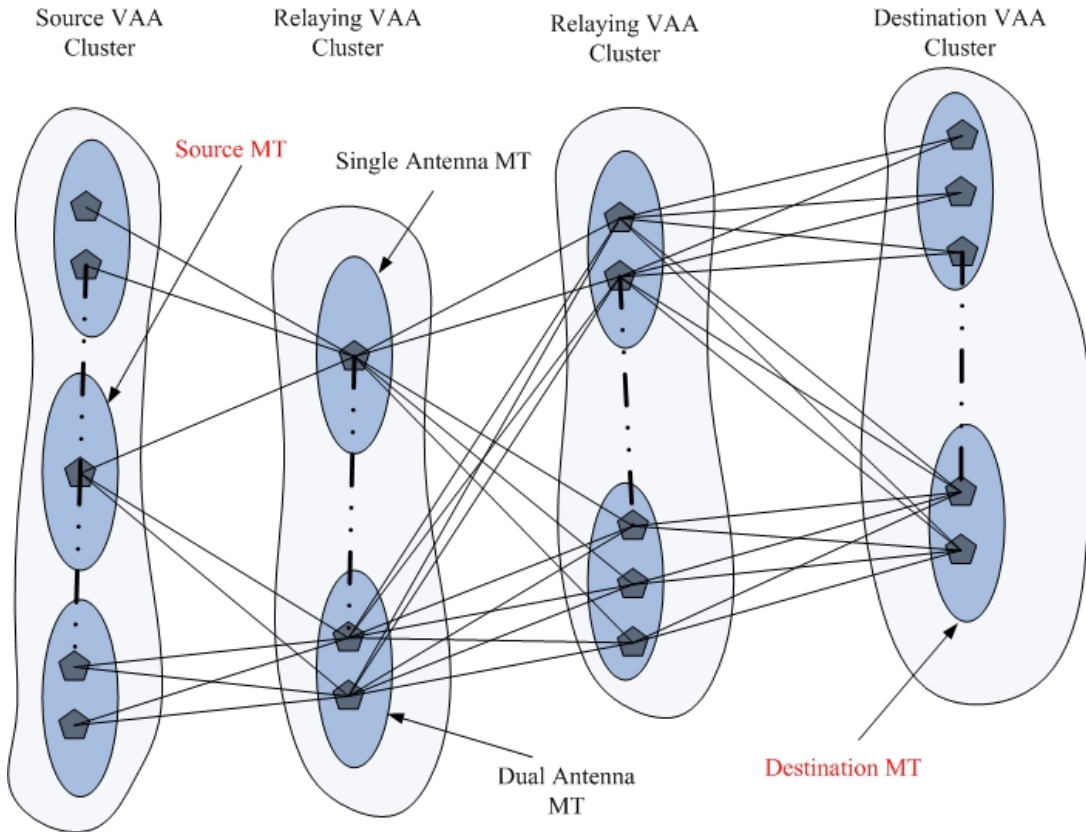


Figure 9. Distributed-MIMO Multi-terminal Relaying Network [After Ref. [32]].

As can be seen, not all mobile terminals can communicate with others because of limited coverage range or incompatibilities in signal modulation and coding

schemes. To take advantage of these relaying topologies one needs to employ algorithms for resource allocation [31], group forming [25], optimum positioning, routing, and synchronization.

b. Cooperative Diversity

Cooperative Diversity is the set of techniques used to achieve spatial diversity in cooperative networks. These techniques were initially applied to achieve spatial diversity between the closely located and correlated antennas in MIMO systems. One can either apply transmit diversity, by employing more than one cooperative transmitter, or receive diversity, by employing more than one cooperative receiver [13]. Of course, both diversity designs can be simultaneously applied to achieve redundancy in every hop between the relays of Figure 9.

c. Three Terminals Relay Network

The relaying method as shown in Figure 8 was introduced in [33]. In Figure 8, the source is considered to have a Line of Sight (LoS) link to both the relay and the destination but the fading components between R-D and S-D are different and independent. The source tries to send data to the destination and it is aided by the relay. This scheme can be full-duplex or half-duplex [30]. Since full-duplex terminals require advanced orthogonal modulation and accurate antenna directivity to avoid interference, only half-duplex schemes are considered here. In the half-duplex case, cooperation takes place in two consecutive time instances. If the LoS link between S and D is lost or interfered with, R can still send data to D. If the S-R or R-D link is down then the S-D link will send data. Spatial diversity combats fading that occurs in one of the channels. Thus, outage probability, which is the probability the link collapses, is diminished, bit error rate (BER) is improved, and redundancy is provided in the destination without additional cost in bandwidth or power.

A critical parameter to achieve high data throughputs is that the distant transmitters have to transmit in such a way that the symbol streams, which are desired to

be received by a specific terminal and be combined at the reception, arrive simultaneously at the receiving terminal [13].

d. Traditional Relaying Protocols

There are three main schemes for achieving cooperation/relaying, namely decode-and-forward, amplify-and-forward, and compress-and-forward. From these the first two are of interest and will be used for simulation. There is also coded cooperation proposed in [24] but because it is not scalable to larger networks it will not be discussed. The decode-and-forward and amplify-and-forward schemes are presented in Figures 10 and 11, respectively.

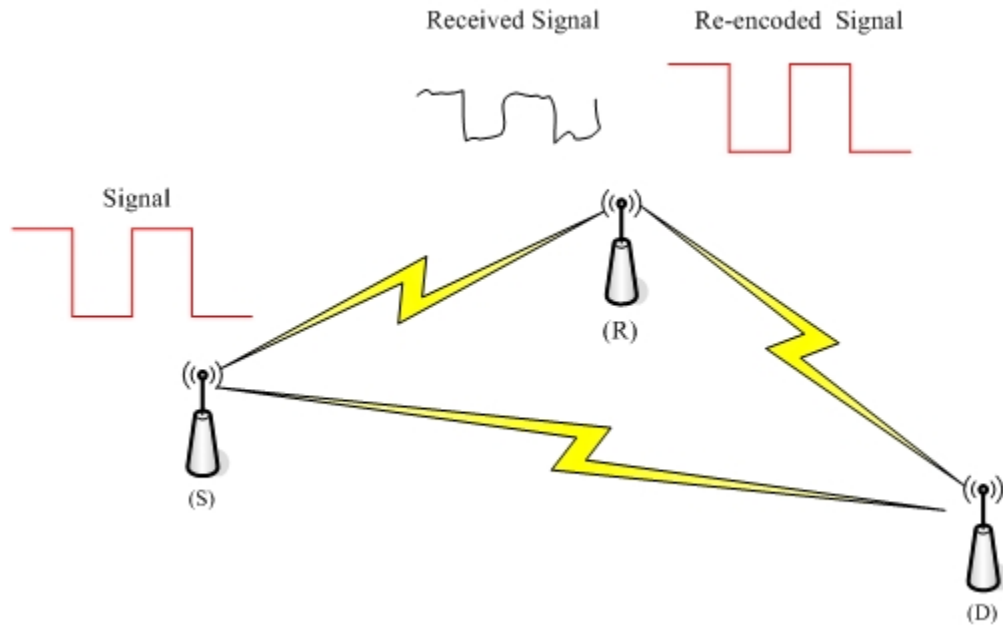


Figure 10. Decode-and-Forward Relaying Protocols in a Three-terminal Wireless Network.

In both decode-and-forward and amplify-and-forward schemes, it can be observed that in the first time slot receive diversity is achieved (R acts as the receiver) and in the second time slot transmit diversity is achieved (both S and R transmit). Briefly it can be said that in the decode-and-forward scheme as seen in Figure 10, the relay fully decodes the received source signal, re-encodes it, and transmits the estimated signal.

In the amplify-and-forward relaying scheme as seen in Figure 11, the received signal is just amplified and transmitted without any decode/encode procedure. Since the received signal in relay also contains noise, in amplify-and-forward the relay also amplifies noise.

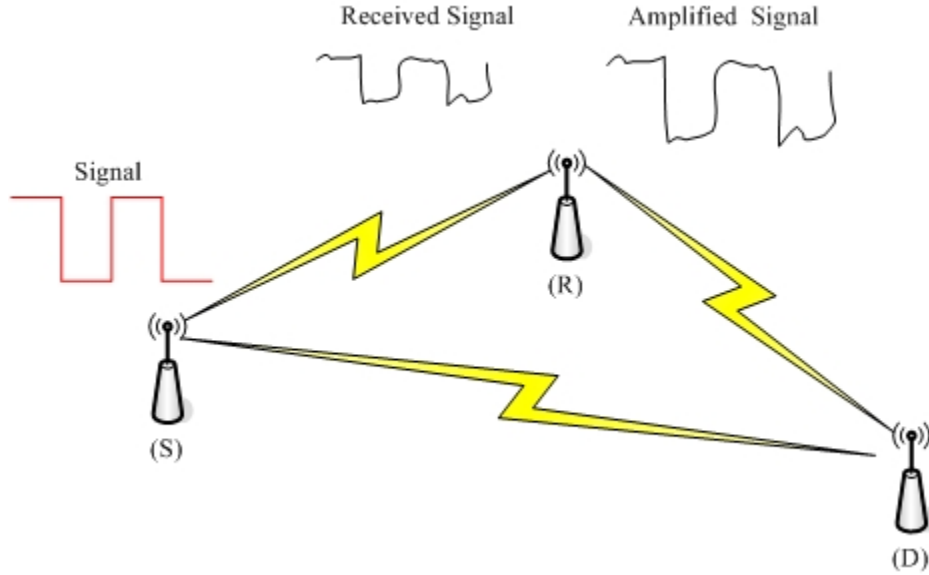


Figure 11. Amplify-and-Forward Relaying Protocols in a Three-terminal Wireless Network.

e. Cooperative Spatial Multiplexing

Cooperative spatial-multiplexing occurs when independent wireless relays deliver different and spatially multiplexed portions of the information signal to the destination [2]. Cooperative spatial multiplexing takes advantage of the spatial (uncorrelated channels due to dispersion of antennas) and frequency (orthogonal frequency channels) diversity gain of a multi-terminal network to increase data rates and decrease outage probability [34] compared to traditional forwarding schemes. In [34] a low complexity cooperative multiplexing scheme for the uplink (mobile terminal to base station) of a relay network is proposed. Another cooperative multiplexing technique for resource constrained devices (sensor networks) is proposed in [2].

f. Cooperative Space-Time Coding

Space-time coding techniques that have been successfully applied to mitigate inter-symbol interference in MIMO communications are being extended to cooperative communications [7, 8, 11, and 35]. Alamouti space-time coding [3] can be easily extended for application in a distributed environment [7]. In this thesis we investigate the distributed form of Alamouti space-time coding for cooperative communications.

D. SUMMARY

In this chapter, we introduced the cooperation in wireless networks, the spatial diversity and spatial multiplexing gains, the cooperative diversity and cooperative multiplexing techniques and the Alamouti space-time coding for MIMO communications. Also the distributed architecture of Alamouti space-time coding was briefly introduced and we analyze the performance of the distributed form of the Alamouti technique, along with cooperative diversity techniques, on specific multi-relaying scenarios in the next chapter [31]. Traditional relaying schemes will also be examined for comparison.

THIS PAGE INTENTIONALLY LEFT BLANK

III. PERFORMANCE ANALYSIS OF COOPERATIVE TECHNIQUES IN MULTI-RELAY CHANNELS

The objective of this chapter is to evaluate the performance of a cooperative diversity scheme and a cooperative space-time coding scheme in a multi-hop relay network. Followed by a description of the topology used, the theoretical formulas describing the non-cooperative and cooperative relaying schemes are introduced. The evaluation of cooperative space-time coding scheme is conducted using a distributed form of the Alamouti space-time coding. Also the bit error performance evaluations of all the schemes in AWGN environment are derived. The theoretical results are compared with simulation results for BPSK.

A. COOPERATIVE COMMUNICATION MODEL

Multi-relay terminal clusters between a source and a destination terminal required for cooperative communication schemes can be created using routing mechanisms developed for wireless ad hoc networks [36-41]. Once formed, these multi-relay terminal clusters can be treated as virtual antenna arrays as described in Chapter II. Figure 12 shows virtual antenna arrays consisting of clusters of two relaying terminals, which are deployed in a way that only one-hop neighborhoods are formed. For example, in the figure, the coverage area (dashed circle) of the cluster on the right most side includes the cluster in the middle but not the one on the left most side and vice versa.

All mobile terminals are assumed to be equipped with single antenna under power restrictions. The destination terminal is not of interest and can be equipped with one or multiple antennas. For this study, only the source mobile terminals, which are depicted on the left side of the network in Figures 13(a) and 13(b), generate information streams. All the other mobile terminals can only relay those information streams and do not generate their own. Hence an uplink is formed from the source mobile terminals on the left side of Figure 13 to the destination terminal on the right hand side of Figure 13. Hence we examine the uplink route that is formed and not the down-link from the right side to the left side of Figure 13.

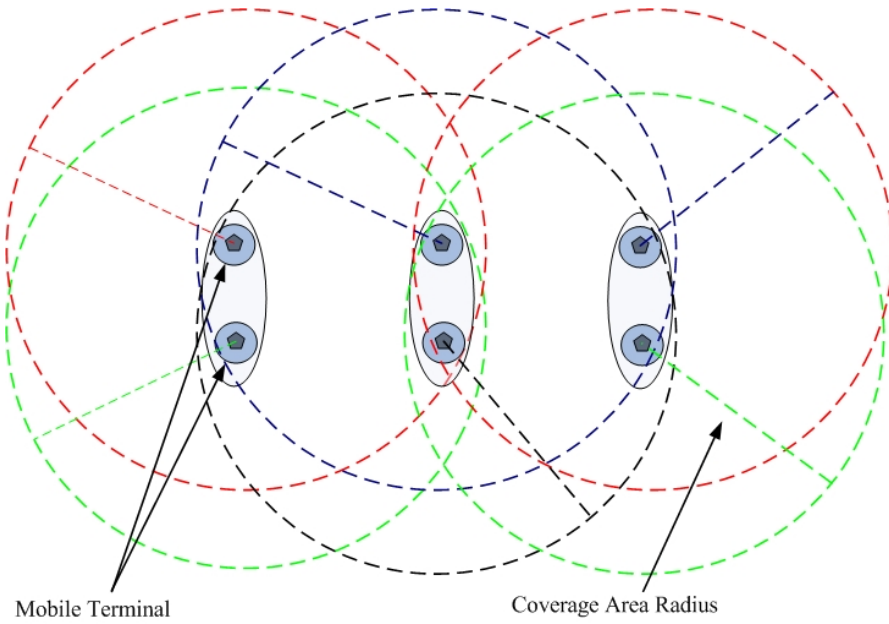


Figure 12. The Coverage Areas of Mobile Terminals. Areas are indicated by the Dashed Circles.

If the clusters contain only one single-antenna mobile terminals, there is no cooperation. In the case of more than one relaying terminal in each cluster, like the one depicted in Figure 13(b), the terminals can cooperate and thus achieve spatial diversity gain.

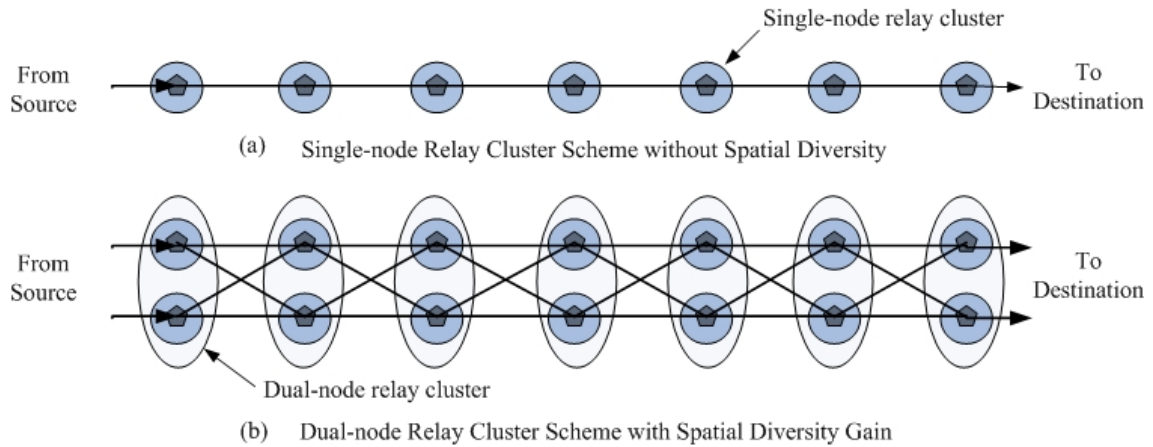


Figure 13. Multi-hop Relaying Topologies of Cooperative and Non-cooperative Schemes. (a) Non-cooperative Scheme and (b) Cooperative Dual-terminal Clustered Scheme.

This work will evaluate the cooperative communication model of Figure 14. Sources and relays are single-antenna mobile terminals. The two source terminals, in the right most side cluster, are denoted as SMT_1 and SMT_2 , respectively. A relay terminal is denoted as RMT_{ji} , for $j=1,2$ and $i=1,\dots,k$; where j indicates whether a relay terminal is on the upper or the lower part of the cluster and i is the number of hops to terminal RMT_{ji} . All terminals in the upper (lower) path are assumed to have the same SNR at reception. All mobile terminals operate in half duplex mode. Source and relaying mobile terminals operate under a total transmitted power constraint P_{max} . Mobile terminals apply coherent detection to the received signal using a matched filter. The destination is assumed to be a dual-antenna terminal. Evaluation can be extended to models containing more than two relaying mobile terminals in each cluster. As direct links (line of sight) can only be established between neighboring mobile terminals, relaying is the only way for communication between the source and destination. Figure 14(a) and 14(b) show the two-hop and multiple-hop cooperative relaying schemes, respectively. These schemes have one or more intermediate clusters of the relaying terminals RMT_{1j} and RMT_{2i} , for $i=1,\dots,k$. Parameter $h_{ji,n}$, for $j=1,2$ and $i=1,2$ and $n=1,\dots,k$, denotes the fading channel coefficient of the n^{th} hop between RMT_{jn-1} and RMT_{in} .

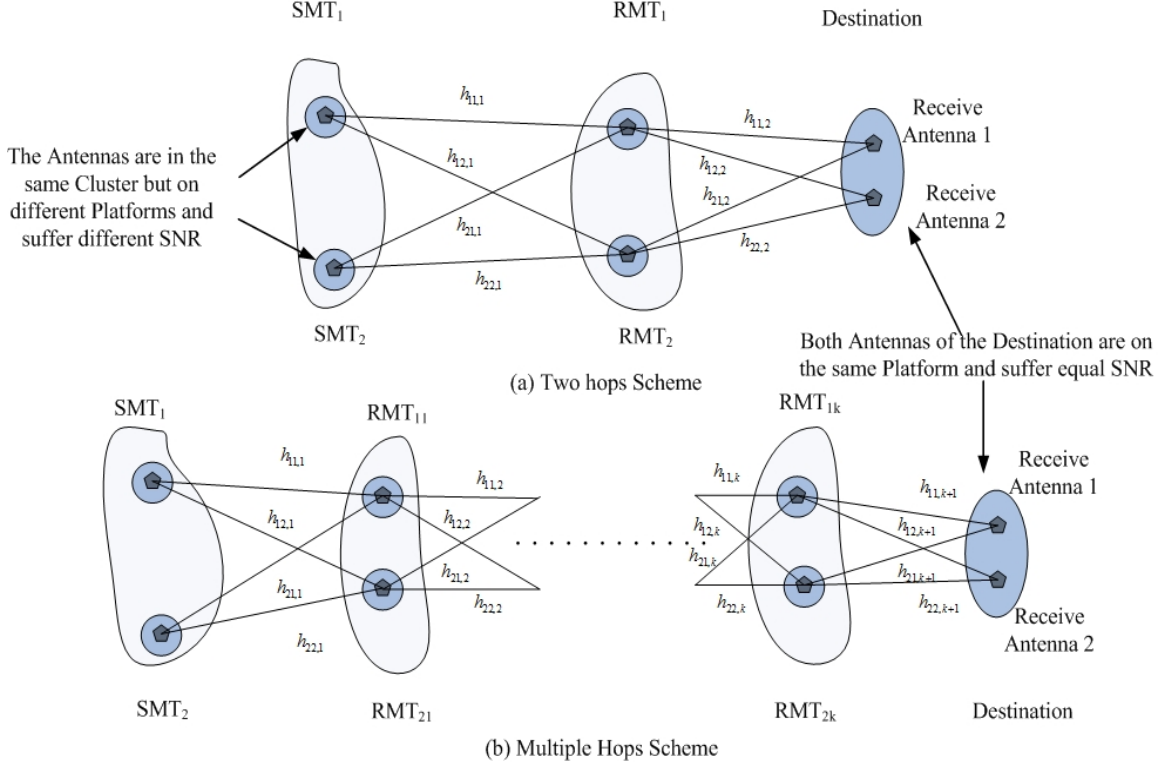


Figure 14. Cooperative Dual-relay Schemes. (a) Two-hop Scheme (b) Multi-hop Scheme.

B. ANALYSIS OF THE RELAYING TECHNIQUES

1. Non-cooperative Multi-hop Scheme

The two non-cooperative methods examined are decode-and-forward and amplify-and-forward. Two sources SMT_1 and SMT_2 transmit two independent signals denoted X_1 and X_2 , respectively, which are relayed to the destination by two separate non-cooperative multi-hop paths. The two parallel paths suffer uncorrelated fading, different noise levels, and no interference between them as shown in Figure 15. Variable R_{ij} denotes the received signal at relaying terminal RMT_{ji} , h_{ji} is the fading path coefficient between terminal RMT_{ji-1} and terminal RMT_{ji} , and \hat{X}_{ji} is the signal transmitted by relaying terminal RMT_{ji} .

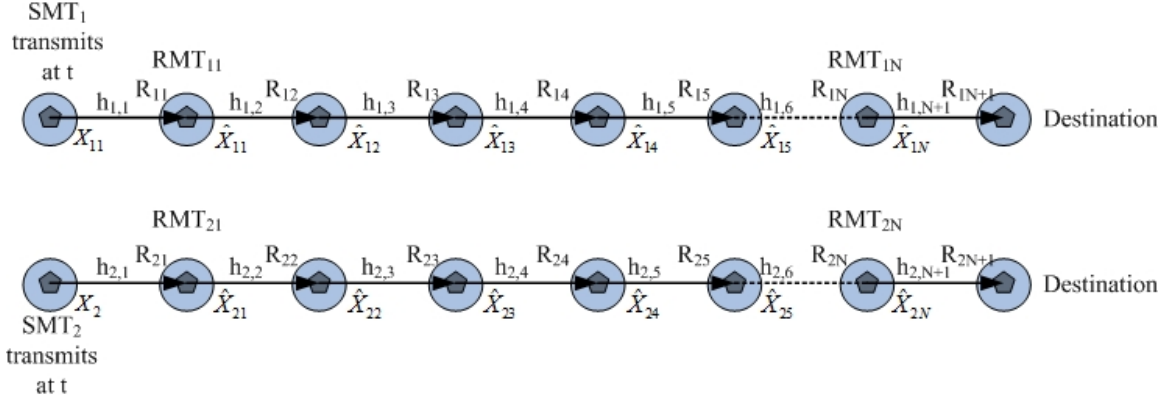


Figure 15. Two Parallel Single-terminal Relay Paths forming a Non-cooperative Multiple-hop Scheme with two sources to the left most side and a destination to the right most side.

a. Decode-and-Forward

Decode-and-forward is the first non-cooperative relaying scheme to be described. The formulas describing the scheme in flat fading are presented. The resulting formulas are used in the simulation of the scheme in the next chapter. The error probability for the two-hop case of decode-and-forward in AWGN is derived as well.

In this scheme, relays RMT_1 and RMT_2 coherently decode the received signals R_1 and R_2 and transmit their estimates \hat{X}_1 and \hat{X}_2 , respectively. The following formulas represent the decode-and-forward scheme in flat fading conditions. The initial transmission sequences for N consecutive time slots from the two sources are

$$X_1 = [X_1(1), X_1(2), \dots, X_1(t), \dots, X_1(N)], \quad (3.1)$$

$$X_2 = [X_2(1), X_2(2), \dots, X_2(t), \dots, X_2(N)]$$

where X_1 are the information symbols of source SMT_1 and X_2 are the information symbols of source SMT_2 . The received signals in the relays RMT_{1i} and RMT_{2i} , corresponding to the transmitted symbols $\hat{X}_{ji-1}(t)$, $j = 1, 2$ and $i = 1, \dots, N+1$, from the relays RMT_{1i-1} and RMT_{2i-1} , respectively, are

$$R_{1i}(t) = h_{1,i}(t) \hat{X}_{1i-1}(t) + n_{0i}(t), \quad (3.2)$$

$$R_{2i}(t) = h_{2,i}(t) \hat{X}_{2i-1}(t) + n_{0i}(t)$$

where n_0 and n_l represent noise received at RMT_{1i} and RMT_{2i}, respectively. For the purpose of simplicity the variable t is dropped from now on. Channel state information (CSI) $h_{j,i}$, for $j=1,2$, and $i=1,...,N+1$, is known at the receiver. The $h_{l,i}^*$ denotes the complex conjugate of $h_{l,i}$. Receiver filters input using CSI to diminish the fading effects as described in Chapter II. The intermediate signals, S_{ji} , calculated in the combiner of RMT_{ji}, are as follows:

$$S_{1i} = h_{1,i}^* R_{1i} = h_{1,i}^* h_{1,i} \hat{X}_{1i} + h_{1,i}^* n_{0i} = \hat{X}_{1i} + h_{1,i}^* n_{0i}, \quad (3.3)$$

$$S_{2i} = h_{2,i}^* R_{2i} = h_{2,i}^* h_{2,i} \hat{X}_{2i} + h_{2,i}^* n_{1i} = \hat{X}_{2i} + h_{2,i}^* n_{1i}.$$

A maximum likelihood detector is used to decode the intermediate signal to the closest reference signal \hat{X}_{ji} which is transmitted from RMT_{ji} under the power constraint of P_{\max} per symbol.

b. Bit Error Probability for Decode-and-forward

In [48] the bit error rate P_b for BPSK modulation with coherent detection in AWGN conditions and noise power spectral density $N_0/2$ for a single-hop relaying network is calculated based on an energy-per-bit to noise power spectral density (PSD) ratio:

$$P_b = Q\left(\sqrt{\frac{2E_b}{N_0}}\right) \quad (3.4)$$

where E_b is the energy per bit and can be represented as the signal power $P_s = E_b/T_b$, where T_b is the bit period. The noise transmission equivalent bandwidth for BPSK is $B = R_b = 1/T_b$; thus the noise power is $P_n = N_0 B = N_0/T_b$ and substituting these into (3.4) yields

$$\begin{aligned} P_b &= Q\left(\sqrt{\frac{2P_s T_b}{N_0}}\right) \\ &= Q\left(\sqrt{2\left(\frac{P_s}{P_n}\right)}\right) \end{aligned}$$

By defining $SNR=P_s/P_n$ the bit error probability P_b is given by

$$P_b = Q\left(\sqrt{2(SNR)}\right). \quad (3.5)$$

In the case of a two-hop relaying scenario with decode-and-forward in AWGN, the probability of error at reception can be calculated based on (3.5). Essentially the total error probability is the sum of the two possible error cases. The first case occurs when there is an error in the first hop, with error probability P_{b1} , and not in the second and the second case occurs when there is an error in the second hop, with error probability P_{b2} , and not in the first. Thus total error probability P_{bt} is

$$P_{bt} = P_{b1}(1 - P_{b2}) + (1 - P_{b1})P_{b2} = P_{b1} + P_{b2} - 2P_{b1}P_{b2}. \quad (3.6)$$

Considering that in consecutive hops the propagation conditions do not change significantly, the bit error probabilities in each can be assumed to be equal.

Substituting $P_{b1} = P_{b2} = P_b$ into (3.6) yields

$$P_{bt} = 2P_b - 2P_b^2 = 2Q\left(\sqrt{2(SNR_r)}\right) - 2Q\left(\sqrt{2(SNR_r)}\right)^2 \quad (3.7)$$

where SNR_r is the SNR at a relay. The developed formulation can be extended to a multi-hop with decode-and-forward relaying scheme for BPSK in AWGN with coherent detection.

c. Amplify-and-Forward

Amplify-and-forward is the second non-cooperative relaying scheme examined in this work. Initially the scheme is described and then the bit error probability for the two-hop case of amplify-and-forward in AWGN is derived.

In this strategy, the relays RMT_{1i} and RMT_{2i} in Figure 15 do not estimate the reference symbol from the received signal. The RMTs do not employ maximum likelihood detectors; instead they transmit the signals \hat{X}_{1i} and \hat{X}_{2i} , which are essentially the signals \hat{S}_{1i} and \hat{S}_{2i} amplified by an amplifier gain ' α ' so that $\alpha\hat{S}_{1i}$ and $\alpha\hat{S}_{2i}$ satisfy the

power constraint P_{max} . The scheme requires no advanced processing and achieves the maximum symbol rate that a non-multiplexing single carrier scheme can achieve.

d. Bit Error Probability for Amplify-and-forward

For the two-hop case of the amplify-and-forward scheme bit error probability P_b at destination is calculated assuming that the noise level in the destination and the relay terminal is the same. Based on (3.4) the bit error probability is

$$P_{bt} = Q\left(\sqrt{2\left(\frac{E_{sd}}{N_{0d}}\right)}\right) \quad (3.8)$$

where E_{sd}/N_{0d} is the signal energy per bit to noise power spectral density ratio at the destination terminal. But the energy of the received signal E_{sd} in the destination also contains the noise present in the relay terminal, which was amplified during the transmission of RMT_{i1}. Thus the portion of the signal energy that benefits detection at the destination is

$$E_{sd} = \frac{P_s}{P_s + P_n} E_b \quad (3.9)$$

where E_b is the bit energy, P_s is the signal power and P_n is the noise power at relay RMT_{i1}. The noise term N_{0t} at the destination is the sum of noise present at destination and the amplified noise from the relay terminal:

$$N_{0t} = N_0 + N_0 \frac{P_s}{P_s + P_n} \quad (3.10)$$

Substituting (3.9) and (3.10) into (3.8) gives

$$P_{bt} = Q\left(\sqrt{2\left(\frac{\frac{P_s}{P_s + P_n} E_b}{N_0 + N_0 \frac{P_s}{P_s + P_n}}\right)}\right) \quad (3.11)$$

Simplifying (3.11) leads to

$$P_{bt} = Q \left(\sqrt{\frac{E_b}{N_0} \frac{2 \frac{P_s}{P_n}}{2 \frac{P_s}{P_n} + 1}} \right) = Q \left(SNR_r \sqrt{\frac{2}{2SNR_r + 1}} \right). \quad (3.12)$$

where $SNR_r = P_s/P_n$.

2. Decode-and-Forward with Cooperative Diversity Scheme

Decode-and-forward with cooperative diversity is the first of the two cooperative relaying schemes (the other is Alamouti cooperative space-time coding) to be examined in this work. We present the scheme first in a flat fading and then in a frequency selective fading environment. Derived equations are then used for simulation. The theoretical error probability for the two-hop case of cooperative diversity scheme in AWGN is also derived. Note that the cooperative diversity scheme examined is for terminals that form dual-terminal clusters.

a. *Decode-and-Forward with Cooperative Diversity Scheme in Flat Fading Channel*

The multiple hop case of the decode-and-forward with cooperative diversity scheme is presented in Figure 16. The scheme applies equations (3.1) – (3.3) of the simple decode-and-forward but the received signal at each receiver is the sum of the received signals from the transmitters of the previous hop, thereby improving the SNR and robustness at reception.

Consider two mobile terminals SMT_1 and SMT_2 that act as sources and transmit separate streams of data of N symbols $X_1(i)$ and $X_2(i)$, respectively. Red dashed lines in Figure 16 denote the links allocated to relay the information of SMT_1 and black solid lines the data of SMT_2 when each source transmits. The two sources do not transmit simultaneously: When SMT_1 transmits SMT_2 is in silence mode and vice versa. This is to avoid interference between the transmitting half-duplex terminals for the single carrier (SC) modulation. Thus SMT_2 can transmit only after the neighbor relays have transmitted the previously received stream by SMT_1 . The next available time slot after t

is the $t+2$ because first hop relays transmit at time $t+1$, so in every two time slots only one of the two sources transmits and the medium is allocated to that source, thus reducing the data rates by one half.

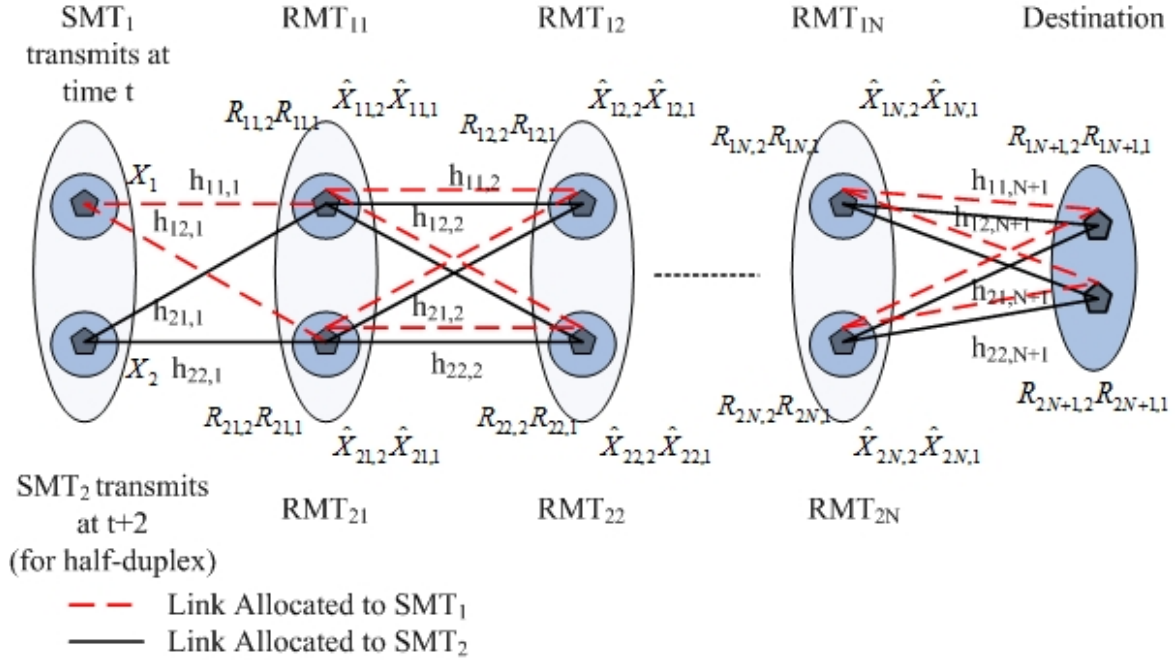


Figure 16. Cooperative Diversity Scheme in Multi-hop Frequency Flat Fading Channel.

The intra-cluster cooperation is limited to time synchronization only, and processing in each RMT is independent. At time t SMT₁ transmits X_1 and RMT₁₁ and RMT₂₁ receive $R_{11,1}$ and $R_{21,1}$, respectively and transmit their maximum-likelihood decoded symbols $\hat{X}_{11,1}$ and $\hat{X}_{21,1}$ to the next relay cluster. In both $R_{ji,k}$ and $\hat{X}_{ji,k}$, $j=1,2$ denotes the upper and lower part of the cluster, respectively, $i=1, \dots, N+1$ denotes the number of hops to RMT_{ji} and $k=1,2$ denotes the initial source SMT_k of the symbol. Next, at time $t+2$ SMT₂ transmits X_2 and RMT₁₁ and RMT₂₁ receive $R_{11,2}$ and $R_{21,2}$, respectively, and transmit their decoded symbols $\hat{X}_{11,2}$ and $\hat{X}_{21,2}$ to the next relay cluster. Hence in the first hop only receive-diversity is achieved as shown in Figure 16. On the other hand after the first hop the scheme achieves spatial diversity of order four since in

each subsequent hop two transmitting terminals and two receiving terminals are employed. The flat fading case, which is used in this work, is realistic for narrowband single carrier modulation. For the slow flat fading case (channel coefficients remain the same for two consecutive symbol transmissions) the respective equations that describe the processing at RMT₁₁ and RMT₂₁ are

$$\begin{aligned} R_{11,1}(t) &= h_{11,i}(t) X_1(t) + n_0(t), \\ R_{21,1}(t) &= h_{12,i}(t) X_1(t) + n_1(t) \end{aligned} \quad (3.13)$$

where n_0 and n_1 represent noise received at RMT₁₁ and RMT₂₁, respectively. The intermediate processing signals calculated in the decoders/combiners of RMT₁₁ and RMT₂₁ are

$$\begin{aligned} S_{11,1}(t) &= h_{11,1}^*(t) h_{11,1}(t) X_1(t) + h_{11,1}^*(t) n_0(t) = X_1(t) + h_{11,1}^*(t) n_0(t), \\ S_{21,1}(t) &= h_{12,1}^*(t) h_{12,1}(t) X_1(t) + h_{12,1}^*(t) n_1(t) = X_1(t) + h_{12,1}^*(t) n_1(t) \end{aligned} \quad (3.14)$$

where $h_{1l,i}^*$ denotes the complex conjugate of $h_{1l,i}$. At subsequent hops, the relays receive the following signals:

$$\begin{aligned} R_{1i,1}(t) &= h_{11,i}(t) \hat{X}_{1i-1,1}(t) + h_{21,i}(t) \hat{X}_{2i-1,1}(t) + n_{0i}(t), \\ R_{2i,1}(t) &= h_{12,i}(t) \hat{X}_{1i-1,1}(t) + h_{22,i}(t) \hat{X}_{2i-1,1}(t) + n_{1i}(t) \end{aligned} \quad (3.15)$$

for $i=2,3,\dots,N+1$, where n_{0i} and n_{1i} represent noise received at RMT_{1i} and RMT_{2i}, respectively. Finally mobile terminals apply coherent detection since the channel state information $\{h_{11,i}, h_{12,i}, h_{21,i}$ and $h_{22,i}\}$ is known in the receiver. At RMT_{1i} and RMT_{2i}, assuming that $\hat{X}_{1i-1,1}(t) = \hat{X}_1(t)$ and $\hat{X}_{2i-1,1}(t) = \hat{X}_1(t)$ in fair propagation conditions and substituting into (3.15) yields

$$\begin{aligned} R_{1i,1}(t) &= (h_{11,i}(t) + h_{21,i}(t)) \hat{X}_1(t) + n_{0i}(t), \\ R_{2i,1}(t) &= (h_{12,i}(t) + h_{22,i}(t)) \hat{X}_1(t) + n_{1i}(t) \end{aligned} \quad (3.16)$$

where the transmitted signals $\hat{X}_{1i,1}$ and $\hat{X}_{2i,1}$ are the reference signals, in the database of RMT_{1i-1} and RMT_{1i-2}, respectively; closest to intermediate signals $S_{11,1}(t)$ and $S_{21,1}(t)$.

Thus the intermediate symbols in the combiner of RMT_{1i} and RMT_{2i} are

$$\begin{aligned} S_{1i,1}(t) &= (h_{11,i}(t) + h_{21,i}(t))^* (h_{11,i}(t) + h_{21,i}(t)) \hat{X}_1(t) + (h_{11,i}(t) + h_{21,i}(t))^* n_{0i}(t) \\ &= \hat{X}_1(t) + (h_{11,i}(t) + h_{21,i}(t))^* n_{0i}(t) \end{aligned} \quad (3.17)$$

$$\begin{aligned} S_{2i,1}(t) &= (h_{12,i}(t) + h_{22,i}(t))^* (h_{12,i}(t) + h_{22,i}(t)) \hat{X}_1(t) + (h_{12,i}(t) + h_{22,i}(t))^* n_{1i}(t) \\ &= \hat{X}_1(t) + (h_{12,i}(t) + h_{22,i}(t))^* n_{1i}(t). \end{aligned}$$

The intermediate signals are then sent to the maximum likelihood detector, which makes the detection decision based on the distance to the reference signals as mentioned before. The decode-and-forward with cooperative diversity scheme presented here is a technique where relays do not make a choice whether they should relay or not; instead they are designated to relay even if they do not decode a correct input sequence. One enhancement that can be applied is the capability for the relay terminal RMT_{ji} to decide, based on channel state information at reception (CSIR), whether or not it is helpful for communication purposes to relay. In this case, for example, when the secondary relay terminal RMT_{2i} works under harsh conditions and decides not to relay, network performance degrades to the non-cooperative decode-and-forward scheme in Figure 15.

b. Bit Error Probability for Decode-and-forward with Cooperative Diversity

The probability that the destination correctly decodes the symbol is equal to the probability that at least one antenna decodes it correctly, hence the probability of symbol error is the probability that both reception antennas decode wrongly. The two-hop case is examined here to determine a lower bound for the bit error probability.

For BPSK in AWGN with power constraint P_{max} at all the terminals, from [42,43,44] for a channel with transmit or receive diversity of order $L=MN$, where M is the number of the transmitters and N the number of the receivers, the probability of error P_b can be expressed as

$$P_b = Q \left(\sqrt{\frac{2 \left| \sum_{i=1}^M \sum_{j=1}^N h_{ij} \right|^2 E_{b_{ij}}}{N_0}} \right), \quad (3.18)$$

where h_{ij} for $i=1, \dots, M$ and $j=1, \dots, N$, are the channel fading coefficients. Let $h_{ij} = 1$ for AWGN. Since diversity order $L=MN$, the probability of error in (3.18) can be simplified to

$$P_b = Q \left(\sqrt{\frac{2 \sum_{l=1}^L E_{b_l}}{N_0}} \right) \quad (3.19)$$

The probability that a relay RMT₁ does not decode correctly is denoted as P_b and can be calculated analogously from (3.19) for $L=1$ since in the link between the source and the RMT₁ there is no diversity gain

$$P_b = Q \left(\sqrt{\frac{2E_b}{N_0}} \right) = Q \left(\sqrt{2SNR_r} \right). \quad (3.20)$$

Finally in the destination terminal, a diversity order of $L=2$, the error probability of the second hop P_{bd} is obtained from (3.19):

$$P_{bd} = Q \left(2 \sqrt{\frac{E_b}{N_0}} \right) = Q \left(2\sqrt{SNR_r} \right). \quad (3.21)$$

For the calculation of the total error probability P_{bt} in the two-hop case, we use the sum of the error probabilities of all the possible cases, in accordance with the bit error probability of the decode-and-forward scheme:

$$P_{bt} = P_{bd}(1 - P_b)(1 - P_b) + (1 - P_{bd})P_bP_b + 1/2P_{bd}P_b(1 - P_b) + 1/2P_{bd}(1 - P_b)P_b$$

$$= P_{bd} (1 - P_b) + (1 - P_{bd}) P_b^2 \quad (3.22)$$

where P_b and P_{bd} are given by (3.20) and (3.21), respectively. There are four possible error cases included in (3.22). The last two terms in (3.22) are multiplied by a factor $\frac{1}{2}$ because the destination can wrongly decode the transmitted signals of the two relays in two equally probable ways, one of which leads to the correct decoding of the original transmitted symbols by the two sources.

Substituting (3.19) and (3.20) into (3.22) yields

$$P_{bt} = Q\left(2\sqrt{SNR_r}\right)\left(1 - Q\left(\sqrt{2SNR_r}\right)\right) + \left(1 - Q\left(2\sqrt{SNR_r}\right)\right)Q\left(\sqrt{2SNR_r}\right)^2 \quad (3.23)$$

where $SNR_r = P_s/P_n$ at the relay nodes.

c. Performance Evaluation of Decode-and-Forward with Cooperative Diversity in Rayleigh Fading Channel

In Figure 17 the bit error probability plot of BPSK for the decode-and-forward with cooperative diversity scheme is presented and compared with the two non-cooperative schemes decode-and-forward and amplify-and-forward. Figure 17 is obtained by simulating the schemes in Matlab for Rayleigh slow flat fading conditions. Since the network resources at each time slot are allocated to only one of the two SMTs, the performance of the two users is exactly the same in a slow fading environment. Thus, only one curve represents this scheme for both the users SMT₁ and SMT₂. The destination terminal exploits receive diversity and chooses to decode one of the two incoming signals at the antennas. For the simulation it is assumed that at all RMT₁s the reception SNR is 3 dB higher than at the RMT₂s, thus the upper part of Figure 15 has 3 dB higher SNR than the lower part. As expected the difference in performance of the two users is almost 3 dB for the non-cooperative schemes. The upper relays of the network do not cooperate with the lower relays in order to improve the performance of user SMT₂. Thus in order for at SMT₂ to achieve same error rate as SMT₁ it should increase transmission power by at least 3 dB.

The performance of the decode-and-forward with cooperative diversity falls between the performance of SMT₁ without diversity (upper bound) and that of SMT₂

without diversity (lower bound). For the cooperative diversity scheme it is obvious that the two users share the medium and achieve the same error rates which is an improvement over the non-cooperative case for user at SMT₂.

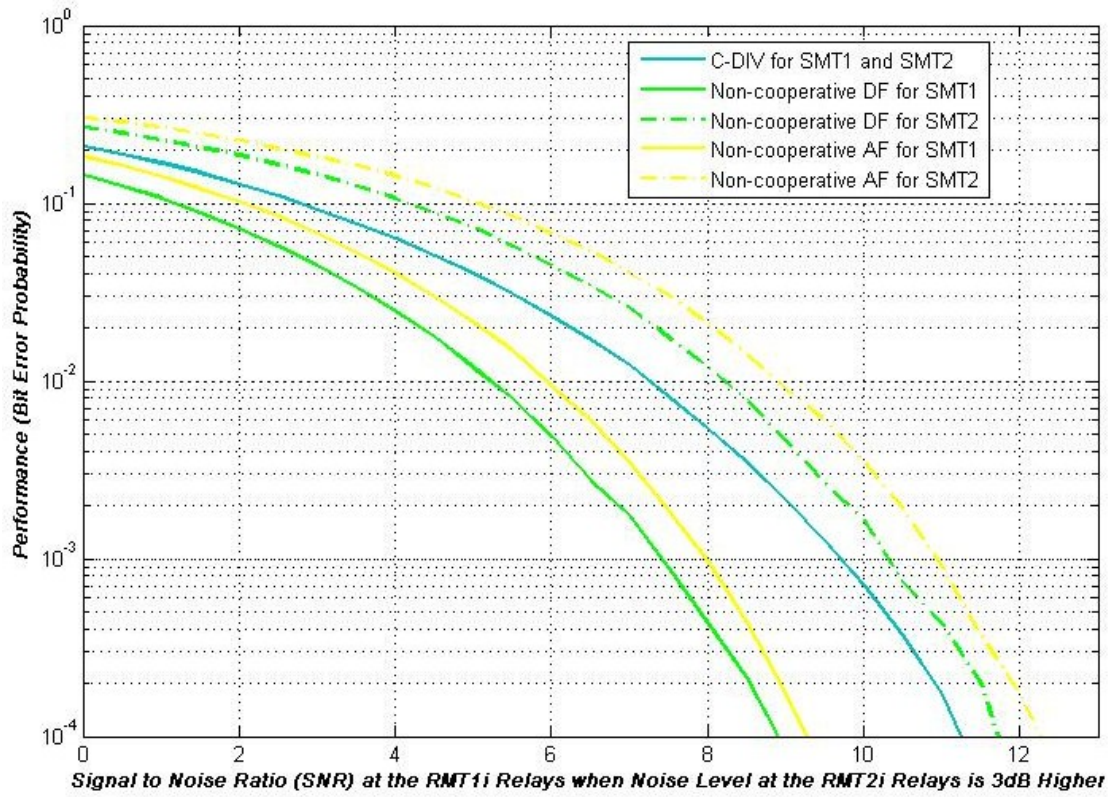


Figure 17. Performance of Two-hop C-DIV and Non-cooperative DF and AF Schemes for a SNR Difference between the Paths of 3 dB in Rayleigh Channel for BPSK.

The error rate for user at SMT₁ increases and the performance is almost 1.5 dB worse than the performance of SMT₁ for the non-cooperative cases. It must be noted that all antennas transmit under the same power constraint P_{max} for every symbol. Thus, for a multiple-hop case (except the two-hop), considering that in cooperative diversity the powers of the received signals are summed, meaning that the received signal power is twice the power of the received signal in the non-cooperative schemes, then in the Figure 17, the cooperative diversity must be plotted by doubling noise in comparison with the non-cooperative decode-and-forward and amplify-and-forward schemes. Hence

the results for decode-and-forward with cooperative diversity (C-DIV) in the multiple hop case are obtained, either for twice the noise level or half the transmitted signal power from each SMT. Thus, if one were to plot the bit error rate versus the absolute noise level for the multi-hop case, the curve for decode-and-forward with cooperative diversity (C-DIV) should be shifted by 3 dB to the left.

d. Decode-and-Forward with Cooperative Diversity in Frequency Selective Channel with ISI

In the frequency selective channel with intersymbol interference (ISI), block coding is used to demonstrate the interference. The frequency selective channel with ISI is depicted in Figure 18. The SMT₁ and SMT₂ transmission scheme is given by (3.1). For the data sequence X_1 , the first relays RMT₁₁ and RMT₂₁ receive

$$R_{11,l}(t) = h_{11,l}(q^{-1})X_1(t) + n_0(t), \quad (3.24)$$

$$R_{21,l}(t) = h_{12,l}(q^{-1})X_1(t) + n_1(t)$$

where $h(q^{-l})$ is given by (2.4). The intermediate signals in the decoder/combiner of RMT₁₁ and RMT₂₁ are

$$S_{11,l}(t) = h_{11,l}^*(q) R_{11,l}(t) = h_{11,l}^*(q) h_{11,l}(q^{-1})X_1(t) + h_{11,l}^*(q) n_0(t), \quad (3.25)$$

$$S_{21,l}(t) = h_{12,l}^*(q) R_{21,l}(t) = h_{12,l}^*(q) h_{12,l}(q^{-1})X_1(t) + h_{12,l}^*(q) n_1(t)$$

where n_0 and n_1 represent noise received at RMT₁₁ and RMT₂₁, respectively.

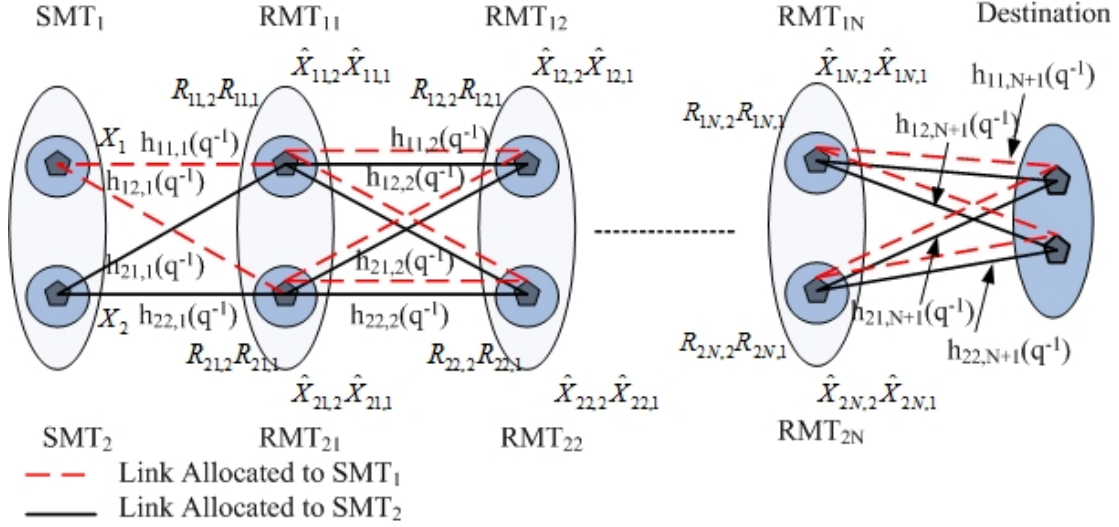


Figure 18. Cooperative Diversity Scheme in Multi-hop Frequency Selective Slow Fading Channel.

After the second hop, for the RMT_{1i} and RMT_{2i} the received signals generally are written as

$$R_{1i,1}(t) = h_{11,i}(q^{-1})\hat{X}_{1i-1,1}(t) + h_{21,i}(q^{-1})\hat{X}_{2i-1,1}(t) + n_{0i}(t), \quad (3.26)$$

$$R_{2i,1}(t) = h_{12,i}(q^{-1})\hat{X}_{1i-1,1}(t) + h_{22,i}(q^{-1})\hat{X}_{2i-1,1}(t) + n_{1i}(t)$$

where n_{0i} and n_{1i} represent noise received at RMT_{1i} and RMT_{2i} , respectively. Like the frequency flat fading case in (3.16), it is assumed that $\hat{X}_{1i-1,1}(t) = \hat{X}_1(t)$ and $\hat{X}_{2i-1,1}(t) = \hat{X}_1(t)$ considering that both are estimations of the same symbol. Hence, the received symbol equations can be written as follows:

$$R_{1i,1}(t) = (h_{11,i}(q^{-1}) + h_{21,i}(q^{-1}))\hat{X}_1(t) + n_{0i}(t), \quad (3.27)$$

$$R_{2i,1}(t) = (h_{12,i}(q^{-1}) + h_{22,i}(q^{-1}))\hat{X}_1(t) + n_{1i}(t).$$

The intermediate signals in the combiner of RMT_{1i} and RMT_{2i} are

$$\begin{aligned}
S_{1i,1}(t) &= (h_{11,i}(q) + h_{21,i}(q))^* R_{1i,1}(t) \\
&= (h_{11,i}(q) + h_{21,i}(q))^* (h_{11,i}(q^{-1}) + h_{21,i}(q^{-1})) \hat{X}_1(t) + (h_{11,i}(q) + h_{21,i}(q))^* n_{0i}(t),
\end{aligned} \tag{3.28}$$

$$\begin{aligned}
S_{2i,1}(t) &= (h_{12,i}(q) + h_{22,i}(q))^* R_{2i,1}(t) \\
&= (h_{12,i}(q) + h_{22,i}(q))^* (h_{12,i}(q^{-1}) + h_{22,i}(q^{-1})) \hat{X}_1(t) + (h_{12,i}(q) + h_{22,i}(q))^* n_{1i}(t).
\end{aligned}$$

Again, the intermediate signals are sent to the maximum likelihood detector, which makes the detection decision and estimates the signals $\hat{X}_{1i,1}$ and $\hat{X}_{2i,1}$ to be transmitted. In the destination terminal, the detector exploits the two signals to enhance signal strength for detection. The same equations describe the system when SMT₂ transmits. This scheme achieves a diversity order of four in each hop count when two mobile terminals relay the signal in every hop. The scheme can be expanded to a multi-terminal scheme by using more than two relaying terminals in the relay cluster. Finally, it must be noted that every transmitted symbol requires intra-cluster transmission-time synchronization.

3. Alamouti Cooperative Space-time Coding

The last scheme discussed will be the distributed implementation of the Alamouti space-time coding used in MIMO communication systems. The scheme presented here is single-carrier oriented but can be used with OFDM. Two cases of this coding scheme will be discussed. The first is when the short-range link, mentioned in Chapter II, in each cluster is used only for time-synchronization purposes, which is for the time being the more realistic scheme. The second case, named dual-antenna Alamouti cooperative space-time coding occurs when the intracluster cooperation includes co-processing between the mobile terminals. It is also the upper bound of cooperation of the single-antenna Alamouti cooperative space-time coding. The dual-antenna cooperative scheme presented here uses the equations of the 2×2 Alamouti space-time coding scheme discussed in Chapter II.

a. Alamouti Cooperative Space-time Coding Scheme in Flat Fading Channel

In Figure 19 the distributed Alamouti cooperative space-time coding scheme (C-STC) is presented, which depicts formation of multiple 2×1 parallel topologies due to cooperation in transmission and independence in reception, which is described later.

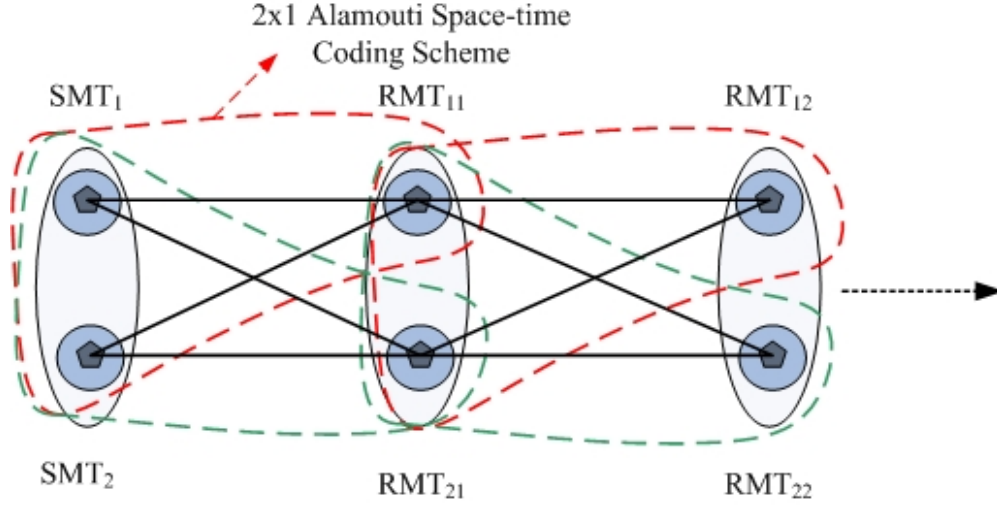


Figure 19. Application of Two Parallel 2-by-1 Distributed Alamouti Space-time Coding Schemes in Consecutive Hops Due to Non-cooperative Processing of Relays in Reception and Synchronization in Transmission.

The system performance between the two independent users SMT_1 and SMT_2 and the destination terminal is evaluated separately. Each cluster consists of two single-antenna mobile terminals. From the network establishment stage one of the two terminals is authorized to be the cluster leader. The criterion can be the channel state information or the SNR at reception. Each single-antenna mobile terminal decodes the input sequence independent from the other terminal of the cluster but relays in cooperation with it. Also, the transmitting terminals are synchronized and cooperate to achieve the space-time transmission sequence. Then, as can be observed in each hop the transmitting terminals form two 2×1 Alamouti cooperative space-time coding schemes. This type of cooperation cannot be achieved in the physical layer alone, but requires cross-layer information exchange with the network layer. Assuming that a mobile

terminal can determine the sender of the received sequences, and then, according to its hierarchy in the cluster, it can retransmit the proper sequence. Thus, the leader of the relay cluster transmits the decoded sequence that was initially transmitted by the leader of the previous relay cluster, and the secondary terminal of the relay cluster transmits the decoded sequence of the secondary terminal of the previous relay cluster.

We now develop the equations used for the frequency flat fading case.

Figure 20 shows the multi-relay scheme for flat fading conditions.

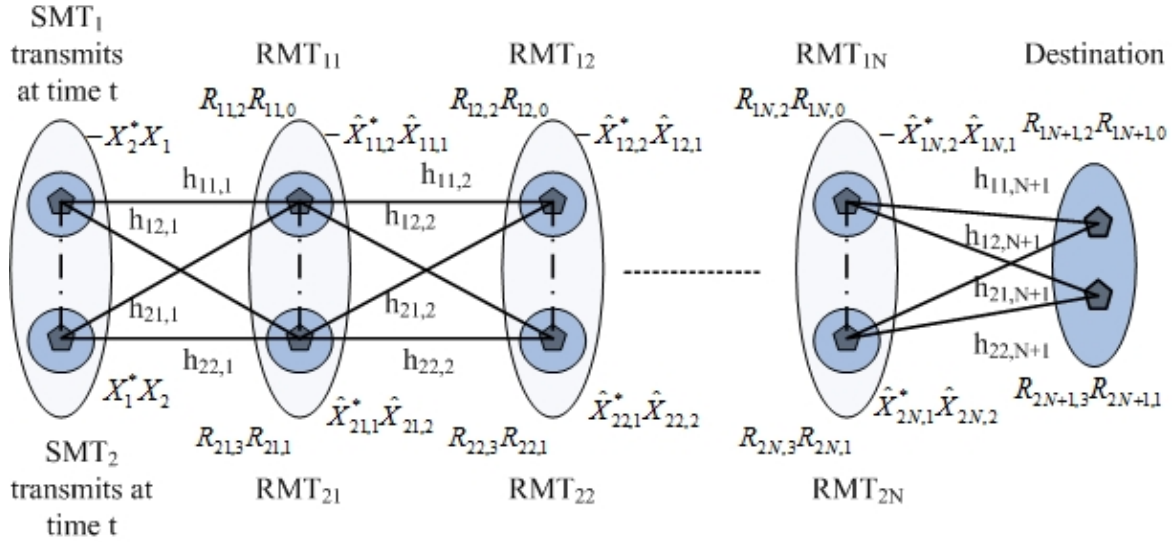


Figure 20. Alamouti Cooperative space-time coding Scheme in Multi-hop Frequency Flat Fading Channel.

The transmission scheme from SMT₁ and SMT₂ is given in Table 2. Note that for flat fading conditions we do not use block coding algorithms.

	SMT ₁	SMT ₂
time t	X_1	X_2
time $t + T$	$-X_2^*$	X_1^*

Table 2. Transmission Sequence for the Dual-Antenna Distributed Alamouti Scheme.

From [17], we make the following assumption:

$$\begin{aligned} h_{11,1}(t) &= h_{11,1}(t+T), \\ h_{21,1}(t) &= h_{21,1}(t+T) \end{aligned} \quad (3.29)$$

where T is the symbol period. As previously mentioned, two 2×1 schemes are formed in the first hop and the relays RMT11 and RMT21 independently decode the incoming sequences $[R_{11,2}, R_{11,0}]$ and $[R_{21,3}, R_{21,1}]$, respectively. The received signals at RMT11 for time instances t and $t+T$ are like the 2×1 MIMO Alamouti case described in Chapter II given by [3]

$$R_{1i,0}(t) = h_{11,i}(t)X_{1i-1,1}(t) + h_{21,i}(t)X_{2i-1,2}(t) + n_{0i}(t), \quad (3.30)$$

$$R_{1i,2}(t) = -h_{11,i}(t)X_{1i-1,2}^*(t) + h_{21,i}(t)X_{2i-1,1}^*(t) + n_{1i}(t)$$

for $i=1$, where n_{01} and n_{11} represent noise at the receiver RMT11 at the first and second transmission periods. The decoded signals are calculated in the combiner of RMT11 as follows:

$$\hat{X}_{1i,1}(t) = h_{11,i}^*(t)R_{1i,0}(t) + h_{21,i}(t)R_{1i,2}^*(t), \quad (3.31)$$

$$\hat{X}_{1i,2}(t) = h_{11,i}^*(t)R_{1i,0}(t) - h_{21,i}(t)R_{1i,2}^*(t)$$

for $i=1$. Estimated symbols are then sent to the maximum likelihood detector. Each relay, namely RMT₁₁ and RMT₂₁, makes separate estimations $[\hat{X}_{11,2}(t), \hat{X}_{11,1}(t)]$ and $[\hat{X}_{21,2}(t), \hat{X}_{21,1}(t)]$. Relays transmit their sequences synchronously [7]. Therefore, at the k^{th} cluster the input sequences at RMT_{1k} and RMT_{2k} are given by (3.30) for $i=k$, and the decoded symbols are given by (3.31) for $i=k$.

Finally, since the destination terminal is a dual-antenna device, the 2×2 distributed Alamouti coding scheme can be used at the final reception. The equations for this step are same as those presented for the MIMO 2×2 case in Chapter II. The received signals at receive antenna 1 of destination are

$$R_{1N+1,0}(t) = h_{11,N+1}(t)X_{1N,1}(t) + h_{21,N+1}(t)X_{2N,2}(t) + n_{0N+1}(t), \quad (3.32)$$

$$R_{1N+1,2}(t) = -h_{11,N+1}(t)X_{1N,2}^*(t) + h_{21,N+1}(t)X_{2N,1}^*(t) + n_{1N+1}(t)$$

and receive antenna 2 of destination the received signals are

$$R_{2N+1,1}(t) = h_{12,N+1}(t)X_{1N,1}(t) + h_{22,N+1}(t)X_{2N,2}(t) + n_{0N+1}(t), \quad (3.33)$$

$$R_{2N+1,3}(t) = -h_{12,N+1}(t)X_{1N,2}^*(t) + h_{22,N+1}(t)X_{2N,1}^*(t) + n_{1N+1}(t)$$

where n_{0N+1} and n_{1N+1} represent noise on the receive antennas at time instances t_1 and t_1+T , respectively. The estimates of the signals are calculated in the decoder/ combiner as follows:

$$\begin{aligned} \hat{X}_{1N+1}(t) = & h_{11,N+1}^*(t)R_{1N+1,0}(t) + h_{21,N+1}(t)R_{1N+1,2}^*(t) + \\ & h_{11,N+1}^*(t)R_{2N+1,1}(t) + h_{21,N+1}(t)R_{2N+1,3}^*(t), \end{aligned} \quad (3.34)$$

$$\begin{aligned} \hat{X}_{2N+1}(t) = & h_{12,N+1}^*(t)R_{1N+1,0}(t) - h_{22,N+1}(t)R_{1N+1,2}^*(t) + \\ & h_{12,N+1}^*(t)R_{2N+1,1}(t) - h_{22,N+1}(t)R_{2N+1,3}^*(t). \end{aligned}$$

The destination terminal decodes symbols using a maximum likelihood detector.

b. Bit Error Probability of Alamouti Cooperative Space-time Coding Scheme

The theoretical bit error probability of BPSK for distributed Alamouti space-time coding scheme in an AWGN two-hop fading environment is derived here. The work is based on related research done in [49] for a dual-antenna remote telemetry transmission scheme with one reception antenna at destination. Similar work is also reported by other researchers [45, 46, 47]. From [42, 43] the bit error probability in AWGN for two transmission antennas and one reception antenna is given by (3.21). Hence the single-hop Alamouti space-time scheme provides the same bit error probability as the decode-and-forward with cooperation. This is expected as the schemes achieve the same diversity order in the reception. However, for Rayleigh fading, the Alamouti cooperative space-time coding performs better since the squares of the fading coefficients

and not the coefficients themselves are added in (3.19). Thus the error probability P_{br} , in relay RMT_j , $j=1,2$ is given by (3.21) for $L=2$. Additionally, in the second hop the 2×2 Alamouti scheme provides twice the diversity gain. Thus the bit error probability at the destination, P_{bd} is given by (3.21) for $L=4$. The total error probability P_{bt} of the scheme consists of four different terms as in (3.22). Considering the same fading conditions and SNRs at both hops, the total error probability is given by

$$\begin{aligned} P_{bt} &= P_{bd}(1 - P_{br})(1 - P_{br}) + 1/2 P_{bd} P_{br}(1 - P_{br}) + 1/2 P_{bd}(1 - P_{br}) P_{br} + (1 - P_{bd}) P_{br} P_{br} \\ &= P_{bd} - P_{bd} P_{br} - P_{bd} P_{br}^2 + P_{br}^2. \end{aligned} \quad (3.35)$$

Substituting P_{br} and P_{bd} from (3.19) for $L=2$ and $L=4$, respectively, into (3.35) yields

$$\begin{aligned} P_{bt} &= Q\left(2\sqrt{\frac{2E_{b_i}}{N_0}}\right) + Q\left(2\sqrt{\frac{E_{b_i}}{N_0}}\right)^2 - Q\left(2\sqrt{\frac{2E_{b_i}}{N_0}}\right)Q\left(2\sqrt{\frac{E_{b_i}}{N_0}}\right) \\ &\quad - Q\left(2\sqrt{\frac{2E_{b_i}}{N_0}}\right)Q\left(2\sqrt{\frac{E_{b_i}}{N_0}}\right)^2. \end{aligned} \quad (3.36)$$

Finally substituting (3.5) into (3.36) yields

$$\begin{aligned} P_{bt} &= Q\left(2\sqrt{(SNR_r)}\right) + Q\left(\sqrt{2(SNR_r)}\right)^2 - Q\left(2\sqrt{(SNR_r)}\right)Q\left(\sqrt{2(SNR_r)}\right) \\ &\quad - Q\left(2\sqrt{(SNR_r)}\right)Q\left(\sqrt{2(SNR_r)}\right)^2 \end{aligned} \quad (3.37)$$

where SNR_r at the relay is $2E_b / N_0$ (see (3.6)). The plots of theoretical bit error probabilities for the aforementioned schemes for BPSK in AWGN conditions are depicted in Figure 21. It can be observed that both cooperative schemes achieve exactly the same performance, measured in bit error probability. This was expected since for AWGN formulas both these schemes are the same and from knowledge that space-time coding compensates for the effect of propagation and not noise at reception. The performance of the cooperative schemes has improved by 1 dB compared to the decode-and-forward and almost by 2 dB compared to the non-cooperative amplify-and-forward.

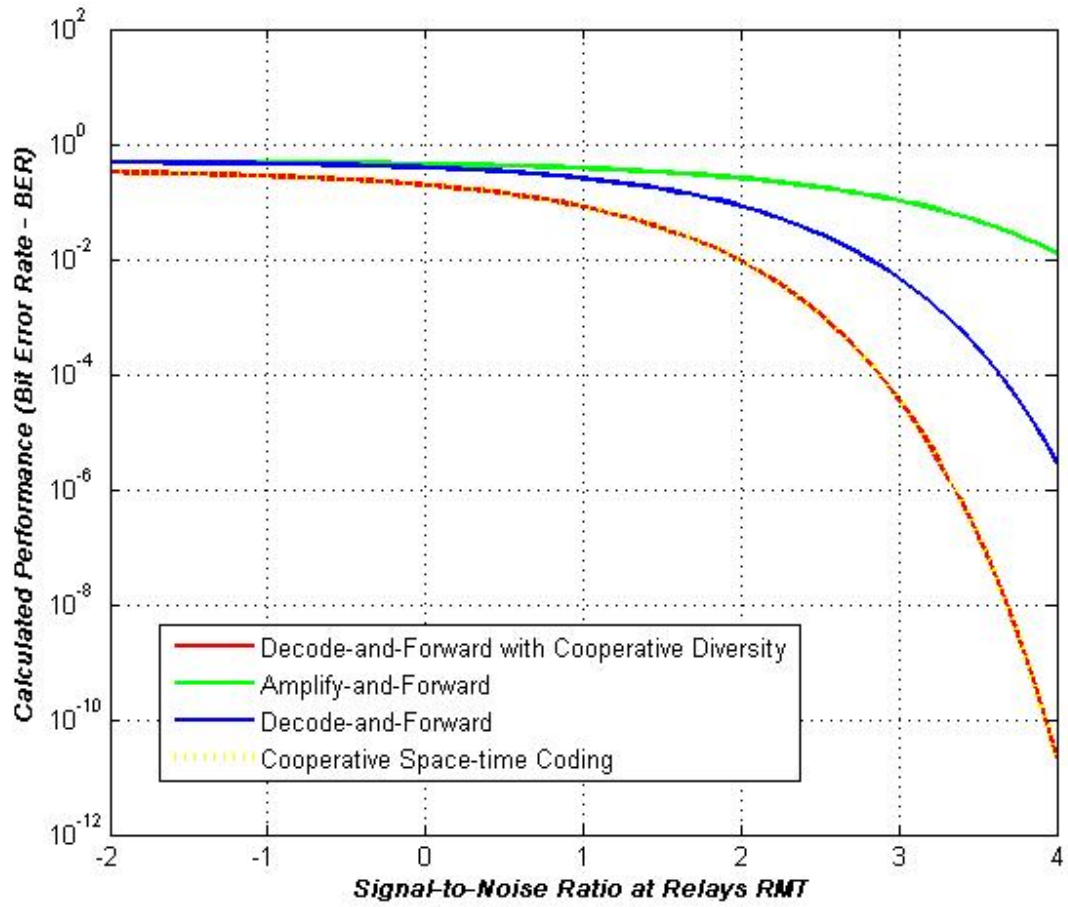


Figure 21. Calculated Performances of Alamouti Cooperative Space-time Coding, Decode-and-Forward with Cooperative Diversity, Decode-and-Forward and Amplify-and-Forward Schemes in AWGN for BPSK in the Two-hop Relaying Network.

c. Alamouti Cooperative Space-time Coding Scheme in Frequency Selective Channel

For the frequency selective fading case the system is depicted in Figure

22.

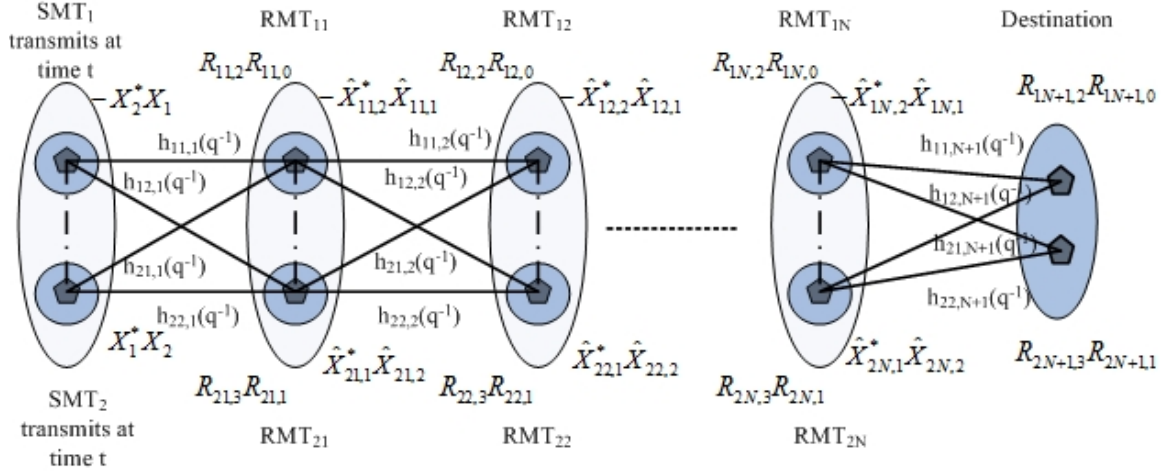


Figure 22. Alamouti Cooperative space-time coding Relaying Scheme in Multi-hop Frequency Selective Fading Channel.

The transmission sequence is given in Table 2, where X_1 and X_2 are given by (3.1). Relays RMT11 and RMT21 independently decode the incoming sequences $[R_{11,2}, R_{11,0}]$ and $[R_{21,3}, R_{21,1}]$, respectively. Channel coefficients remain the same for all frame transmission periods. The received signals at RMT11 are given by

$$R_{li,0}(t) = h_{1i,1}(q^{-1})X_{li-1,1}(t) + h_{2i,1}(q^{-1})X_{2i-1,2}(t) + n_{0i}(t), \quad (3.38)$$

$$R_{li,2}(t) = -h_{1i,1}(q^{-1})X_{li-1,2}^*(t) + h_{2i,1}(q^{-1})X_{2i-1,1}^*(t) + n_{li}(t)$$

for $i=1$, where n_{0i} and n_{li} represent noise at the receiver RMT11 in time periods $[t, t+NT]$ and $[t+NT, t+2NT]$, respectively and N is the number of symbols in the transmitted frame and T is the symbol period. The RMT11 decoder calculates the estimations of the input signals

$$\hat{X}_{li,1}(t) = h_{li,1}^*(q)R_{li,0}(t) + h_{2i,1}(q^{-1})R_{li,2}^*(t), \quad (3.39)$$

$$\hat{X}_{li,2}(t) = h_{li,1}^*(q)R_{li,0}(t) - h_{2i,1}(q^{-1})R_{li,2}^*(t)$$

for $i=1$, where $h(q)$ represents an anti-causal channel filter. As a result, mobile terminal RMT12 estimates $\hat{X}_{21,1}(t)$ and $\hat{X}_{21,2}(t)$. At the k th cluster the input sequences for terminal RMT1i are given by (3.38) for $i=k$. The symbols estimated in the combiner of RMT1k

are given by (3.39) for $i=k$. Estimations are then made into the maximum likelihood decoder. Finally, at destination the input signals, at the receive antenna 1 are

$$R_{1N+1,0}(t) = h_{11,N+1}(q^{-1})X_{1N,1}(t) + h_{21,N+1}(q^{-1})X_{2N,2}(t) + n_{0N+1}(t), \quad (3.40)$$

$$R_{1N+1,2}(t) = -h_{11,N+1}(q^{-1})X_{1N,2}^*(t) + h_{21,N+1}(q^{-1})X_{2N,1}^*(t) + n_{1N+1}(t)$$

where n_{0N+1} and n_{1N+1} represent noise at the destination antennas. At receive antenna 2 the received signals are

$$R_{2N+1,1}(t) = h_{12,N+1}(q^{-1})X_{1N,1}(t) + h_{22,N+1}(q^{-1})X_{2N,2}(t) + n_{0N+1}(t), \quad (3.41)$$

$$R_{2N+1,3}(t) = -h_{12,N+1}(q^{-1})X_{1N,2}^*(t) + h_{22,N+1}(q^{-1})X_{2N,1}^*(t) + n_{1N+1}(t).$$

The combiner estimates the symbols and then a maximum likelihood decoder decodes them as follows:

$$\begin{aligned} \hat{X}_{1N+1}(t) = & h_{11,N+1}^*(q)R_{1N+1,0}(t) + h_{21,N+1}(q^{-1})R_{1N+1,2}^*(t) + \\ & h_{11,N+1}^*(q)R_{2N+1,1}(t) + h_{21,N+1}(q^{-1})R_{2N+1,3}^*(t), \end{aligned} \quad (3.42)$$

$$\begin{aligned} \hat{X}_{2N+1}(t) = & h_{12,N+1}^*(q)R_{1N+1,0}(t) - h_{22,N+1}(q^{-1})R_{1N+1,2}^*(t) + \\ & h_{12,N+1}^*(q)R_{2N+1,1}(t) - h_{22,N+1}(q^{-1})R_{2N+1,3}^*(t). \end{aligned}$$

A critical issue addressed in [7] is how the receiver combines the incoming streams arriving from different paths with different phases. This problem is common in all the schemes that exploit transmission diversity, such as decode-and-forward with cooperative diversity and Alamouti cooperative space-time coding. Generally, in these schemes the transmission for the two transmitters in a relay cluster is not simultaneous [7]. The receivers, in the establishment stage of the network, inform transmitting terminals with what time difference they should transmit, in order that the signals arrive simultaneously for reception at the destination.

d. Performance Evaluation of Cooperative Alamouti Space-time Coding in Rayleigh Fading Channel

In Figure 23 the performance of Alamouti cooperative space-time coding (C-STC) scheme is compared to that of decode-and-forward with cooperative diversity (C-DIV), non-cooperative decode-and-forward (DF) and non-cooperative amplify-and-forward (AF) schemes. The simulation was run for BPSK modulated streams in a Rayleigh flat fading environment. The blue lines represent the performances of the Alamouti cooperative space-time coding scheme and the red lines are the dual-antenna Alamouti cooperative space-time coding (DC-STC). This scheme is for dual-antenna terminals and thus uses a 2×2 Alamouti space-time coding scheme, as described in Chapter II.

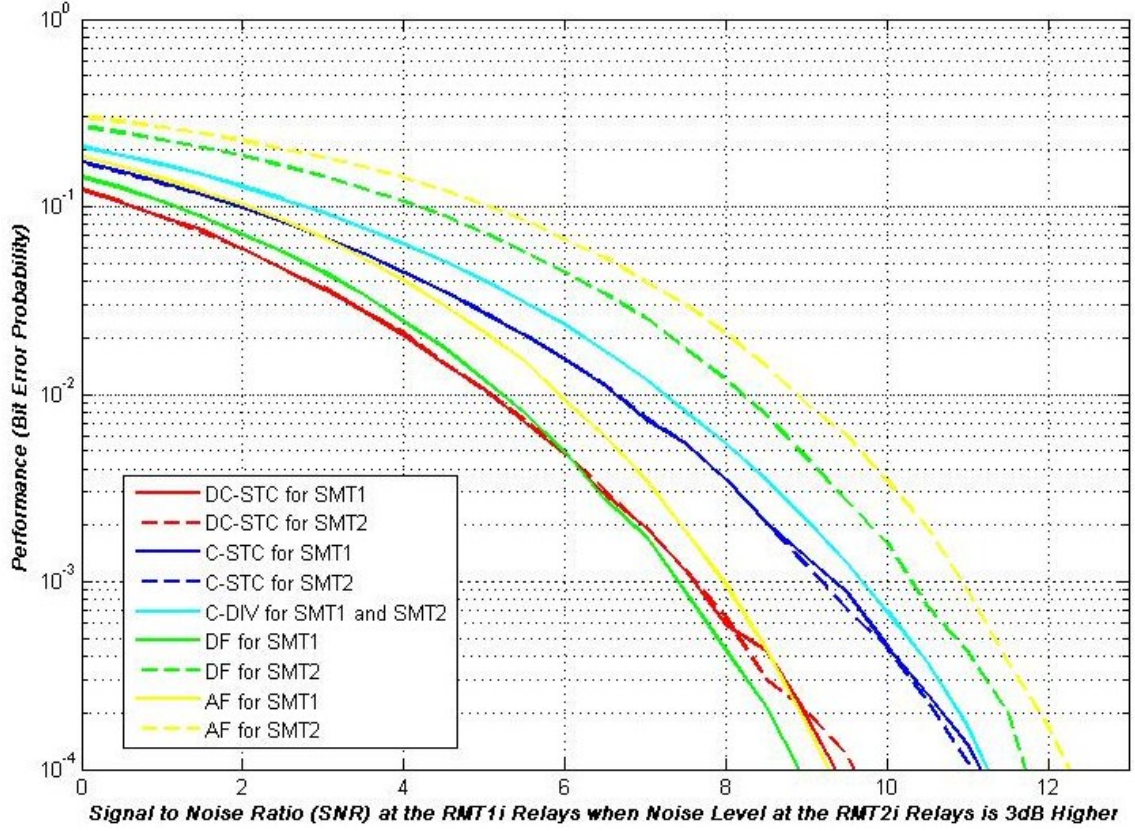


Figure 23. Performance of Two-hop Cooperative C-STC and C-DIV and Non-cooperative DF and AF Schemes for a SNR Difference between the Paths of 3 dB in Rayleigh Channel for BPSK.

Relays, RMT_{1i} have a 3 dB higher SNR than RMT_{2i} . In Alamouti cooperative space-time coding the medium is equally shared by the two users. The effect of this cooperation can be observed in Figure 23 where their performances are almost equal for low SNRs and very close for higher SNRs. It is clear that user SMT_2 with Alamouti cooperative space-time coding can improve its performance almost by 3 dB compared to the non-cooperative schemes, and close to 2 dB compared to the cooperative diversity scheme. Like in the case of decode-and-forward with cooperative diversity, considering the noise level and not SNR at reception, plots can be shifted to the left another 3 dB.

C. SUMMARY

In this chapter, the formulas describing the cooperative diversity scheme and the Alamouti space-time coding scheme were presented and will be used to obtain simulation results in the next chapter. Additionally expressions for the probabilities of error were derived for BPSK in AWGN for decode-and-forward, amplify-and-forward, cooperative diversity and Alamouti space-time coding schemes and presented as plots (see Figure 21). The next chapter will present the simulation results for MPSK and M-QAM signals. The slow frequency selective fading channels are also simulated using Stanford University Interim (SUI) channel models.

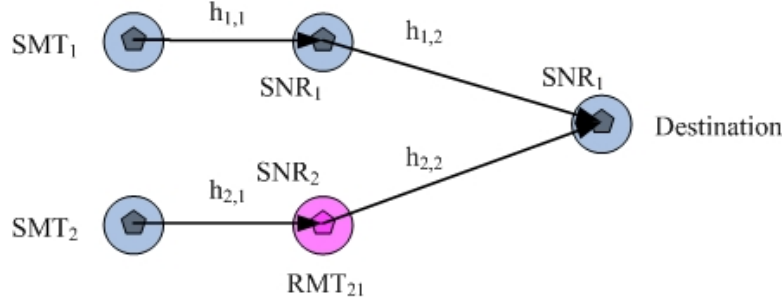
IV. SIMULATION RESULTS

This chapter completes the work done in Chapter III by simulating the discussed schemes with Matlab software. Specifically, this chapter presents the performance results and makes comparisons between decode-and-forward, amplify-and-forward, decode-and-forward with cooperative diversity and cooperative Alamouti space-time coding schemes. Also dual-antenna Alamouti cooperative space-time coding scheme is included for comparison. The results are divided based on the modulation scheme. The first set of results presented is for the phase modulation, such as BPSK and QPSK and the next set of results is for quadrature amplitude modulation (QAM) schemes, specifically 16-QAM and 64-QAM. The work is concentrated on the dual-hop case, but in BPSK and QPSK cases the results are expanded to six hops. Finally, since amplify-and-forward relaying scheme always performs worse than decode-and-forward relaying scheme, it will not be discussed further on.

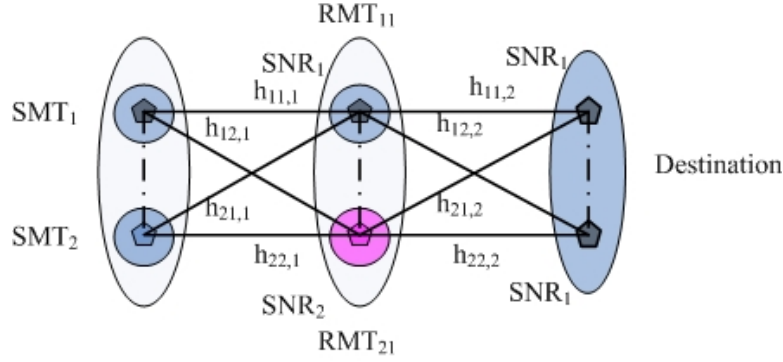
A. SIMULATION MODEL

The simulation goal was to reach a bit error probability of at most 10^{-4} . The Monte Carlo averaging method is used for the simulation. The flat fading scenario was simulated using Rayleigh fading model and in that case a simulation run consisted of at least *1,000,000* coded symbol transmissions for each nominal signal-to-noise ratio (SNR) value and the results are averaged using 10 runs. The outdoor frequency selective fading scenarios are simulated using SUI1, SUI3, and SUI6 channel models with frames of *200* symbols being transmitted. Thus a simulation for a nominal SNR value consisted of $1,000,000/200=5000$ frame transmissions. SUI channel models, discussed in Appendix A, simulate three common types of residential terrains found across the United States (types A, B and C) [48]. SUI1 is simulating a light channel scenario and SUI3 and SUI6 are for simulating to be very harsh propagation scenarios based on tables given in Appendix A. Since channel coefficients, in simulation, remain the same for two consecutive frame transmissions, channels are characterized as slow channels.

The simulation code used in this work is presented in Appendix B. The two-hop topologies that are examined in this work are depicted in Figure 24. In Figure 24(a) is the non-cooperative topology and in Figure 24(b) is the cooperative topology. The simulated multiple hops topologies, examined later, are an extension of the two-hop topologies. All wireless terminals in simulation have single omni-directional antennas, though the ‘Dualhop.m’ Matlab file in Appendix B provides the choice to obtain directivity with the antennas. This is because the specific part of code that simulates the SUI fading channels was taken and modified in [21]. All antenna elements are considered to be uncorrelated, thus in ‘Dualhop.m’ parameters ρ_{tx} and ρ_{rx} are set to zero. The relaying terminals are divided into two sets based on the noise level at their reception antennas. In Figure 24, the terminals in blue color have SNR1 at reception and those in magenta have SNR2. This is done to account for the different conditions in the paths for user SMT1 and user SMT2. In the simulation the difference in SNR between blue and magenta wireless terminals is 3 dB. Both SMTs have equal symbol transmission power P_{max} . Figures present the symbol error probability and not the bit error probability because of the different modulation schemes in use.



(a) Non-cooperative Two Hop Scheme



(b) Cooperative Two Hop Scheme

Figure 24. Relay Schemes for Simulation. (a) Non-cooperative Two Hop (b) Cooperative Two Hop Scheme.

B. SIMULATION RESULTS FOR BPSK AND QPSK

The simulated BPSK and QPSK constellation values under the power constraint $P_{max} = \frac{1}{2} = 0.5$, resulting in a total power constraint for the two sources equal to one, are

$$BPSK : X_{1,2}(t) = \pm \frac{1}{\sqrt{2}} = \left[\frac{1}{\sqrt{2}}, -\frac{1}{\sqrt{2}} \right], \quad (4.1)$$

$$QPSK : X_{1,2}(t) = (\pm 1 \pm j) / 2 = \left[\frac{1+j}{2}, \frac{1-j}{2}, \frac{-1+j}{2}, \frac{-1-j}{2} \right].$$

1. BPSK in Rayleigh Channel

Figures 25, 26 and 27 show the performances of the relaying schemes in Rayleigh channel and an SNR difference between the two paths of 0 dB, 5 dB, and 9 dB,

respectively; the SNR in RMT_2 (SNR_2), as depicted in Figure 24, is lower than the SNR at RMT_1 (SNR_1) by these values. For the two non-cooperative schemes the performance difference between SMT_1 and SMT_2 increases linearly with the SNR difference and remains zero for the cooperative schemes.

In Figure 25, where the SNR difference between the two paths is 0 dB, the non-cooperative decode-and-forward (DF) reaches the target probability of 10^{-4} for SNR_1 around 9 dB. Decode-and-forward with cooperative diversity (C-DIV) performs same as the DF scheme. This happens because conditions in both paths are the same and thus no spatial diversity advantage exists. Alamouti cooperative space-time coding (C-STC) outperforms the other schemes by 0.5 dB at the target probability of 10^{-4} in the lower SNR region and performs close to that of the C-DIV in the higher SNR region. However, considering that the performance of C-STC can be shifted by 3 dB at the target probability of 10^{-4} (see Chapter III) to the left, its performance is better by at least 3.5 dB in the lower SNR region and 4 dB in the higher SNR region compared to the other schemes; hence, keeping the error probability the same, potentially the terminals achieve energy savings (up to 50%) when they cooperate. On the other hand, by keeping the same transmission power the terminals can extend coverage ranges at each hop up to $\sim 20\%$ in an urban area cellular radio environment (where path loss exponent is from 2.7 to 3.5), based on the log-distance path loss model [59]. The performance difference for users SMT_1 and SMT_2 in C-STC is zero and remains such in all the simulation scenarios. Finally, the dual-antenna Alamouti cooperative space-time coding (DC-STC) performs 3 dB better than C-STC at the target probability of 10^{-4} .

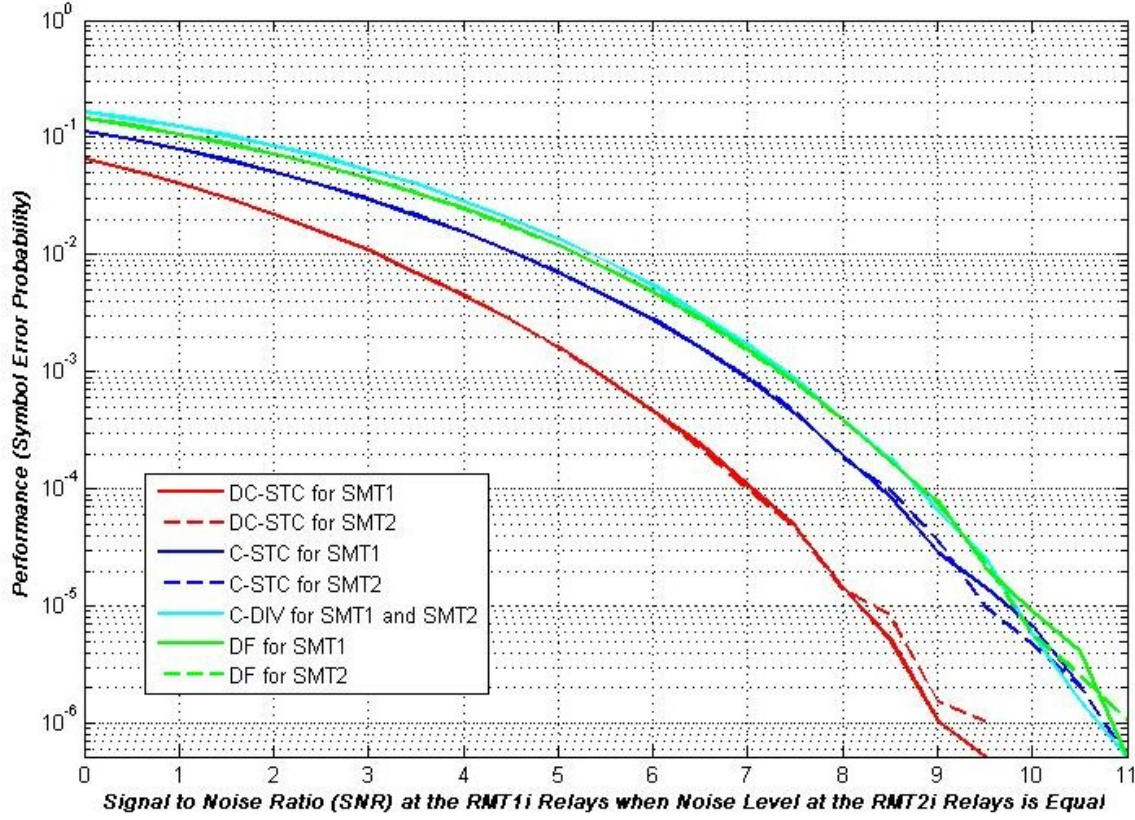


Figure 25. Performance of Two-hop Cooperative C-STC, C-DIV and Non-cooperative DF Schemes for a SNR Difference between the Paths of 0 dB in Rayleigh Channel for BPSK.

In Figures 26 and 27, we notice that C-DIV scheme performance remains good as the SNR difference between the two paths increases and, along with DF for SMT₁, provides the best error probability performance. This comes at the cost of doubling the transmitted power since two relays transmit simultaneously the same signal. By reducing the transmission energy of the relays by one half, the C-DIV error probability plots, in Figures 26 and 27, are shifted to the right but are still better, in the cases of high SNR difference between the two paths, compared to the other schemes except for the case of DF for SMT₁.

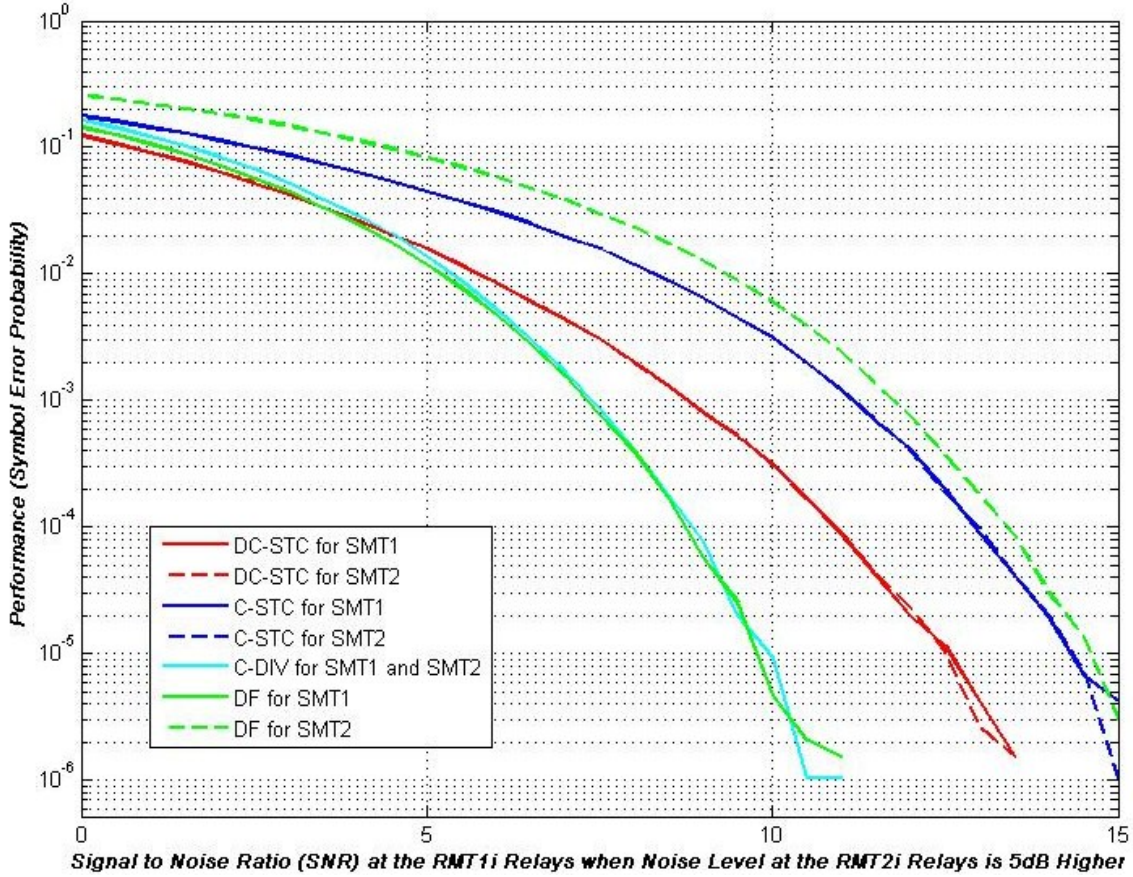


Figure 26. Performance of Two-hop Cooperative C-STC, C-DIV and Non-cooperative DF Schemes for a SNR Difference between the Paths of 5 dB in Rayleigh Channel for BPSK.

In Figure 27, when the 3 dB shift for C-STC is taken into account, its performance is better than that of SMT₂ but worse than that of SMT₁ in the DF scheme. As the SNR difference increases, the C-STC performance does not improve as the C-DIV performance and is closer to the performance of SMT₂ in the DF. Yet C-STC, as C-DIV does, shares energy consumption equally among all transmitters in contrast to the DF scheme where the secondary path's transmitters consume more power in order to achieve the same target error probability with the transmitters of the path with the higher SNR. Hence, as in Figure 25 where the SNR difference was set to zero, in the case of high SNR difference between the paths, the cooperative schemes reallocate the power resources of the relaying system in a manner that extends the lifetime of the relays of the SNR₂ path.

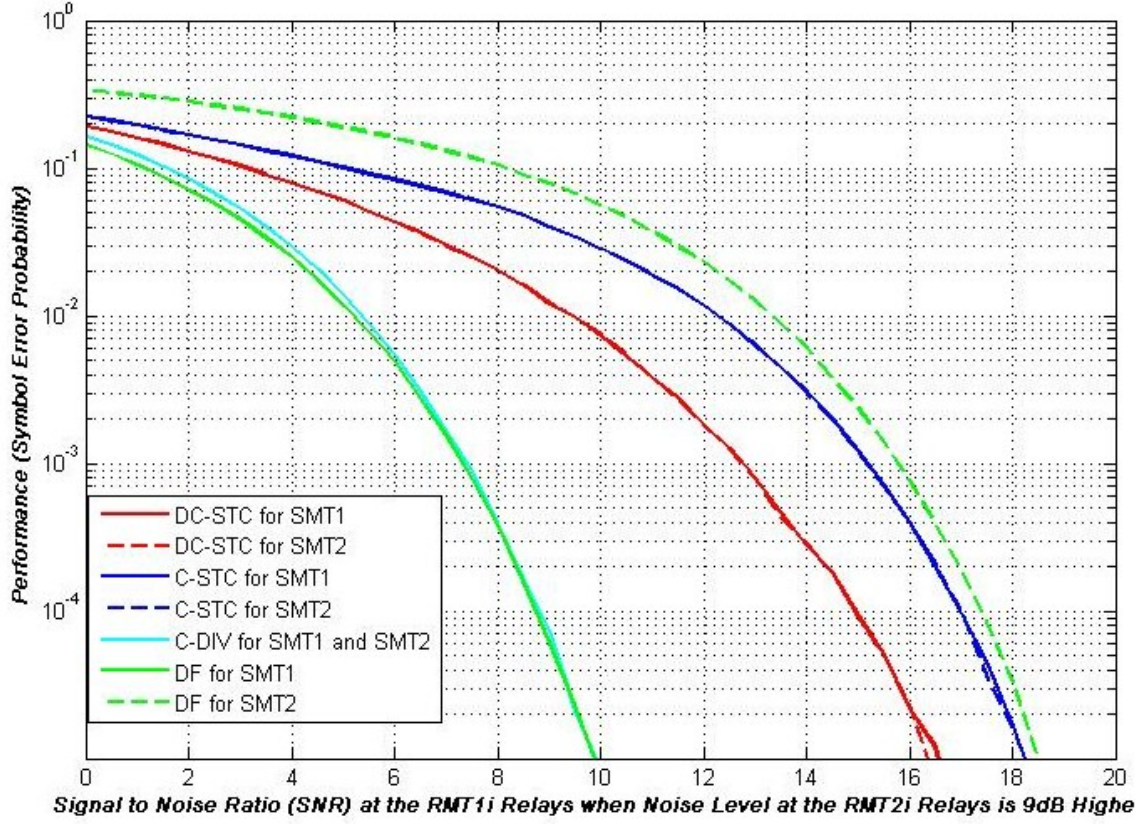


Figure 27. Performance of Two-hop Cooperative C-STC, C-DIV and Non-cooperative DF Schemes for a SNR Difference between the Paths of 9 dB in Rayleigh Channel for BPSK.

2. BPSK in SUI Channels

In Figure 28 the performances of users SMT_1 and SMT_2 in the SUI1 channel (terrain type 'A'), described in Appendix A, and for an SNR difference of 3 dB between paths are shown. In comparison with Figure 23, for the Rayleigh fading with 3 dB SNR difference, the performances of all the schemes are worse with the exception of DC-STC. In the lower SNR ($SNR < 10$ dB) region of the figure the performance plots of the two users, for the DF scheme, have a difference of approximately 2 dB, and the C-STC performance is approximately in the middle of the two non-cooperative DF users. For SNRs higher than 12 dB the performances of DF and C-DIV saturate slightly above the target probability of 10^{-4} .

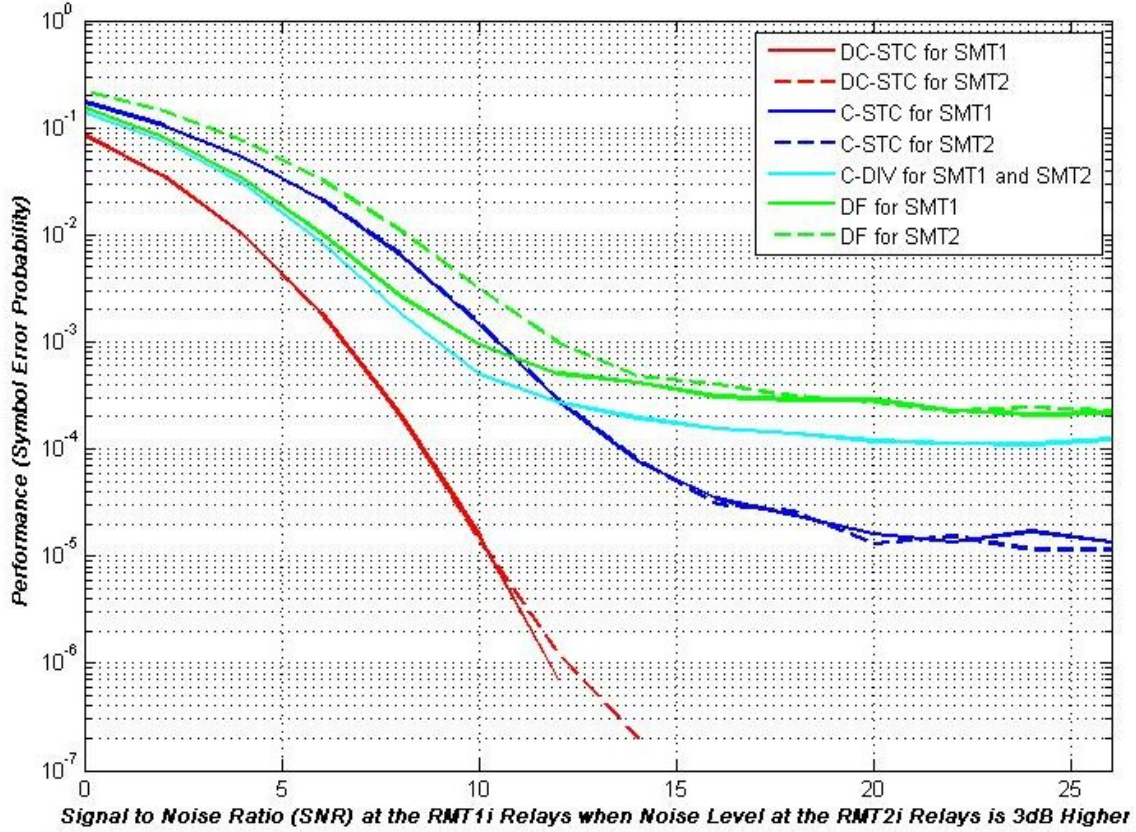


Figure 28. Performance of Two-hop Cooperative C-STC, C-DIV and Non-cooperative DF Schemes for a SNR Difference between the Paths of 3 dB in SUI1 Channel for BPSK.

The C-STC error probability continues to fall, providing a performance difference of 8 dB over the C-DIV at the target probability of 10^{-4} (11 dB in terms of SNR per signal). The DC-STC error probability also falls rapidly. Though terrain ‘A’ is a dense urban terrain, the SUI1 model is a light interference model for this terrain where the secondary paths of the channel have small delays and even smaller relative powers than the main path. The SUI3 and SUI6 models, as mentioned earlier, have stronger secondary paths, and thus the overall error probabilities for all the relaying schemes are in higher levels.

In a SUI3 environment the C-STC performance is degraded as can be observed in Figure 29. None of the schemes approached the target probability of 10^{-4} for SNR lower than 20 dB. The DC-STC outperforms all others but only reaches a 10^{-2} error probability for SNR greater than 13 dB.

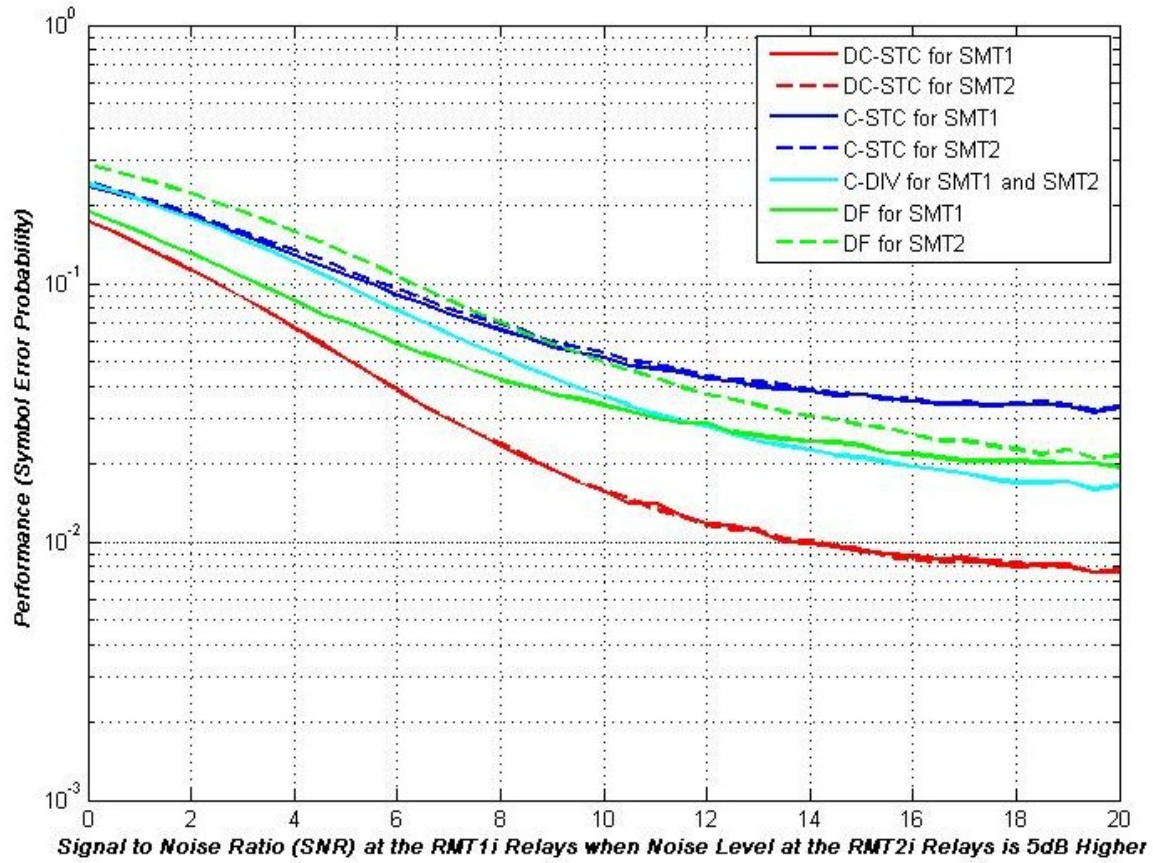


Figure 29. Performance of Two-hop Cooperative C-STC, C-DIV and Non-cooperative DF Schemes for a SNR Difference between the Paths of 3 dB in SUI3 Channel for BPSK.

Figure 30 presents the error performance results in a SUI6 channel. SUI6 represents type ‘C’ terrain (see Appendix A.) which is a light obstacle density terrain. All schemes perform slightly better than in SUI3 and for high SNRs the performances converge at a probability close to 10^{-2} . The C-STC scheme has improved performance and the DC-STC has outperformed the other techniques.

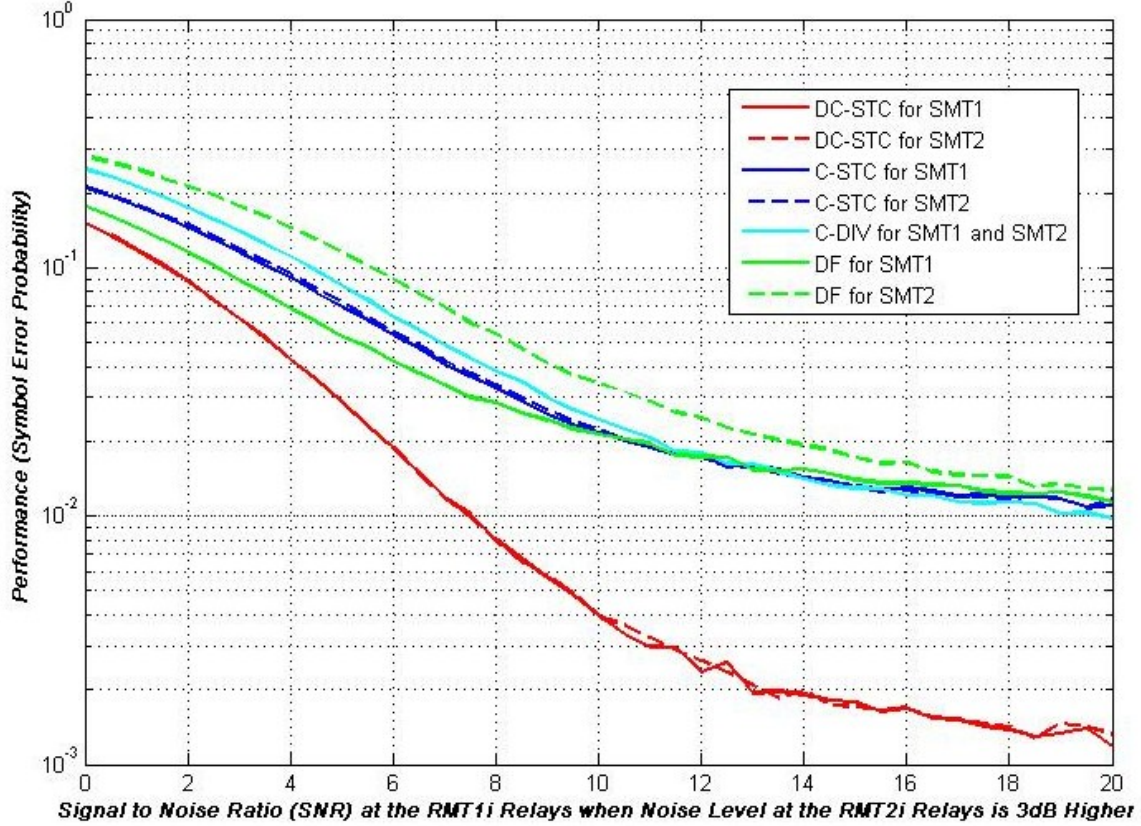


Figure 30. Performance of Two-hop Cooperative C-STC, C-DIV and Non-cooperative DF Schemes for a SNR Difference between the Paths of 3 dB in SUI6 Channel for BPSK.

3. QPSK in Rayleigh Channel

We now extend the simulation to include QPSK in Rayleigh and SUI channels. Figure 31 presents results for QPSK in a Rayleigh channel. The shape and the relative positioning of the error probability plots are very similar to those of BPSK in Rayleigh fading channel as shown in Figure 23. The plots for QPSK are shifted at least 4 dB to the right along the SNR axis, compared to the BPSK case, i.e., to obtain the same error probability, the scheme requires 4 dB more SNR than BPSK. This occurs for all the probability plots of SMT₁ and the cooperative schemes of SMT₂. On the other hand, the error probability plot of SMT₂ for the DF scheme is shifted even more to the right, increasing the performance difference between SMT₁ and SMT₂ in the non-cooperative schemes.

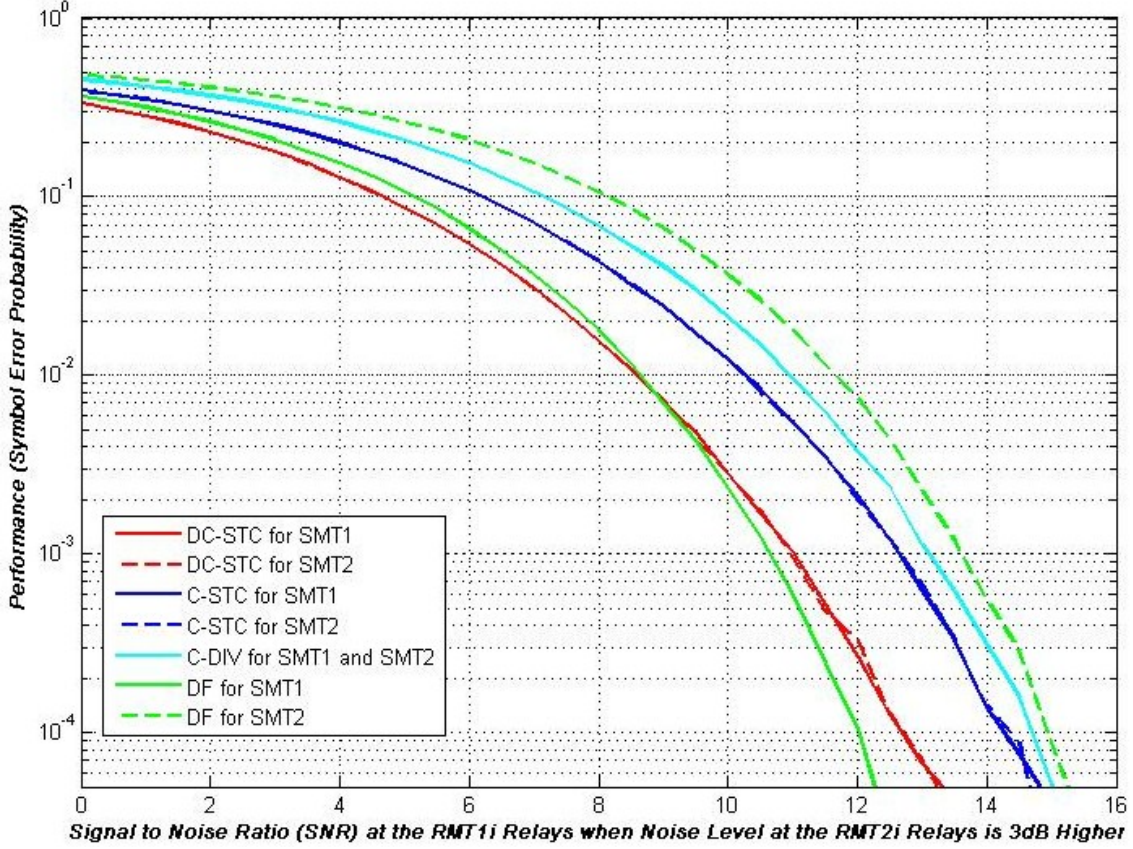


Figure 31. Performance of Two-hop Cooperative C-STC, C-DIV and Non-cooperative DF Schemes for a SNR Difference between the Paths of 3 dB in Rayleigh Channel for QPSK.

4. QPSK in SUI Channels

Similar observations to the aforementioned for the Rayleigh fading case are also applicable to the results for the frequency selective channels shown in Figures 32-34. Figure 32 shows the results of the relaying schemes in SUI1 channel. Similar to the results for the SUI1 case for BPSK, in the higher SNR region the C-STC scheme performs better than C-DIV and DF cases. The DC-STC scheme again outperforms all other techniques and has a performance difference over C-STC of around 10 dB at the target probability of 10^{-4} .

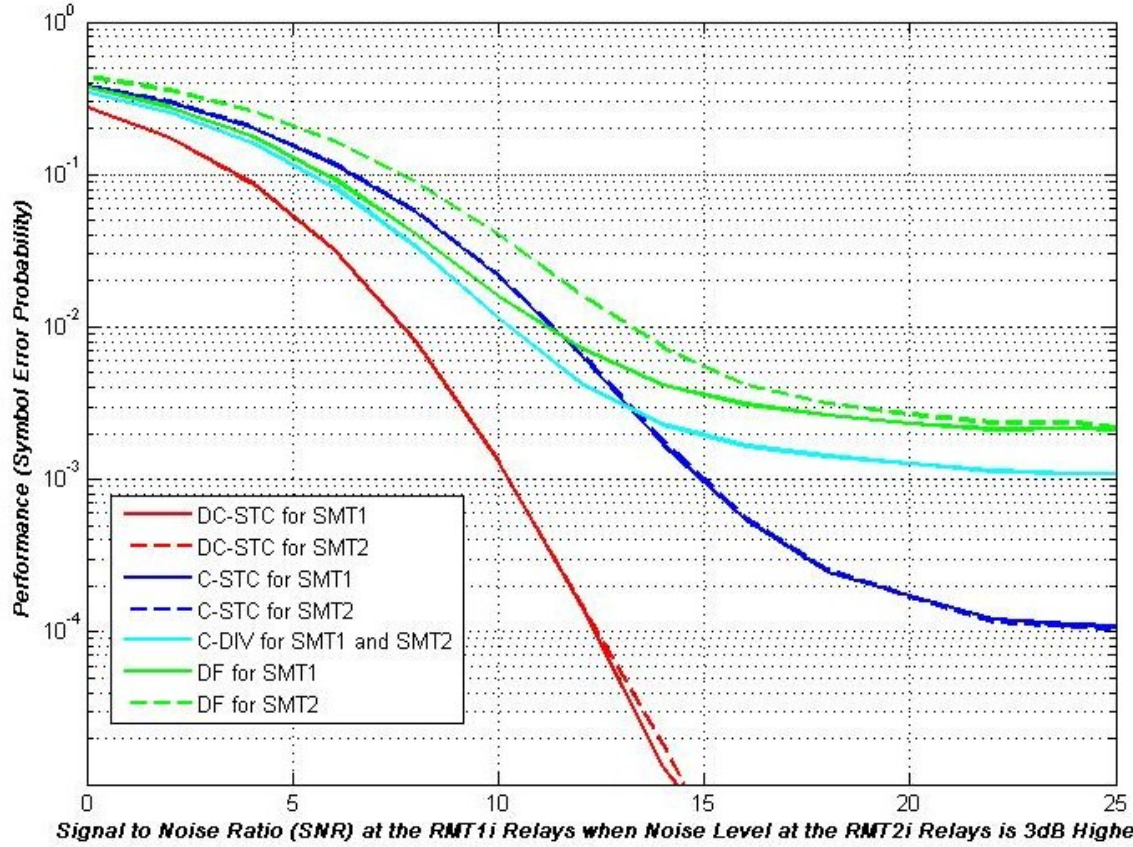


Figure 32. Performance of Two-hop Cooperative C-STC, C-DIV and Non-cooperative DF Schemes for a SNR Difference between the Paths of 3 dB in SUI1 Channel for QPSK.

In the SUI3 channel, as shown in Figure 33, the C-STC scheme for QPSK, unlike the BPSK case (see Figure 29), performs better than the other schemes in all SNR ranges. None of the schemes however reach the target probability of 10^{-4} in the SNR range simulated. The best error probability observed is 10^{-1} for SNRs more than 16 dB, which is not acceptable performance for most wireless communication applications.

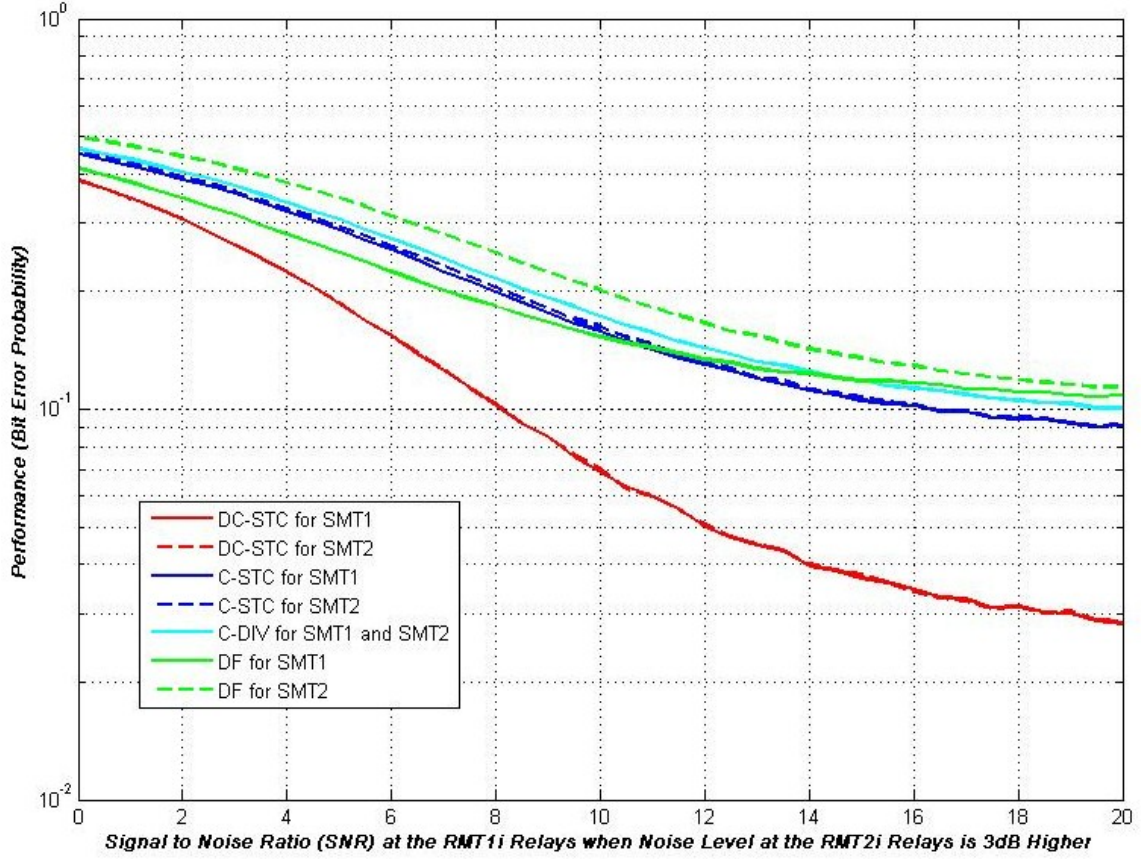


Figure 33. Performance of Two-hop Cooperative C-STC, C-DIV and Non-cooperative DF Schemes for a SNR Difference between the Paths of 3 dB in SUI3 Channel for QPSK.

Figure 34 shows the simulation results in a SUI6 channel. The performance of the non-cooperative schemes and C-DIV are close. The C-STC scheme performs better in SUI6 than in SUI3. A 10 dB performance difference between C-STC scheme and the other simulated schemes is noticed in the SNR range simulated. Also, no scheme reaches the target error probability of 10^{-4} .

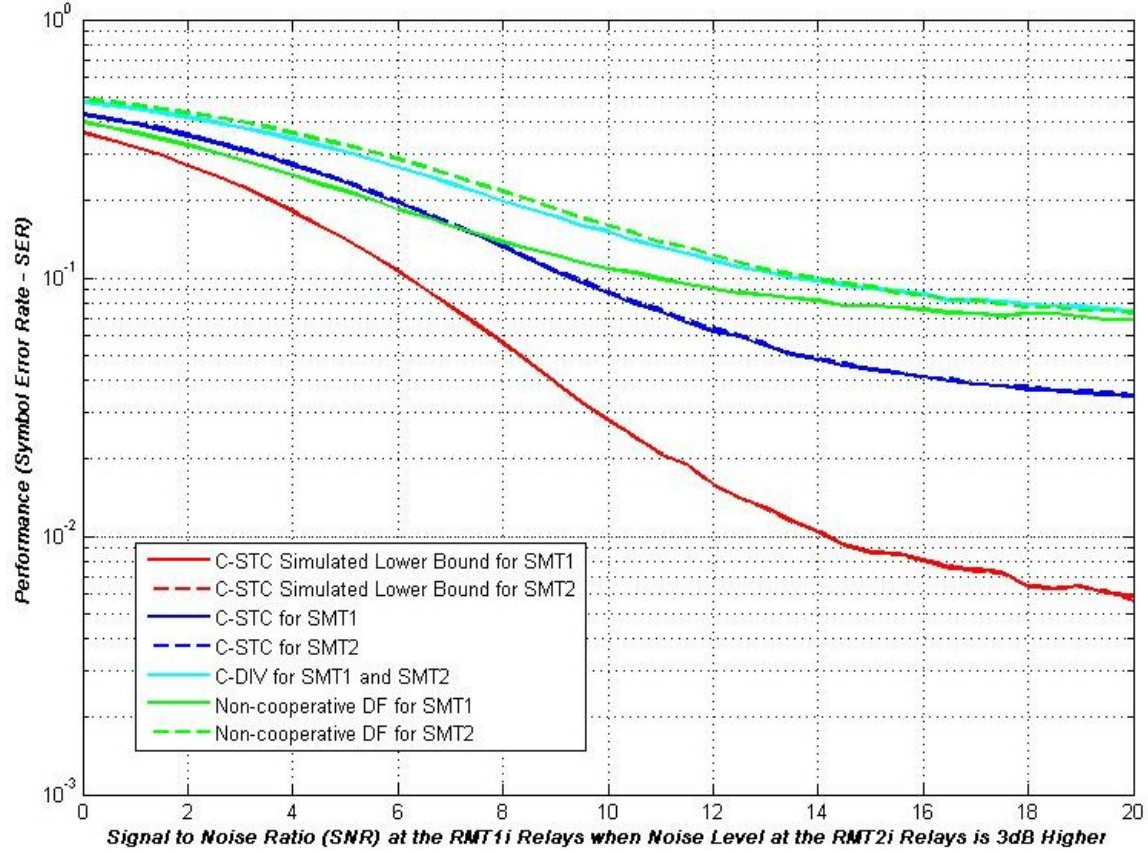


Figure 34. Performance of Two-hop Cooperative C-STC, C-DIV and Non-cooperative DF Schemes for a SNR Difference between the Paths of 3 dB in SUI6 Channel for QPSK.

5. Multiple Hops in SUI1 Channel for BPSK and QPSK

Figure 35 presents error probability over multiple hops. The SUI1 channel is used with SNR_{1i} set to 8 dB and SNR_{2i} to 5 dB. What can be noticed is that error probabilities tend to increase slowly at each hop. Between the second and the sixth hop, the error probability increase is less than a factor of 10 while the differences between the performances of the schemes remained the same.

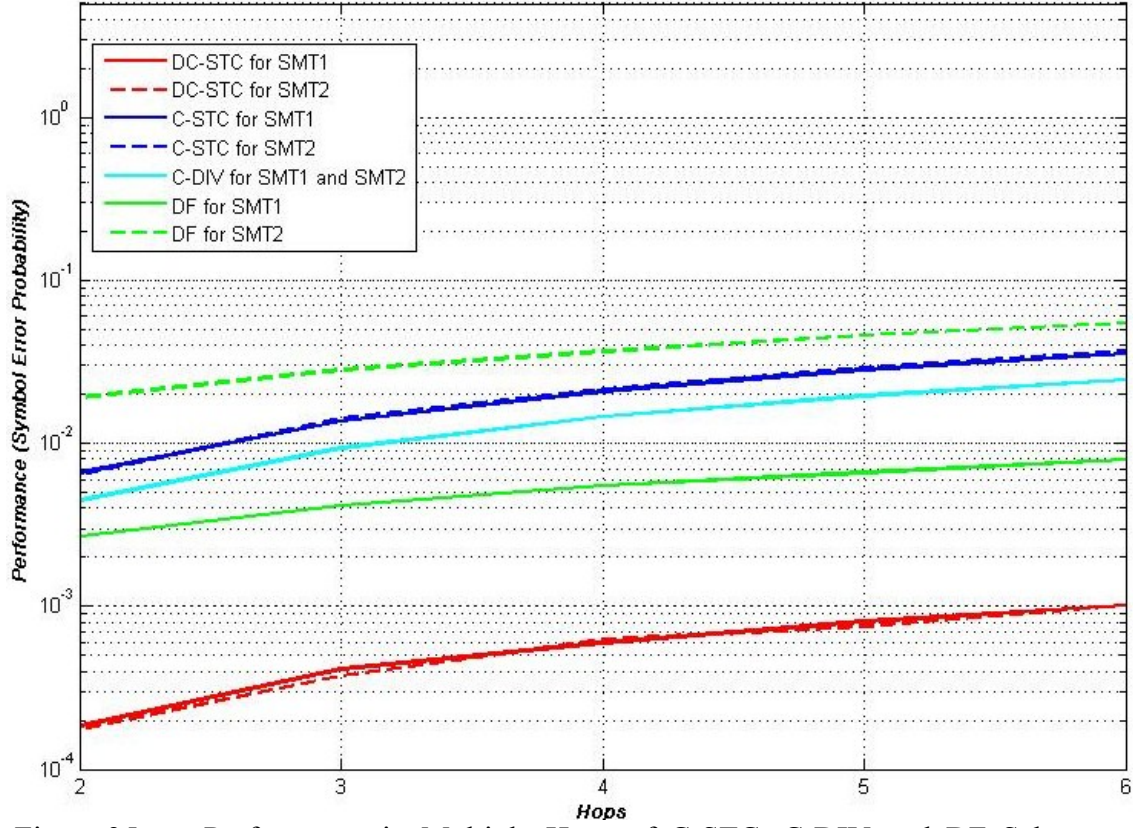


Figure 35. Performance in Multiple Hops of C-STC, C-DIV and DF Schemes for BPSK in SUI1 Channel and an SNR Difference between the Paths of 3 dB in the Low SNR Region.

Figure 36 presents the multihop results for QPSK. The performance trends are similar to those of BPSK as the number of hops increases, but the performance is worse in comparison with Figure 35. Note that all error probabilities have increased by more than a factor of 10.

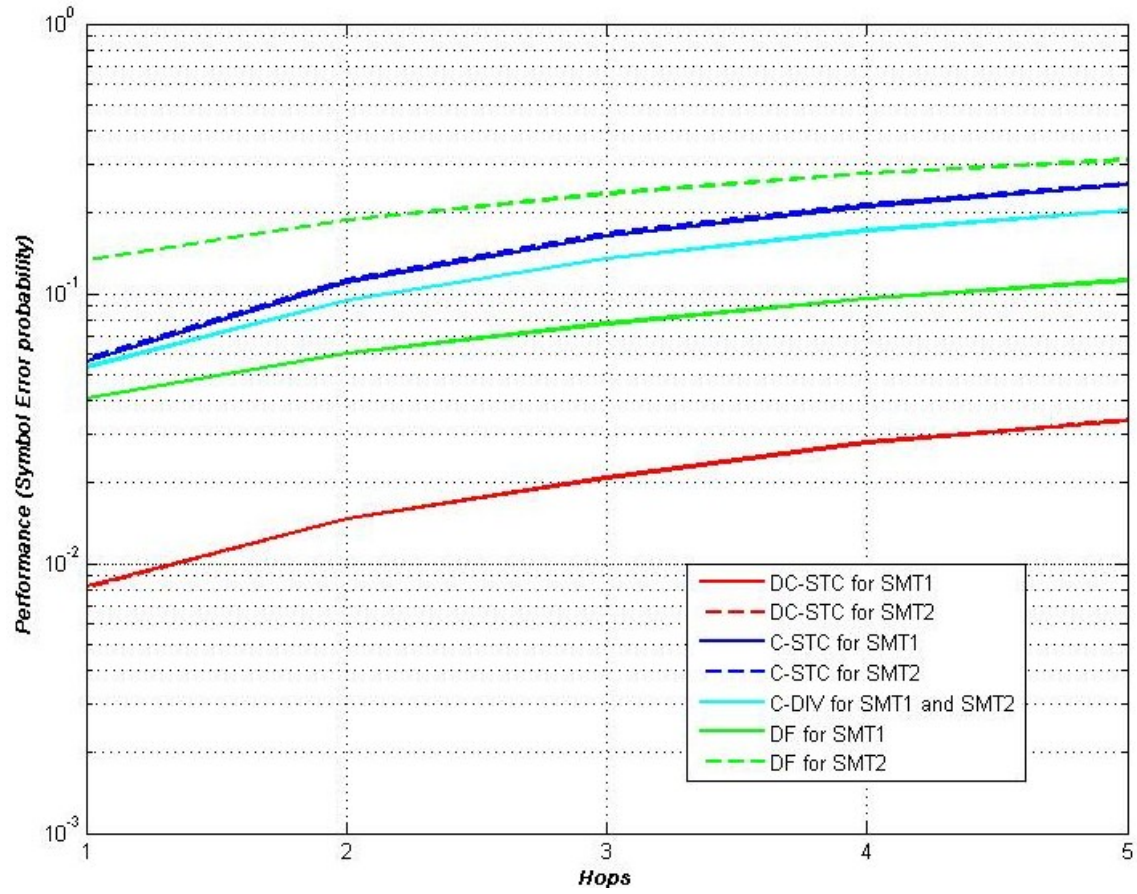


Figure 36. Performance in Multiple Hops of C-STC, C-DIV and DF Schemes for QPSK in SUI1 Channel and an SNR Difference between the Paths of 3 dB in the Low SNR Region.

C. SIMULATION RESULTS FOR QAM

In this section the simulation results for 16-QAM and 64-QAM modulated signals are presented. The rectangular QAM constellations used in the simulation are depicted in Figure 37.

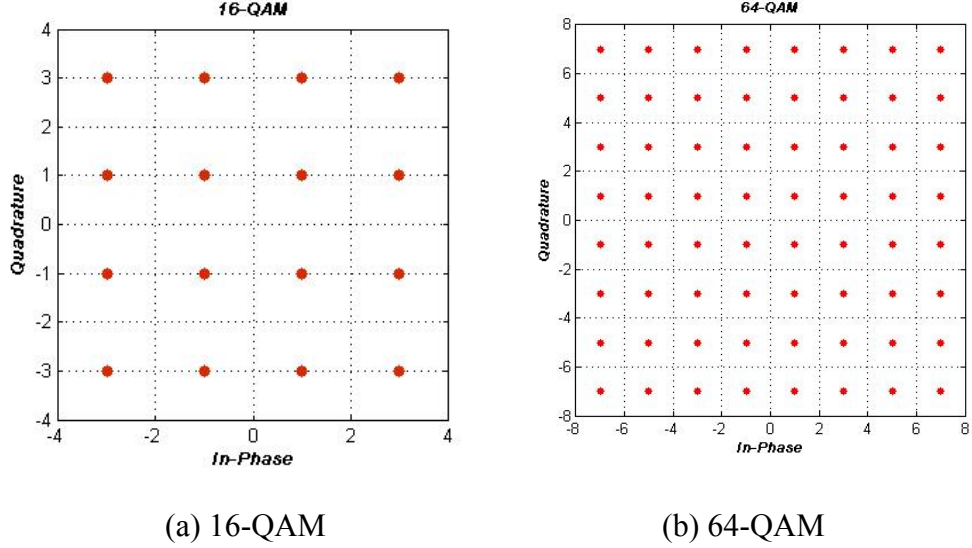


Figure 37. Constellations used in the Simulation: (a) 16-QAM Rectangular and (b) 64-QAM Rectangular.

1. 16-QAM

In Figure 38 the performance of C-STC can be compared to that of C-DIV and DF schemes for 16-QAM modulated streams in a Rayleigh channel. For DF the performance difference between the two users is equal to the SNR difference. The C-DIV improves the performance of SMT_2 and reduces the performance of SMT_1 to the middle of the performance difference of the two users in the non-cooperative case. C-DIV performance is similar to that of C-STC.

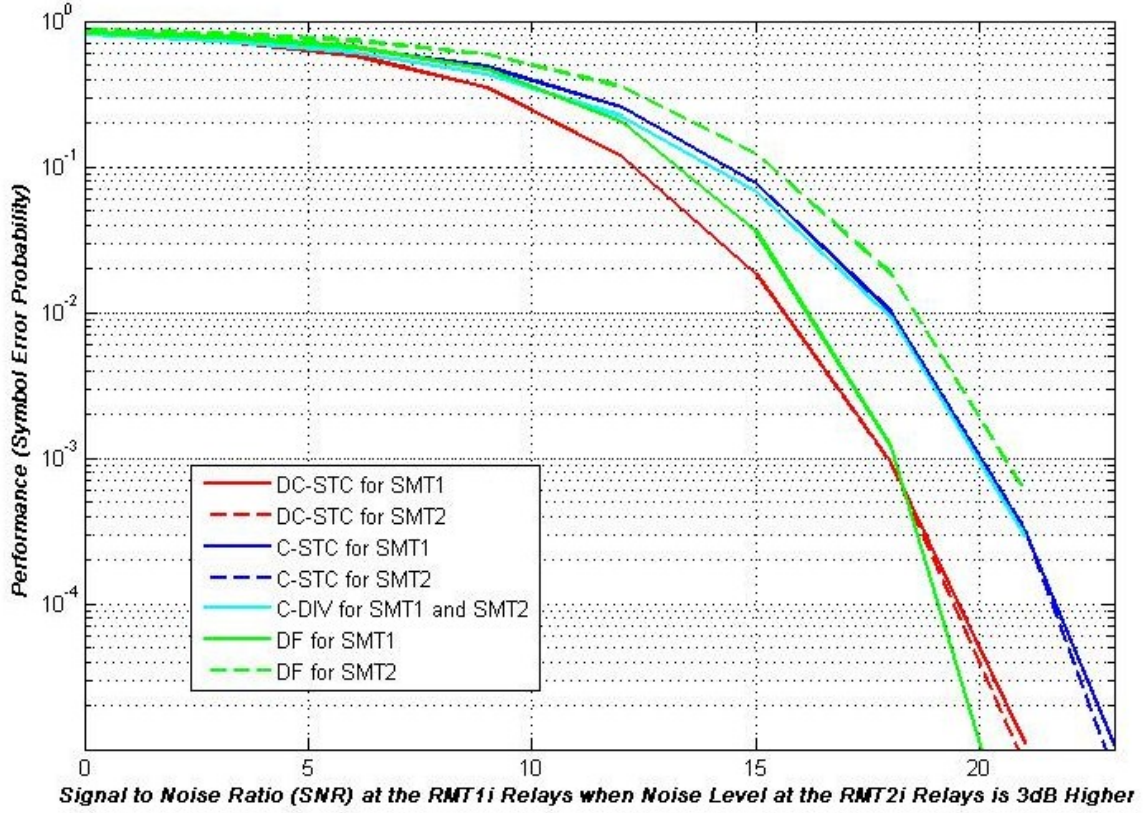


Figure 38. Performance of Two-hop Cooperative C-STC, C-DIV and Non-cooperative DF Schemes for a SNR Difference between the Paths of 3 dB in Rayleigh Channel for 16-QAM.

In Figure 39, the performances in the SUI1 fading environment for 16-QAM are shown. Like the SUI1 cases of the PSK, for SNRs beyond 25 dB the performances saturate. The C-DIV scheme, as can be observed in Figure 39, shows the worst performance in the SUI1 fading environment. The C-STC and the DC-STC schemes, for SNRs beyond 15 dB, perform better than other schemes, although no scheme achieves the desired error probability of 10^{-4} .

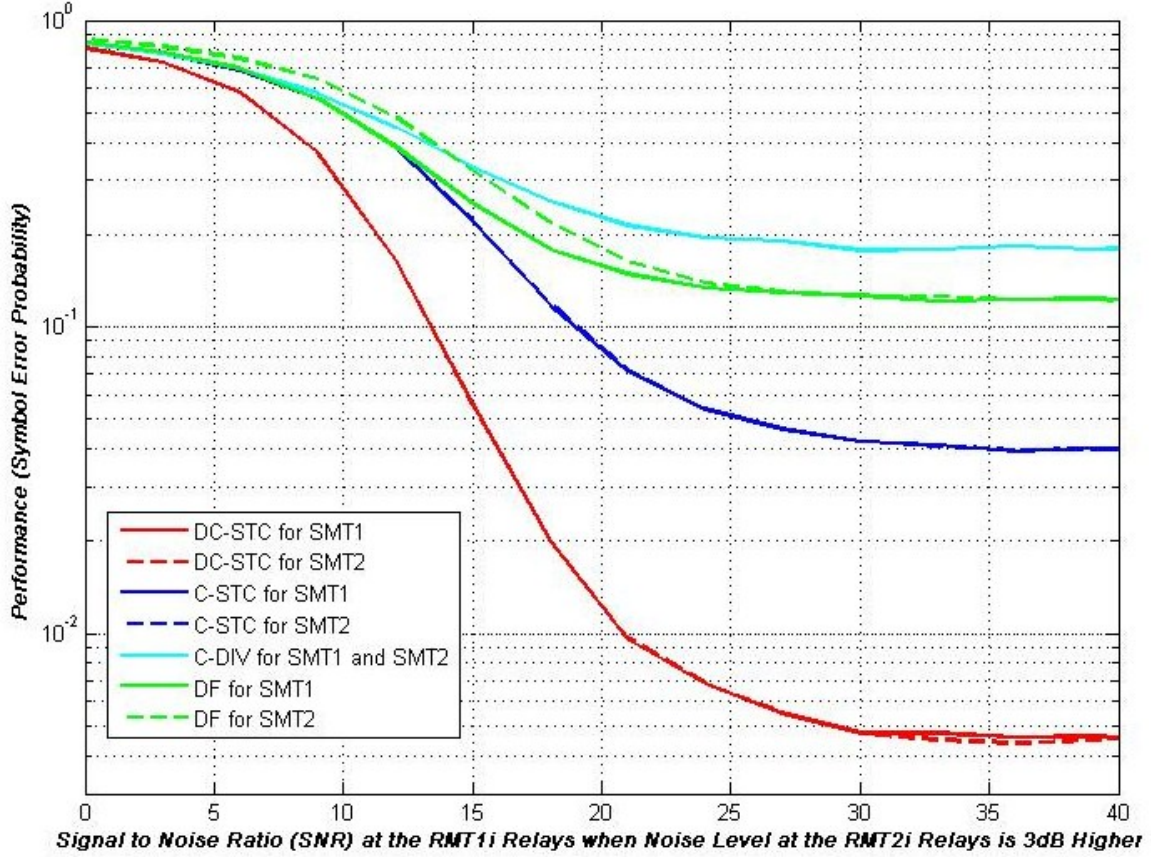


Figure 39. Performance of Two-hop Cooperative C-STC, C-DIV and Non-cooperative DF Schemes for a SNR Difference between the Paths of 3 dB in SUI1 Channel for 16-QAM.

The results for SUI3 and SUI6 channels are not presented, but like PSK modulations, the performances degrade in comparison to the SUI1 channel case.

2. 64-QAM

The observations for the 64-QAM case are similar to the simulation results for the 16-QAM case. Figure 40 presents the acquired performances in a Rayleigh channel. Again, all the performances are worse compared to the equivalent performances for the 16-QAM case.

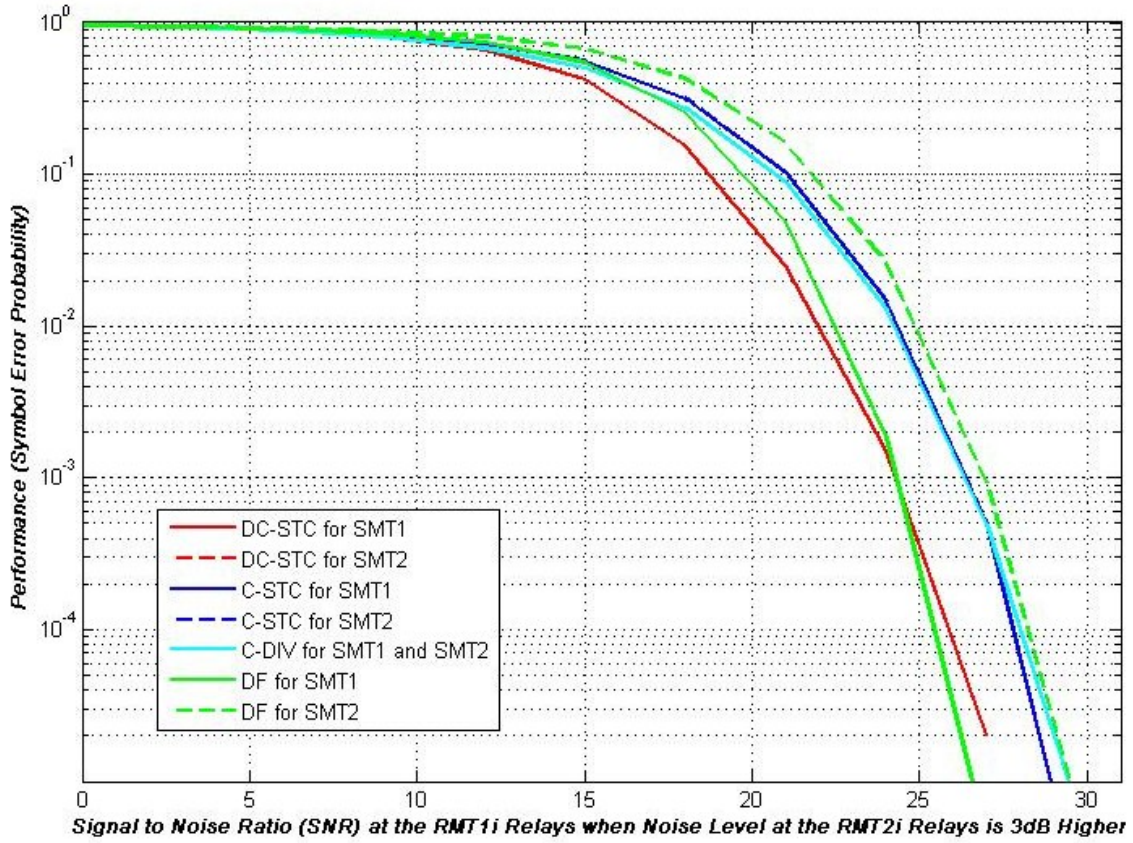


Figure 40. Performance of Two-hop Cooperative C-STC, C-DIV and Non-cooperative DF Schemes for a SNR Difference between the Paths of 3 dB in Rayleigh Fading Conditions for 64-QAM.

Figure 41 presents the results for 64-QAM in a SUI1 channel. None of the error plots fall below 10^{-1} for SNRs up to 40 dB.

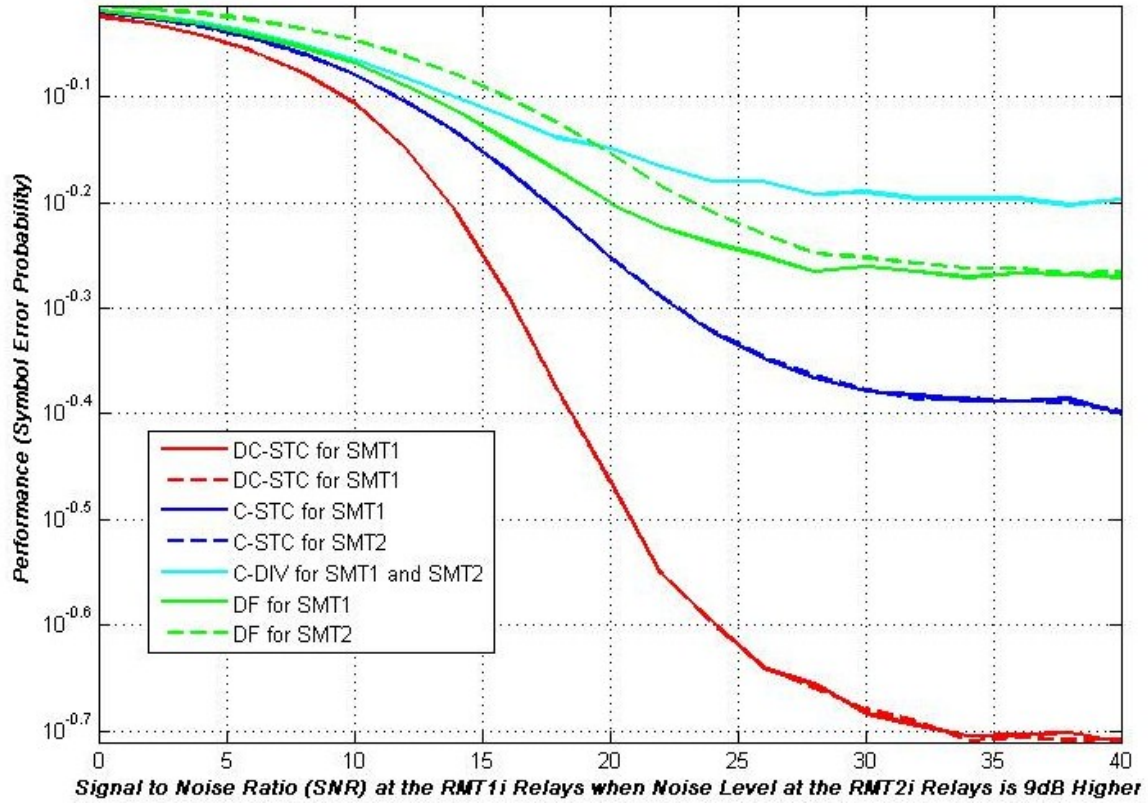


Figure 41. Performance of Two-hop Cooperative C-STC, C-DIV and Non-cooperative DF Schemes for a SNR Difference between the Paths of 3 dB in SUI1 Fading Conditions for 64-QAM.

In the SC modulation implemented in this work the error probabilities are high for QAM; the use of OFDM may improve the error probabilities.

D. SUMMARY

Chapter IV presented the results of simulation using Matlab. Results were obtained for BPSK, QPSK, 16-QAM and 64-QAM modulations in Rayleigh and SUI channels. In the next chapter the significant results and conclusions obtained here are summarized and presented with some suggestions for future work.

THIS PAGE INTENTIONALLY LEFT BLANK

V. CONCLUSIONS AND FUTURE WORK

In this chapter the work done in this thesis is summarized, the significant results obtained from the theoretical investigation and simulations are presented and some suggestions for future work are provided.

A. SUMMARY OF WORK

Multi-cluster relay schemes for single-antenna terminals for cooperative and non-cooperative communications in Rayleigh and SUI channels are presented. For the purpose of this thesis, each cluster consisted of two terminals. The non-cooperative relaying schemes introduced were decode-and-forward where the relay terminal fully decodes the received symbol and retransmits and amplify-and-forward where the relay terminal just amplifies the received signal and noise after compensating the fading effect. The cooperative schemes discussed here are decode-and-forward with cooperative diversity (C-DIV) and Alamouti cooperative space-time coding (C-STC). C-DIV applies spatial transmit and receive diversity through cooperation and C-STC is based on a distributed version of the 2×1 Alamouti space-time coding scheme [3]. The error probabilities for the aforementioned schemes were calculated for a two-hop relay scenario in an AWGN channel. The Alamouti cooperative space-time coding for dual-antenna terminals (DC-STC) is also presented. The simulations for the two-hop scenario were performed for BPSK, QPSK and QAM in AWGN, Rayleigh, and SUI channels.

B. SIGNIFICANT RESULTS

Calculations of the symbol error probability for the C-STC and the C-DIV schemes showed that in the AWGN channel both schemes performed similarly and were better than the DF and AF schemes by 1 dB and 2 dB, respectively, for the two-hop relaying case with two relaying terminals. For PSK, the cooperative schemes in Rayleigh and SUI channels achieved or were very close to the target error probability of 10^{-4} . For

QAM the resulting error probabilities were high in both Rayleigh and SUI fading scenarios. This indicates the use of PSK rather than QAM as more reliable in single-carrier multi-hop relay scenarios.

An important result observed in the simulation was that the performance difference between the two users had diminished in the cooperative schemes. The performances of the cooperative schemes in PSK were better or close to the target error probability of 10^{-4} , which did not always occur for the non-cooperative case of SMT₂. This diminishing of the performance difference indicates sharing of the resources between the two users and between the relays in the cluster and that only cooperation can facilitate communications in cases where recovery of both user signals are important, which is a common scenario for tactical military communications. The improved resource sharing potentially leads to better coverage areas and extended terminal lifetime. As an example, for BPSK in a single hop scenario the energy consumption of both users can be reduced by almost 50% when they cooperated. Alternatively, a 20% increase of coverage range can be achieved based on the log-distance path loss model when keeping the same energy consumption and sharing it equally.

Another significant observation is that C-DIV performed well in cases where the SNR difference between the paths was high. C-STC didn't perform as well and was very close to the performance of SMT₂ in the non-cooperative case. On the other hand C-STC performed better than other schemes in severe channel fading conditions.

In the multihop scenarios we observed that adding more hops to the route of the signal as expected degraded the performance, but by no more than a factor of 10 for a scenario of six hops. Hence multihop relay topologies for cooperative schemes do not severely degrade the quality of the signal and keep error probabilities lower than the multihop non-cooperative schemes.

C. SUGGESTIONS FOR FUTURE WORK

Listed below are some suggestions for improvements that can be made or extensions of the research based on the work reported in this thesis.

In this work a single carrier narrowband modulation was considered. Modern wireless systems however have adopted orthogonal frequency division multiplexing (OFDM) techniques along with forward error correction. Since OFDM is known to provide increased data rates and reliability, a future thesis may extend the investigation of the schemes studied in this work to OFDM based cooperative schemes. Use of OFDM can probably facilitate the use of QAM which in this work did not perform adequately well. Also, investigation can include smart relaying techniques which were not taken into account in this work, like the choice of the relay terminal to relay a signal or not.

In order to perform well, the cooperative schemes require network establishment, time synchronization, and terminal localization for simultaneous receptions in order to eliminate any undesired interference. Hence, investigation is required on how to implement the distributed cooperative algorithms in an environment where terminals are randomly dispersed.

The performance measure used in the simulation was the symbol error probability (SER) as a function of SNR in the relay. The actual performance of the investigated schemes cannot be completely evaluated only by the error probability, but also needs to take into account other parameters such as achieved data rates, outage probabilities, and power consumption. A future thesis effort may analyze the behavior of the schemes as a function of these parameters.

Finally the equations for the symbol error probabilities derived here are exclusively for the two-hop scheme in the AWGN environment. Performance evaluations for fading environments and for multihop schemes are suggested to be derived; also, work can be extended from dual-terminal clusters to multi-terminal clustered networks.

THIS PAGE INTENTIONALLY LEFT BLANK

APPENDIX A. STANFORD UNIVERSITY INTERIM MODELS

This appendix lists the six Stanford University Interim models used in this work

SUI – 1 Channel				
	Tap 1	Tap 2	Tap 3	Units
Delay	0	0.2	0.4	μs
Power	0	-3	-10	dB
K-factor	10	10	10	
Doppler	0.4	0.4	0.4	Hz
Terrain Type: C, Antenna correlation: 0.7, RMS Delay Spread: 0.1 μs				

SUI – 2 Channel				
	Tap 1	Tap 2	Tap 3	Units
Delay	0	0.3	0.6	μs
Power	0	-3	-8	dB
K-factor	5	5	5	
Doppler	0.4	0.4	0.4	Hz
Terrain Type: C, Antenna correlation: 0.5, RMS Delay Spread: 0.2 μs				

SUI – 3 Channel				
	Tap 1	Tap 2	Tap 3	Units
Delay	0	0.5	1	μs
Power	0	-5	-10	dB
K-factor	0	0	0	
Doppler	0.4	0.4	0.4	Hz
Terrain Type: B, Antenna correlation: 0.25, RMS Delay Spread: 0.3 μs				

SUI – 4 Channel				
	Tap 1	Tap 2	Tap 3	Units
Delay	0	2	4	μs
Power	0	-4	-8	dB
K-factor	0	0	0	
Doppler	1	1	1	Hz
Terrain Type: B, Antenna correlation: 0.5, RMS Delay Spread: 1.3 μs				

SUI – 5 Channel				
	Tap 1	Tap 2	Tap 3	Units
Delay	0	4	11	μs
Power	0	-3	-5	dB
K-factor	0	0	0	
Doppler	2	2	2	Hz
Terrain Type: A, Antenna correlation: 0.5, RMS Delay Spread: 3.1 μs				

SUI – 6 Channel				
	Tap 1	Tap 2	Tap 3	Units
Delay	0	14	20	μs
Power	0	-10	-12	dB
K-factor	0	0	0	
Doppler	0.4	0.4	0.4	Hz
Terrain Type: A, Antenna correlation: 0.25, RMS Delay Spread: 5.2 μs				

For a given close-in reference distance d_0 , the median path loss (PL in dB) is given by $PL = A + 10\gamma \log_{10}(d / d_0) + s$ for $d > d_0$ where $A = 20 \log_{10}(4\pi d_0 / \lambda)$, (λ being the wavelength in m), γ is the path-loss exponent with $\gamma = (a - bh_b + c/h_b)$ for h_b between 10m and 80m (h_b is the height of the base station in m), $d_0 = 100\text{m}$ and a, b, c are constants dependent on the terrain category [56].

Model Parameter	Terrain Type A	Terrain Type B	Terrain Type C
<i>a</i>	4.6	4	3.6
<i>b</i>	0.0075	0.0065	0.005
<i>c</i>	12.6	17.1	20

APPENDIX B. MATLAB SOURCE CODE

This appendix lists the MATLAB codes used in this work

Dualhop.m

```
% Parameters
clear all; clc;
M = input('give M-PSK order (2,4)or QAM order(16, 64):');
if M == 2;
    dh = [1 -1]/(sqrt(2)); % Possible symbols BPSK
else if M == 4;
    dh = [1+j -1+j 1-j -1-j]/(2); % Possible symbols QPSK
else if M == 16;
    qamOrder = M; temp = 0:1:15; dh = qammod(temp, qamOrder); % 16QAM
else qamOrder = M; temp = 0:1:63; dh = qammod(temp, qamOrder); % 64QAM
end
end
end
b = input('For frequency selective channel press 0 and for flat channel press 1:');
number = 5000; number1 = number*200; % STBC
if b == 1
    a = input('For AWGN channel press 0 and for Rayleigh channel press 1:');
    SUI_index = 1; rho_tx = 0; rho_rx = 0; direct = 0;
else SUI_index = input('Choose SUI propagation model [1:6]:');
    direct = input('For omni antennas press 0, for antennas with directivity 30deg press 1:');
    rho_tx = input('If transmission antennas suffer correlation choose (1) else (0):');
    rho_rx = input('If reception antennas suffer correlation choose (1) else (0):');
end
MonteCarlo = 10; SNR = 0:2:40; % Length of SNR
SER_matrix_avg = zeros(1, length(SNR));
SER_matrix_avg1 = zeros(1, length(SNR));
SER_matrix_avg2 = zeros(1, length(SNR));
SER_matrix_avg3 = zeros(1, length(SNR));
SER_matrix_avg4 = zeros(1, length(SNR));
SER_matrix_avg5 = zeros(1, length(SNR));
SER_matrix_avg6 = zeros(1, length(SNR));
SER_matrix_avg7 = zeros(1, length(SNR));
SER_matrix_avg8 = zeros(1, length(SNR));
for e=1:MonteCarlo
    SER_matrix = [];
    SER_matrix1 = [];
    SER_matrix2 = [];
    SER_matrix3 = [];
    SER_matrix4 = [];
    SER_matrix5 = [];
    SER_matrix6 = [];
    SER_matrix7 = [];
    SER_matrix8 = [];
for SNR1 = 0:2:40 % SNR at receivers side
    SNR2 = SNR1-3; tot_errors = 0; tot_errors1 = 0;
```

```

%% CSTC Alamouti. Full Data Exchange in Intracluster Link
for i = 1:number
    if M == 2;
        Datar1 = randint(200,1,M); Data1 = pskmod(Datar1,M)/(sqrt(2));
        Datar2 = randint(200,1,M); Data2 = pskmod(Datar2,M)/(sqrt(2));
    else if M==4;
        Data1 = ((2*round(rand(200,1))-1)+ j*(2*round(rand(200,1))-
1))/(2);
        Datar1 = pskdemod(2*Data1,M);%random data QPSK
        Data2 = ((2*round(rand(200,1))-1)+ j*(2*round(rand(200,1))-
1))/(2);
        Datar2 = pskdemod(2*Data2,M); %random data QPSK
    else
        Datar1 = randint(200,1,qamOrder);Data1 =
gammod(Datar1,qamOrder);%16QAM
        Datar2 = randint(200,1,qamOrder);Data2 =
gammod(Datar2,qamOrder);%64QAM
    end
end
%% Building the Channel from Sources to Relays
[h11,h12,h21,h22] = TwobyTwo_channel (SUI_index,direct,rho_tx, rho_rx);%
SUI fading channel
if b == 1;% Flat fading channel
    if a == 1;
        h = randn(4,1)/sqrt(2)+j*randn(4,1)/sqrt(2);
        h11=h(1);h12=h(2);h21=h(3);h22=h(4);%Rayleigh
    else h11=1;h12=1;h21=1;h22=1;%AWGN
    end
end
R1 = awgn(filter(h11,1,Data1) + filter(h12,1,Data2), SNR1, 'measured');%
Received signals
R2 = awgn(filter(h21,1,Data1) + filter(h22,1,Data2), SNR2,'measured');
R3 = awgn(filter(h11,1,-conj(Data2)) + filter(h12,1,conj(Data1)), SNR1,
'measured');
R4 = awgn(filter(h21,1,-conj(Data2)) + filter(h22,1,conj(Data1)),
SNR2, 'measured');
s0 = non_causal_filter(conj(h11),transpose(R1)) +
filter(h12,1,conj((transpose(R3)))) + ...
non_causal_filter(conj(h21),transpose(R2)) +
filter(h22,1,conj((transpose(R4))));
s1 = non_causal_filter(conj(h12),transpose(R1)) + filter(-
h11,1,conj((transpose(R3)))) + ...
non_causal_filter(conj(h22),transpose(R2)) + filter(-
h21,1,conj((transpose(R4))));
H = [h11,h12,h21,h22];
% Maximum Likelihood Detector, Computing the distances
if M == 2;
    [decoded1, sa] = ML_BPSK (dh, s0);
    decoded1= transpose(decoded1);%BPSK
    [decoded2, sb] = ML_BPSK (dh, s1);
    decoded2= transpose(decoded2);%BPSK
else if M==4;
    [decoded1, sa] = ML_QPSK (dh, s0);
    decoded1= transpose(decoded1);%QPSK
    [decoded2, sb] = ML_QPSK (dh, s1);
    decoded2= transpose(decoded2);%QPSK
    else [decoded1, sa] = ML_QAM (dh, s0, qamOrder, H);
        decoded1= transpose(decoded1);%QAM
        [decoded2, sb] = ML_QAM (dh, s1, qamOrder, H);
        decoded2= transpose(decoded2);%QAM
    end
end

```

```

end
%% From relays to Destination
[h11,h12,h21,h22] = TwobyTwo_channel (SUI_index,direct,rho_tx, rho_rx); %
SUI fading channel
if b == 1;% Flat fading channel
    if a == 1;
        h = randn(4,1)/sqrt(2)+j*randn(4,1)/sqrt(2);
        h11=h(1);h12=h(2);h21=h(3);h22=h(4);%Rayleigh
    else h11=1;h12=1;h21=1;h22=1;%AWGN
    end
end
R1 = awgn(filter(h11,1,decoded1) + filter(h12,1,decoded2), SNR1,
'measured');% Received signals
R2 = awgn(filter(h21,1,decoded1) + filter(h22,1,decoded2),
SNR1,'measured');
R3 = awgn(filter(h11,1,-conj(decoded2)) + filter(h12,1,conj(decoded1)),
SNR1, 'measured');
R4 = awgn(filter(h21,1,-conj(decoded2)) + filter(h22,1,conj(decoded1)),
SNR1,'measured');
s0 = non_causal_filter(conj(h11),transpose(R1)) +
filter(h12,1,conj((transpose(R3)))) + ...
non_causal_filter(conj(h21),transpose(R2)) +
filter(h22,1,conj((transpose(R4)))));
s1 = non_causal_filter(conj(h12),transpose(R1)) + filter(-
h11,1,conj((transpose(R3)))) + ...
non_causal_filter(conj(h22),transpose(R2)) + filter(-
h21,1,conj((transpose(R4)))));
H = [h11,h12,h21,h22];
% Maximum Likelihood Detector, Computing the distances
if M == 2;
    [decoded1, sa] = ML_BPSK (dh, s0);
    decoded1= transpose(decoded1);%BPSK
    decoded1 = pskdemod(decoded1,M);
    [decoded2, sb] = ML_BPSK (dh, s1);
    decoded2= transpose(decoded2);%BPSK
    decoded2 = pskdemod(decoded2,M);
else if M==4;
    [decoded1, sa] = ML_QPSK (dh, s0);
    decoded1= transpose(decoded1);%QPSK
    decoded1 = pskdemod(decoded1,M);
    [decoded2, sb] = ML_QPSK (dh, s1);
    decoded2= transpose(decoded2);%QPSK
    decoded2 = pskdemod(decoded2,M);
else
    [decoded1, sa] = ML_QAM (dh, s0, qamOrder, H);
    decoded1= transpose(decoded1);
    decoded1 = qamdemod(decoded1,qamOrder);%QAM
    [decoded2, sb] = ML_QAM (dh, s1, qamOrder, H);
    decoded2= transpose(decoded2);
    decoded2 = qamdemod(decoded2,qamOrder);%QAM
end
end
errors = sum(decoded1~=Datar1); tot_errors = tot_errors+errors;
errors1 = sum(decoded2~=Datar2);tot_errors1 = tot_errors1+errors1;
end
ber = tot_errors/(number1); %Computing the SER for spesific SNR
ber1 = tot_errors1/(number1); %Computing the SER for spesific SNR
SER_matrix = [SER_matrix, ber];%Computing the SER matrix
SER_matrix1 = [SER_matrix1, ber1];%Computing the SER matrix

```



```

%% CSTC Alamouti. Time Synchronization Only in Intracluster Link
tot_errors = 0; tot_errors1 = 0;
for i = 1:number
    if M == 2;
        Datar1 = randint(200,1,M); Data1 = pskmod(Datar1,M)/(sqrt(2));
        Datar2 = randint(200,1,M); Data2 = pskmod(Datar2,M)/(sqrt(2));
    else if M==4;
        Data1 = ((2*round(rand(200,1))-1)+ j*(2*round(rand(200,1))-
1))/(2);
        Datar1 = pskdemod(2*Data1,M);%random data QPSK
        Data2 = ((2*round(rand(200,1))-1)+ j*(2*round(rand(200,1))-
1))/(2);
        Datar2 = pskdemod(2*Data2,M); %random data QPSK
    else
        Datar1 = randint(200,1,qamOrder);Data1 =
qammod(Datar1,qamOrder);%16QAM
        Datar2 = randint(200,1,qamOrder);Data2 =
qammod(Datar2,qamOrder);%64QAM
    end
end
%% Building the Channel for the first 2x1 system
[h1,h2] = TwobyOne_channel (SUI_index,direct,rho_tx);% SUI fading channel
if b == 1;% Flat fading channel
    if a == 1;
        h = randn(2,1)/sqrt(2)+j*randn(2,1)/sqrt(2);
        h1=h(1);h2=h(2);%Rayleigh
    else h1=1;h2=1;%AWGN
    end
end
R1 = awgn(filter(h1,1,Data1) + filter(h2,1,Data2), SNR1,
'measured');%Received signals
R2 = awgn(filter(h1,1,-conj(Data2)) + filter(h2,1,conj(Data1)), SNR1,
'measured');
s0 = non_causal_filter(conj(h1),transpose(R1)) +
filter(h2,1,conj((transpose(R2))));
s1 = non_causal_filter(conj(h2),transpose(R1)) + filter(-
h1,1,conj((transpose(R2))));
H=[h1,h2];
% Maximum Likelihood Detector, Computing the distances
if M == 2;
    [decoded11, s11] = ML_BPSK (dh, s0);decoded11=
transpose(decoded11);%BPSK
    [decoded12, s12] = ML_BPSK (dh, s1);decoded12=
transpose(decoded12);%BPSK
else if M==4;
    [decoded11, s11] = ML_QPSK (dh, s0);decoded11=
transpose(decoded11);%QPSK
    [decoded12, s12] = ML_QPSK (dh, s1);decoded12=
transpose(decoded12);%QPSK
    else
        [decoded11, s11] = ML_QAM (dh, s0, qamOrder, H);
        decoded11= transpose(decoded11);%QAM
        [decoded12, s12] = ML_QAM (dh, s1, qamOrder, H);
        decoded12= transpose(decoded12);%QAM
    end
end
%% Building the Channel for the second 2x1 system
[h1,h2] = TwobyOne_channel (SUI_index,direct,rho_tx);% SUI fading channel
if b == 1;% Flat fading channel
    if a == 1;
        h = randn(2,1)/sqrt(2)+j*randn(2,1)/sqrt(2);
        h1=h(1);h2=h(2);%Rayleigh

```

```

        else h1=1;h2=1;%AWGN
    end
end
R1 = awgn(filter(h1,1,Data1) + filter(h2,1,Data2), SNR2,
'measured');%Received signals
R2 = awgn(filter(h1,1,-conj(Data2)) + filter(h2,1,conj(Data1)), SNR2,
'measured');
s0 = non_causal_filter(conj(h1),transpose(R1)) +
filter(h2,1,conj((transpose(R2))));
s1 = non_causal_filter(conj(h2),transpose(R1)) + filter(-
h1,1,conj((transpose(R2))));H=[h1,h2];
% Maximum Likelihood Detector, Computing the distances
if M == 2;
    [decoded21, s21] = ML_BPSK (dh, s0);
    decoded21= transpose(decoded21);%BPSK
    [decoded22, s22] = ML_BPSK (dh, s1);
    decoded22= transpose(decoded22);%BPSK
else if M==4;
    [decoded21, s21] = ML_QPSK (dh, s0);
    decoded21= transpose(decoded21);%QPSK
    [decoded22, s22] = ML_QPSK (dh, s1);
    decoded22= transpose(decoded22);%QPSK
    else
        [decoded21, s21] = ML_QAM (dh, s0, qamOrder, H);
        decoded21= transpose(decoded21);%QAM
        [decoded22, s22] = ML_QAM (dh, s1, qamOrder, H);
        decoded22= transpose(decoded22);%QAM
    end
end
%% From relays to Destination
[h11,h12,h21,h22] = TwobyTwo_channel (SUI_index,direct,rho_tx, rho_rx);%
SUI fading channel
if b == 1;% Flat fading channel
    if a == 1;
        h = randn(4,1)/sqrt(2)+j*randn(4,1)/sqrt(2);
        h11=h(1);h12=h(2);h21=h(3);h22=h(4);%Rayleigh
    else h11=1;h12=1;h21=1;h22=1;%AWGN
    end
end
R1 = awgn(filter(h11,1,decoded11) + filter(h12,1,decoded22),
SNR1,'measured');% Received signals
R2 = awgn(filter(h21,1,decoded11) + filter(h22,1,decoded22),
SNR1,'measured');
R3 = awgn(filter(h11,1,-conj(decoded12)) + filter(h12,1,conj(decoded21)),
SNR1,'measured');
R4 = awgn(filter(h21,1,-conj(decoded12)) + filter(h22,1,conj(decoded21)),
SNR1,'measured');
s0 = non_causal_filter(conj(h11),transpose(R1)) +
filter(h12,1,conj((transpose(R3))));
...
non_causal_filter(conj(h21),transpose(R2)) +
filter(h22,1,conj((transpose(R4))));
s1 = non_causal_filter(conj(h12),transpose(R1)) + filter(-
h11,1,conj((transpose(R3))));
...
non_causal_filter(conj(h22),transpose(R2)) + filter(-
h21,1,conj((transpose(R4))));
H = [h11,h12,h21,h22];
% Maximum Likelihood Detector, Computing the distances
if M == 2;
    [decoded1, sa] = ML_BPSK (dh, s0);
    decoded1= transpose(decoded1);%BPSK
    decoded1 = pskdemod(decoded1,M);
    [decoded2, sb] = ML_BPSK (dh, s1);
    decoded2= transpose(decoded2);%BPSK

```

```

        decoded2 = pskdemod(decoded2,M);
    else if M==4;
        [decoded1, sa] = ML_QPSK (dh, s0);
        decoded1= transpose(decoded1);%QPSK
        decoded1 = pskdemod(decoded1,M);
        [decoded2, sb] = ML_QPSK (dh, s1);
        decoded2= transpose(decoded2);%QPSK
        decoded2 = pskdemod(decoded2,M);
    else
        [decoded1, sa] = ML_QAM (dh, s0, qamOrder, H);
        decoded1= transpose(decoded1);
        decoded1 = qamdemod(decoded1,qamOrder);%QAM
        [decoded2, sb] = ML_QAM (dh, s1, qamOrder, H);
        decoded2= transpose(decoded2);
        decoded2 = qamdemod(decoded2,qamOrder);%QAM
    end
end
errors = sum(decoded1~=Datar1);tot_errors = tot_errors+errors;
errors1 = sum(decoded2~=Datar2);tot_errors1 = tot_errors1+errors1;
end
ber = tot_errors/(number1); %Computing the SER for spesific SNR
ber1 = tot_errors1/(number1); %Computing the SER for spesific SNR
SER_matrix2 = [SER_matrix2, ber];%Computing the SER matrix
SER_matrix3 = [SER_matrix3, ber1];%Computing the SER matrix

%% C-Div DF
tot_errors = 0;
for i = 1:number
    if M == 2;
        Datar = randint(200,1,M); Data = pskmod(Datar,M)/(sqrt(2)); %Random
data BPSK
    else if M==4;
        Data = ((2*round(rand(200,1))-1)+ j*(2*round(rand(200,1))-
1))/(2);
        Datar = pskdemod(2*Data,M);%random data QPSK
    else
        Datar = randint(200,1,qamOrder);Data =
gammod(Datar,qamOrder);%16QAM
    end
end
%% Building the Channel for the first 1x1 system
[h1] = OnebyOne_channel (SUI_index,direct);% SUI fading channel
if b == 1;% Flat fading channel
    if a == 1;
        h1 = randn(1,1)/sqrt(2)+j*randn(1,1)/sqrt(2);%Rayleigh
    else h1=1;%AWGN
    end
end
R1 = awgn(filter(h1,1,Data), SNR1, 'measured');
s0 = non_causal_filter(conj(h1),transpose(R1)); H=h1;
% Maximum Likelihood Detector, Computing the distances
if M == 2;
    [decoded1, sa] = ML_BPSK (dh, s0);
    decoded1= transpose(decoded1);%BPSK
else if M==4;
    [decoded1, sa] = ML_QPSK (dh, s0);
    decoded1= transpose(decoded1);%QPSK
    else
        [decoded1, sa] = ML_QAM (dh, s0, qamOrder, H);
        decoded1= transpose(decoded1);%QAM
    end
end
%% Building the Channel for the second 1x1 system

```

```

[h1] = OnebyOne_channel (SUI_index,direct);% SUI fading channel
if b == 1;% Flat fading channel
    if a == 1;
        h1 = randn(1,1)/sqrt(2)+j*randn(1,1)/sqrt(2);%Rayleigh
    else h1=1;%AWGN
    end
end
R1 = awgn(filter(h1,1,Data), SNR1, 'measured');
s0 = non_causal_filter(conj(h1),transpose(R1)); H=h1;
% Maximum Likelihood Detector, Computing the distances
if M == 2;
    [decoded2, sb] = ML_BPSK (dh, s0);
    decoded2= transpose(decoded2);%BPSK
else if M==4;
    [decoded2, sb] = ML_QPSK (dh, s0);
    decoded2= transpose(decoded2);%QPSK
    else [decoded2, sb] = ML_QAM (dh, s0, qamOrder, H);
    decoded2= transpose(decoded2);%QAM
end
end
%% From relays to Destination
[h11,h12,h21,h22] = TwobyTwo_channel (SUI_index,direct,rho_tx, rho_rx);%
SUI fading channel
if b == 1;% Flat fading channel
    if a == 1; % Rayleigh
        h = randn(4,1)/sqrt(2)+j*randn(4,1)/sqrt(2);
        h11=h(1);h12=h(2);h21=h(3);h22=h(4);%Rayleigh
    else h11=1;h12=1;h21=1;h22=1;%AWGN
    end
end
R1 = awgn(filter(h11,1,decoded1) + filter(h12,1,decoded2), SNR1,
'measured');
R2 = awgn(filter(h21,1,decoded1) + filter(h22,1,decoded2),
SNR1,'measured');
s0 = non_causal_filter(conj(h11+h12),transpose(R1));
s1 = non_causal_filter(conj(h21+h22),transpose(R2));
H = [h11+h12,h21+h22];
s = s0/2+s1/2;
% Maximum Likelihood Detector, Computing the distances
if M == 2;
    [decoded, sa] = ML_BPSK (dh, s);
    decoded = transpose(decoded);%BPSK
    decoded = pskdemod(decoded,M);
else if M==4;
    [decoded, sa] = ML_QPSK (dh, s0);
    decoded = transpose(decoded);%QPSK
    decoded = pskdemod(decoded,M);
    else [decoded, sa] = ML_QAM (dh, s0, qamOrder, H);
    decoded = transpose(decoded);
    decoded = qamdemod(decoded,qamOrder);%QAM
end
end
errors = sum(decoded~=Datar); tot_errors = tot_errors+errors;
end
ber = tot_errors /(number1);
SER_matrix4 = [SER_matrix4, ber];%Computing the SER matrix

%% Non-Cooperative DF (Two parallel channels)
tot_errors = 0; tot_errors1 = 0;
for i = 1:number
    if M == 2;

```

```

        Datar = randint(200,1,M); Data = pskmod(Datar,M)/(sqrt(2));
%Random data BPSK
        else if M==4;
            Data = ((2*round(rand(200,1))-1)+ j*(2*round(rand(200,1))-
1))/(2);
            Datar = pskdemod(2*Data,M);%random data QPSK
        else
            Datar = randint(200,1,qamOrder);Data =
gammod(Datar,qamOrder);%16QAM
        end
    end
%% Building the 1st Channel from Source to Relay
    [h1] = OnebyOne_channel (SUI_index,direct);% SUI fading channel
    if b == 1;% Flat fading channel
        if a == 1;
            h1 = randn(1,1)/sqrt(2)+j*randn(1,1)/sqrt(2);%Rayleigh
        else h1=1;%AWGN
        end
    end
    R = awgn(filter(h1,1,Data), SNR1, 'measured');
    s0 = non_causal_filter(conj(h1),transpose(R));H = h1;
% Maximum Likelihood Detector, Computing the distances
    if M == 2;
        [X, sa] = ML_BPSK (dh, s0);X= transpose(X);%BPSK
    else if M==4;
        [X, sa] = ML_QPSK (dh, s0);X= transpose(X);%QPSK
        else [X, sa] = ML_QAM (dh, s0, qamOrder, H);X= transpose(X);%QAM
        end
    end
%% Building the Channel from Relay to Destination
    [h1] = OnebyOne_channel (SUI_index,direct);% SUI fading channel
    if b == 1;% Flat fading channel
        if a == 1;
            h1 = randn(1,1)/sqrt(2)+j*randn(1,1)/sqrt(2);%Rayleigh
        else h1=1;%AWGN
        end
    end
    R = awgn(filter(h1,1,X), SNR1, 'measured');
    s0 = non_causal_filter(conj(h1),transpose(R));H=h1;
% Maximum Likelihood Detector, Computing the distances
    if M == 2;
        [decoded3, sa] = ML_BPSK (dh, s0);
        decoded3= transpose(decoded3);%BPSK
        decoded3 = pskdemod(decoded3,M);
    else if M==4;
        [decoded3, sa] = ML_QPSK (dh, s0);
        decoded3= transpose(decoded3);%QPSK
        decoded3 = pskdemod(decoded3,M);
        else [decoded3, sa] = ML_QAM (dh, s0, qamOrder, H);
            decoded3= transpose(decoded3);
            decoded3 = qamdemod(decoded3,qamOrder);%QAM
        end
    end
    errors = sum(decoded3~=Datar); tot_errors = tot_errors+errors;
end
ber = tot_errors /(number1); %Computing the SER for spesific SNR
SER_matrix5 = [SER_matrix5, ber];%Computing the SER matrix
%% 2nd Channel
for i = 1:number
    if M == 2;
        Datar1 = randint(200,1,M); Data1 = pskmod(Datar1,M)/(sqrt(2));
%Random data BPSK

```

```

        else if M==4;
            Data1 = ((2*round(rand(200,1))-1)+ j*(2*round(rand(200,1))-
1)))/(2);
            Datar1 = pskdemod(2*Data1,M);%random data QPSK
        else
            Datar1 = randint(200,1,qamOrder);Data1 =
gammod(Datar1,qamOrder);%16QAM
        end
    end
%% Building the 2nd Channel from Source to Relay
[h1] = OnebyOne_channel (SUI_index,direct);% SUI fading channel
if b == 1;% Flat fading channel
    if a == 1;
        h1 = randn(1,1)/sqrt(2)+j*randn(1,1)/sqrt(2);%Rayleigh
    else h1=1;%AWGN
    end
end
R = awgn(filter(h1,1,Data1), SNR1, 'measured');
s0 = non_causal_filter(conj(h1),transpose(R));H = h1;
% Maximum Likelihood Detector, Computing the distances
if M == 2;
    [X1, sa] = ML_BPSK (dh, s0);X1= transpose(X1);%BPSK
else if M==4;
    [X1, sa] = ML_QPSK (dh, s0);X1= transpose(X1);%QPSK
    else [X1, sa] = ML_QAM (dh, s0, qamOrder, H);X1=
transpose(X1);%QAM
    end
end
%% Building the 2nd Channel from Relay to Destination
[h1] = OnebyOne_channel (SUI_index,direct);% SUI fading channel
if b == 1;% Flat fading channel
    if a == 1;
        h1 = randn(1,1)/sqrt(2)+j*randn(1,1)/sqrt(2);%Rayleigh
    else h1=1;%AWGN
    end
end
R = awgn(filter(h1,1,X1), SNR2, 'measured');
s0 = non_causal_filter(conj(h1),transpose(R));H = h1;
% Maximum Likelihood Detector, Computing the distances
if M == 2;
    [decoded4, sa] = ML_BPSK (dh, s0);
    decoded4= transpose(decoded4);%BPSK
    decoded4 = pskdemod(decoded4,M);
else if M==4;
    [decoded4, sa] = ML_QPSK (dh, s0);
    decoded4= transpose(decoded4);%QPSK
    decoded4 = pskdemod(decoded4,M);
    else [decoded4, sa] = ML_QAM (dh, s0, qamOrder, H);
    decoded4= transpose(decoded4);
    decoded4 = qamdemod(decoded4,qamOrder);%QAM
    end
end
errors1 = sum(decoded4~=Datar1); tot_errors1 = tot_errors1+errors1;
end
ber1 = tot_errors1 /(number1); %Computing the SER for spesific SNR
SER_matrix6 = [SER_matrix6, ber1];%Computing the SER matrix

%% Non-Cooperative AF. (Two parallel channels)
tot_errors = 0; tot_errors1 = 0;
for i = 1:number
    if M == 2;

```

```

Datar = randint(200,1,M); X = pskmod(Datar,M)/(sqrt(2));%Random data BPSK
else if M==4;
    X = ((2*round(rand(200,1))-1)+ j*(2*round(rand(200,1))-1))/(2);
    Datar = pskdemod(2*X,M);%random data QPSK
else
    Datar = randint(200,1,qamOrder);X =
gammod(Datar,qamOrder);%16QAM
end
end
%% Building the Channel from Source to Relay
[H] = OnebyOne_channel (SUI_index,direct);% SUI fading channel
if b == 1;% Flat fading channel
    if a == 1;
        H = randn(1,1)/sqrt(2)+j*randn(1,1)/sqrt(2);%Rayleigh
    else H=1;%AWGN
    end
end
R = awgn(filter(H,1,X), SNR1, 'measured');
S = non_causal_filter(conj(H),transpose(R));
%% Building the Channel from Relay to Destination
[H] = OnebyOne_channel (SUI_index,direct);% SUI fading channel
if b == 1;% Flat fading channel
    if a == 1;
        H = randn(1,1)/sqrt(2)+j*randn(1,1)/sqrt(2);%Rayleigh
    else H=1;%AWGN
    end
end
for k=1:length(S)
    S(k) = sqrt(X(k)*X(k)')*S(k)/sqrt(S(k)*S(k)');
end
S = transpose(S);
R = awgn(filter(H,1,S), SNR1, 'measured');
s0 = non_causal_filter(conj(H),transpose(R));
% Maximum Likelihood Detector, Computing the distances
if M == 2;
    [decoded3, sa] = ML_BPSK (dh, s0);
    decoded3= transpose(decoded3);%BPSK
    decoded3 = pskdemod(decoded3,M);
else if M==4;
    [decoded3, sa] = ML_QPSK (dh, s0);
    decoded3= transpose(decoded3);%QPSK
    decoded3 = pskdemod(decoded3,M);
else
    [decoded3, sa] = ML_QAM (dh, s0, qamOrder, H);
    decoded3= transpose(decoded3);
    decoded3 = qamdemod(decoded3,qamOrder);%QAM
end
end
errors = sum(decoded3~=Datar); tot_errors = tot_errors+errors;
end
ber = tot_errors /(number1); %Computing the SER for spesific SNR
SER_matrix7 = [SER_matrix7, ber];%Computing the SER matrix
%% 2nd Channel
for i = 1:number
    if M == 2;
        Datar = randint(200,1,M); X = pskmod(Datar,M)/(sqrt(2)); %Random data
BPSK
    else if M==4;
        X = ((2*round(rand(200,1))-1)+ j*(2*round(rand(200,1))-1))/(2);
        Datar = pskdemod(2*X,M);%random data QPSK
    else
        Datar = randint(200,1,qamOrder);X =
gammod(Datar,qamOrder);%16QAM

```

```

        end
    end
    %% Building the Channel from Source to Relay
    [H] = OnebyOne_channel (SUI_index,direct);% SUI fading channel
    if b == 1;% Flat fading channel
        if a == 1;
            H = randn(1,1)/sqrt(2)+j*randn(1,1)/sqrt(2);%Rayleigh
        else H=1;%AWGN
        end
    end
    end
    R = awgn(filter(H,1,X), SNR2, 'measured');
    S = non_causal_filter(conj(H),transpose(R));
    %% Building the Channel from Relay to Destination
    [H] = OnebyOne_channel (SUI_index,direct);% SUI fading channel
    if b == 1;% Flat fading channel
        if a == 1;
            H = randn(1,1)/sqrt(2)+j*randn(1,1)/sqrt(2);%Rayleigh
        else H=1;%AWGN
        end
    end
    end
    for k=1:length(S)
        S(k) = sqrt(X(k)*X(k)')*S(k)/sqrt(S(k)*S(k)');
    end
    S = transpose(S);
    R = awgn(filter(H,1,S), SNR2, 'measured');
    s0 = non_causal_filter(conj(H),transpose(R));
    % Maximum Likelihood Detector, Computing the distances
    if M == 2;
        [decoded4, sa] = ML_BPSK (dh, s0);
        decoded4= transpose(decoded4);%BPSK
        decoded4 = pskdemod(decoded4,M);
    else if M==4;
        [decoded4, sa] = ML_QPSK (dh, s0);
        decoded4= transpose(decoded4);%QPSK
        decoded4 = pskdemod(decoded4,M);
    else
        [decoded4, sa] = ML_QAM (dh, s0, qamOrder, H);
        decoded4= transpose(decoded4);
        decoded4 = qamdemod(decoded4,qamOrder);%QAM
    end
    end
    errors1 = sum(decoded4~=Datar); tot_errors1 = tot_errors1+errors1;
end
ber = tot_errors1 /(number1); %Computing the SER for spesific SNR
SER_matrix8 = [SER_matrix8, ber];%Computing the SER matrix
end
SER_matrix_avg = SER_matrix_avg + SER_matrix;
SER_matrix_avg1 = SER_matrix_avg1 + SER_matrix1;
SER_matrix_avg2 = SER_matrix_avg2 + SER_matrix2;
SER_matrix_avg3 = SER_matrix_avg3 + SER_matrix3;
SER_matrix_avg4 = SER_matrix_avg4 + SER_matrix4;
SER_matrix_avg5 = SER_matrix_avg5 + SER_matrix5;
SER_matrix_avg6 = SER_matrix_avg6 + SER_matrix6;
SER_matrix_avg7 = SER_matrix_avg7 + SER_matrix7;
SER_matrix_avg8 = SER_matrix_avg8 + SER_matrix8;
% Plot
end
SER_matrix_avg = SER_matrix_avg /MonteCarlo;
SER_matrix_avg1 = SER_matrix_avg1 /MonteCarlo;
SER_matrix_avg2 = SER_matrix_avg2 /MonteCarlo;
SER_matrix_avg3 = SER_matrix_avg3 /MonteCarlo;
SER_matrix_avg4 = SER_matrix_avg4 /MonteCarlo;
SER_matrix_avg5 = SER_matrix_avg5 /MonteCarlo;

```



```

SER_matrix_avg6 = SER_matrix_avg6 /MonteCarlo;
SER_matrix_avg7 = SER_matrix_avg7 /MonteCarlo;
SER_matrix_avg8 = SER_matrix_avg8 /MonteCarlo;
%% Plot Average
figure (MonteCarlo+1)
semilogy (SNR, SER_matrix_avg, 'r');
hold on; semilogy (SNR, SER_matrix_avg1, 'r--'); hold on;
semilogy (SNR, SER_matrix_avg2, 'b');
hold on; semilogy (SNR, SER_matrix_avg3, 'b--'); hold on;
semilogy (SNR, SER_matrix_avg4, 'c');
hold on; semilogy (SNR, SER_matrix_avg5, 'g'); hold on;
semilogy (SNR, SER_matrix_avg6, 'g--');
hold on; semilogy (SNR, SER_matrix_avg7, 'y'); hold on;
semilogy (SNR, SER_matrix_avg8, 'y--'); grid

```

ML-BPSK

```

function [decoded, s] = ML_BPSK (dh, S);
% Author : Konstantinos Alexopoulos, Naval Postgraduate School, June
2008
% This function compute symbol distances for baseband BPSK
for i=1:length(S)
    d11 = ((dh(1)-real(S(i)))^2+(imag(S(i)))^2);
    d12 = ((dh(2)-real(S(i)))^2+(imag(S(i)))^2);
    D1 = [d11 d12]; %Distances for the received symbol
    [sc1, pos1] = min(D1);
    decoded(i)=[dh(pos1)]; %The decisions
    s(i) = sc1;
end

```

ML-QPSK

```

function [decoded, s] = ML_QPSK (dh, S);
% Author : Konstantinos Alexopoulos, Naval Postgraduate School, June
2008
% This function compute symbol distances for baseband QPSK
%Computing the distances for the first symbol
for i=1:length(S)
    d11 = ((real(dh(1))-real(S(i)))^2+(imag(dh(1))-imag(S(i)))^2);
    d12 = ((real(dh(2))-real(S(i)))^2+(imag(dh(2))-imag(S(i)))^2);
    d21 = ((real(dh(3))-real(S(i)))^2+(imag(dh(3))-imag(S(i)))^2);
    d22 = ((real(dh(4))-real(S(i)))^2+(imag(dh(4))-imag(S(i)))^2);
    D1 = [d11 d12 d21 d22]; %Distances for the received symbol
    [sc1, pos1] = min(D1);
    decoded(i)=[dh(pos1)]; %The decisions
    s(i) = sc1;
end

```

ML-QAM

```

function [decoded, s] = ML_QAM (dh, S, QAM_order, H);
% Author : Konstantinos Alexopoulos, Naval Postgraduate School, June
2008
% This function compute symbol distances for baseband QPSK

```

```

%Computing the distances for the first symbol
for j=1:length(S)
    for i=1:QAM_order
        D1(i) = ((real(dh(i))-real(S(j)))^2+(imag(dh(i))-
imag(S(j)))^2);
    end
%Building the decisions vector for the first symbol
    for k = 1:QAM_order
        X1_dec(k) = ((abs(dh(k)))^2)*sum(sum((abs(H)).^2)-1)+D1(k);
    end
    [sc1, posil] = min(X1_dec);
    decoded(j)=[dh(posil)];%The decisions
    s(j) = sc1;
end

```

OnebyOne_channel

```

function [h1] = OnebyOne_channel (SUI_index,direct);
% Title      : Correlated MISO channel creator based on 3-tap SUI
channels
% Author     : Derya Saglam, Naval Postgraduate School, November
2004
% Modified   : Konstantinos Alexopoulos, Naval Postgraduate School,
June 2008
% SUI_index  : SUI channel index, 1-6
% direct     : antenna directivity; 0=Omni antenna, 1=30deg
directional antenna
% rho_rx     : receive correlation coefficient
% Output :
%   h1       : SIMO channels
% -----

% Square root of the correlation matrix
Rr = 1;

% Generating two independent SUI channels
[h1 paths_r1 paths_c1 Fnorm] = SUI_model(SUI_index,direct);

k = length(h1);

V = zeros(1,k);
V(1,:) = transpose(paths_r1);
paths_r1 = V(1,:);
% Adding the LOS components to the correlated paths
h1 = paths_r1 + transpose(paths_c1);

% Multiplying all coefficients with F normalization factor
h1 = h1 * 10^(Fnorm/20);

```

TwobyOne_channel

```

function [h1,h2] = TwobyOne_channel (SUI_index,direct,rho_tx);

```

```

% Title      : Correlated MISO channel creator based on 3-tap SUI
channels
% Author     : Derya Saglam, Naval Postgraduate School, November
2004
% Modified   : Konstantinos Alexopoulos, Naval Postgraduate School,
June 2008
% SUI_index  : SUI channel index, 1-6
% direct     : antenna directivity; 0=Omni antenna, 1=30deg
directional antenna
% rho_tx     : transmit correlation coefficient
% Output :
%   h1, h2   : MISO channels
% -----

% Square root of the correlation matrix
Rt = sqrtm([1 rho_tx;rho_tx' 1]);

% Generating two independent SUI channels
[h1 paths_r1 paths_c1 Fnorm] = SUI_model(SUI_index,direct);
[h2 paths_r2 paths_c2 Fnorm] = SUI_model(SUI_index,direct);

k = length(h1);

V = zeros(k,2);
V(:,1) = paths_r1;
V(:,2) = paths_r2;

% Generating the correlated part of the channel assuming that tap
correlations are identical
for i = 1:k
    V(k,:) = V(k, :)* Rt;
end
paths_r1 = V(:,1);
paths_r2 = V(:,2);

% Adding the LOS components to the correlated paths
h1 = paths_r1 + paths_c1;
h2 = paths_r2 + paths_c2;

h1 = transpose(h1); h2 = transpose(h2);

% Multiplying all coefficients with F normalization factor
h1 = h1 * 10^(Fnorm/20);
h2 = h2 * 10^(Fnorm/20);

```

OnebyTwo_channel

```

function [h1,h2] = OnebyTwo_channel (SUI_index,direct,rho_rx);
% Title      : Correlated MISO channel creator based on 3-tap SUI
channels
% Author     : Derya Saglam, Naval Postgraduate School, November
2004

```

```

% Modified      : Konstantinos Alexopoulos, Naval Postgraduate School,
June 2008
% SUI_index     : SUI channel index, 1-6
% direct        : antenna directivity; 0=Omni antenna, 1=30deg
directional antenna
% rho_rx        : receive correlation coefficient
% Output :
%   h1, h2      : SIMO channels
% -----

% Square root of the correlation matrix
Rr = sqrtm([1 rho_rx;rho_rx' 1]);

% Generating two independent SUI channels
[h1 paths_r1 paths_c1 Fnorm] = SUI_model(SUI_index,direct);
[h2 paths_r2 paths_c2 Fnorm] = SUI_model(SUI_index,direct);

k = length(h1);

V = zeros(2,k);
V(1,:) = transpose(paths_r1);
V(2,:) = transpose(paths_r2);

% Generating the correlated part of the channel assuming that tap
correlations are identical
for i = 1:k
    V(:,k) = Rr * V(:,k) ;
end
paths_r1 = V(1,:);
paths_r2 = V(2,:);

% Adding the LOS components to the correlated paths
h1 = paths_r1 + transpose(paths_c1);
h2 = paths_r2 + transpose(paths_c2);

% Multiplying all coefficients with F normalization factor
h1 = h1 * 10^(Fnorm/20);
h2 = h2 * 10^(Fnorm/20);

```

TwobyTwo_channel

```

function [h11,h12,h21,h22] = TwobyTwo_channel (SUI_index,direct,rho_tx,
rho_rx);
% Title      : Correlated MISO channel creator based on 3-tap SUI
channels
% Author     : Derya Saglam, Naval Postgraduate School, November
2004
% Modified   : Konstantinos Alexopoulos, Naval Postgraduate School,
June 2008
% SUI_index  : SUI channel index, 1-6
% direct     : antenna directivity; 0=Omni antenna, 1=30deg
directional antenna
% rho_tx     : transmit correlation coefficient

```

```

% rho_rx          : receive correlation coefficient
% Output :
% h11, h12, h12, h22      : MIMO channels
% -----

% Square roots of the correlation matrices
Rr = sqrtm([1 rho_rx;rho_rx' 1]);
Rt = sqrtm([1 rho_tx;rho_tx' 1]);

% Generating four independent SUI channels
[h11 paths_r11 paths_c11 Fnorm] = SUI_model(SUI_index,direct);
[h12 paths_r12 paths_c12 Fnorm] = SUI_model(SUI_index,direct);
[h21 paths_r21 paths_c21 Fnorm] = SUI_model(SUI_index,direct);
[h22 paths_r22 paths_c22 Fnorm] = SUI_model(SUI_index,direct);

G = [];

% Generating the correlated part of the channel assuming that tap
correlations are identical
for i = 1:length(h11)
    H = Rr * [paths_r11(i) paths_r12(i);paths_r21(i) paths_r22(i)] *
    Rt;
    G = [G ;H];
end

H = reshape(G,2,6);

paths_r11 = H(1,1:3);
paths_r12 = H(1,4:6);
paths_r21 = H(2,1:3);
paths_r22 = H(2,4:6);

% Adding the LOS components to the correlated paths
h11 = paths_r11 + transpose(paths_c11);
h12 = paths_r12 + transpose(paths_c12);
h21 = paths_r21 + transpose(paths_c21);
h22 = paths_r22 + transpose(paths_c22);

% Multiplying all coefficients with F normalization factor
h11 = h11 * 10^(Fnorm/20);
h12 = h12 * 10^(Fnorm/20);
h21 = h21 * 10^(Fnorm/20);
h22 = h22 * 10^(Fnorm/20);

```

LIST OF REFERENCES

- [1] T. M. Cover and A. A. El Gamal, "Capacity theorems for the relay channel," *IEEE Trans. Inf. Theory*, vol. IT-25, no. 5, pp. 572–584, September 1979.
- [2] G. J. Foschini, "Layered Space-Time Architecture for Wireless Communication in a Fading Environment When Using Multi-Element Antennas," *Bell Laboratories Technical Journal* 41–59, October 1996.
- [3] S. M. Alamouti, "A simple transmit diversity technique for wireless communications," *IEEE J. Select. Areas Commun.*, vol. 16, pp. 1451–1458, October 1998.
- [4] E. Lindskog and A. Paulraj, "A Transmit Diversity Scheme for Channels with Intersymbol Interference," *Proceedings of IEEE International Conference on Communications, 2000*, Vol. 1, pp. 307-311, June 18, 2000.
- [5] K. Mehrotra and I.V. McLoughlin, "Time Reversal Space-Time Block Coding with Channel Estimation Errors," *Proceedings of the Fourth Pacific Rim Joint Conference on Information, Communications and Signal Processing*, Vol. 1, pp. 617-620, December 15, 2003.
- [6] H. D. Saglam, "Simulation Performance of Multiple-Input Multiple-Output Systems Employing Single-Carrier Modulation And Orthogonal Frequency Division Multiplexing," Master's Thesis, Naval Postgraduate School, Monterey, CA, December 2004.
- [7] D. K. Borah, G. Moreno-Crespo and S. Nammi, , "Distributed Alamouti Transmit Diversity Technique for Co-Operative Communications," *Vehicular Technology Conference, 2007, VTC2007- Spring. IEEE 65th*, pp. 2210-2214, April 2007
- [8] E. Kurniawan, A.S. Madhukumar and F. Chin, "Performance Analysis of Distributed Space Time Coding: A Geometric Approach," *PIMRC 2007, IEEE 18th International Symp.*, September 2007
- [9] Y. Zhang, W. Genyuan and M.G. Amin, "Cooperative Spatial Multiplexing in Multi-Hop Wireless Networks," *ICASSP 2006 Proceedings. 2006 IEEE International Conference on Volume 4*, May 2006.
- [10] S. W. Kim, "Cooperative spatial multiplexing in mobile ad hoc networks," *Mobile Ad hoc and Sensor Systems Conf., IEEE International Conference*, Nov. 2005.
- [11] J.N. Laneman and G.W. Wornell, "Distributed space-time-coded protocols for exploiting cooperative diversity in wireless networks," *Information Theory, IEEE Transactions on Volume 49, Issue 10*, October 2003.

- [12] E. C. van der Meulen, "*Transmission of information in a T-terminal discrete memoryless channel*," Ph.D. dissertation, Univ. California, Berkeley, CA, Jun. 1968.
- [13] V. Stankovic, A. Host-Madsen, and Z. Xiong, "*Cooperative diversity for wireless ad hoc networks*," *IEEE Signal Processing Magazine*, vol. 23, pp. 37-49, Sep. 2006.
- [14] A. Sendonaris, E. Erkip, and B. Aazhang, "*User cooperation diversity - Part I: system description*," *IEEE Trans. Commun.*, vol. 51, pp. 1927-1938, Nov. 2003.
- [15] A. Sendonaris, E. Erkip, and B. Aazhang, "*User cooperation diversity - Part II: implementation aspects and performance analysis*," *IEEE Trans. Commun.*, vol. 51, pp. 1939-1948, Nov. 2003.
- [16] J-S. Yoon, J-H. Kim, and H-K. Song, "*Modified Space Time Coded Cooperative Scheme by Amplify-and-Forward for OFDMA Uplink System*," *IEEE Congress on Image and Signal Processing*, 2008.
- [17] J. N. Laneman, "*Cooperative diversity in wireless networks: Algorithms and architectures*," Ph.D. dissertation, MIT, Cambridge, MA, Aug. 2002.
- [18] A. Nosratinia and A. Hedayat, "*Cooperative communication in wireless networks*," *IEEE Commun. Mag.*, vol. 42, no. 10, pp. 74-80, Oct. 2004.
- [19] R. Pabst, B. H. Walker, D. C. Schultz, P. Herhold, H. Yanikomeroglu, S. Mukherjee, H. Viswanathan, M. Lott, W. Zirwas, M. Dohler, H. Aghvami, D. D. Falconer, and G. P. Fettweis, "*Relay-based deployment concepts for wireless and mobile broadband radio*," *IEEE Commun. Mag.*, vol. 42, no. 9, pp. 80-89, Sep. 2004.
- [20] R. C. King, "*Multiple access channels with generalized feedback*," Ph.D. dissertation, Stanford Univ., Stanford, CA, March 1978.
- [21] B. Schein and R. G. Gallager, "*The Gaussian parallel relay network*," in *Proc IEEE Int. Symp. Information Theory*, Sorrento, Italy, June 2000, p. 22.
- [22] B. E. Schein, "*Distributed coordination in network information theory*," Ph.D. dissertation, MIT, Cambridge, MA, October 2001.
- [23] M. Gastpar, G. Kramer, and P. Gupta, "*The multiple-relay channel: Coding and antenna-clustering capacity*," in *Proc. IEEE Int. Symp. Information Theory*, Lausanne, Switzerland, June/July 2002, p. 136.
- [24] T. Hunter and A. Nosratinia, "*Diversity through coded cooperation*," *IEEE Transactions on Wireless Communications*, vol. 5, no. 2, February 2006, pp. 283-289.

- [25] A. Nosratinia and T. E. Hunter, "Grouping and partner selection in cooperative wireless networks," *IEEE Journal on Selected Areas in Communications*, vol. 25, no. 2, February 2007, pp. 369-378.
- [26] Y-W Hong, W-J Huang, F-H Chiu, and C.-C. J. Kuo, "Cooperative Communications in Resource-Constrained Wireless Networks," *IEEE Processing Magazine*, vol. 24, pp. 47-57, May 2007.
- [27] H. Li and Q. Zhao, "Distributed modulation for cooperative wireless communications," *IEEE Signal Processing Magazine*, vol. 23, pp. 30-36, September 2006.
- [28] A. Darmawan, S.W. Kim and H. Morikawa, "Amplify-and-Forward Scheme in Cooperative Spatial Multiplexing," *Mobile and Wireless Communications Summit*, 16th IST, July 2007.
- [29] T. Koike, H. Murata and S. Yoshida, "Iterative FDE for DD-Based Cooperative Relaying with FD-STBC in Quasi-Synchronous Networks," *Personal, Indoor and Mobile Radio Communications, IEEE 17th International Symposium*, September 2006.
- [30] E. Biglieri, R. Calderbank, A. Constantinides, A. Goldsmith, A. Paulraj and H.V. Poor, "MIMO Wireless Communications," Cambridge University Press 2007.
- [31] F. H.P. Fitzek (Editor) and M.D. Katz (Editor), "Cooperation in Wireless Networks: Principles and Applications. Real Egoistic Behavior is to Cooperate," Springer, 2006.
- [32] P. Gupta and P.R. Kumar, "Towards an Information Theory of Large Networks: An Achievable Rate Region," *IEEE Transactions on Information Theory*, vol. 49, No. 8, August 2003.
- [33] E. van der Meulen, "Three Terminal Communication Channels," *Adv. Appl. Prob.*, 3:120-154, 1971.
- [34] S. Zhang and V. K. N. Lau, "Design and Analysis of Multiple-Relay Selection for Cooperative Spatial Multiplexing," *IEEE ICC*, pp. 903-907, 2008.
- [35] G. S. Rajan and B. S. Rajan, "Distributed Space-Time Codes for Cooperative Networks with Partial CSI," *IEEE WCNC*, 2007.
- [36] M. A. Tope, "Performance Evaluation of a Cooperative Diversity Enhanced Ad Hoc Network," Master's Thesis, Naval Postgraduate School, Monterey, CA, December 2002.
- [37] C.E. Perkins and E. M. Royer, "Ad-Hoc On-Demand Distance Vector Routing," *Proceedings of 2nd IEEE Workshop on Mobile Computing Systems and Applications*, pp. 90 – 100, New Orleans LA, February 1999.

- [38] V.D. Park and M.S. Corson, “*A Highly Adaptive Distributed Routing Algorithm for Mobile Wireless Networks*,” *Proceedings of INFOCOM '97*, Vol. 3, pp. 1405 – 1413, April 1997.
- [39] M.S. Corson and A. Ephremides, “*A Distributed Routing Algorithm for Mobile Wireless Networks*,” *ACM/Baltzer Wireless Journal*, Vol. 1, No. 1, pp. 61-81, February 1995.
- [40] D.B Johnson and D.A. Matlz, “*Dynamic Source Routing in ad hoc networks*,” *Mobile Computing*, Kluwer Academic Publishers, pp. 153-181, 1996.
- [41] C.E. Perkins and P. Bhagwat, “*Highly Dynamic Destination-Sequence Distance Vector routing (DSDV) for mobile computers*,” *Proceedings of SIGCOMM '94, Conference on Communications Architectures, Protocols and Applications*, pp. 234-244, August 1994.
- [42] B. Vucetic and J. Yuan, “*Space-Time Coding*,” Wiley, 1st Edition, 2003.
- [43] M. A. Jensen, R. C. Crummett and A. L. Anderson, “*Orthogonal Space-time Coding for Self-interference Suppression in Multi-antenna Telemetry Transmission*,” Brigham Young University, UT, supported by National Science Foundation under Wireless Initiative Grant CCR 99-79452.
- [44] M. M. Carvalho and J.J. Garcia-Lua-Aceves, “*Analytical Modeling of Ad Hoc Networks that utilize Space-time Coding*,” *Modeling and Optimization in Mobile, Ad Hoc and Wireless Networks, 2006 4th International Symposium on Volume*, Issue 03-06, pp. 1-11, April 2006.
- [45] Y. Chang and Y. Hua, “*Diversity Analysis of Orthogonal Space-time Modulation for Distributed Wireless Relays*,” in *IEEE J. Sel. Areas Communications*, vol. 22, no. 8, pp. 1099-1109, August 2004.
- [46] Y. Hua, Y. Mei and Y. Chang, “*Wireless Antennas – making Wireless Communications perform like Wireline Communications*,” in *IEEE AP-S Topical Conference on Wireless Communications Technology*, Honolulu Hawaii, pp. 1-27, invited paper, October 2003.
- [47] P. A. Anghel and M. Kaveh, “*On the Performance of Distributed Space-time Coding System with one and two Non-regenerative Relays*,” *IEEE Transactions on Wireless Communications*, vol. 5, no. 3, pp. 682-691, March 2006.
- [48] IEEE 802.16 Broadband Wireless Access Working Group, “*Channel Models for Fixed Wireless Applications*,” IEEE 802.16a.3c-01/01, March 2001.
- [49] T. S. Rappaport, “*Wireless Communications*,” Prentice Hall Communications Engineering and Emerging Technologies Series, 2nd Edition, 2002.

INITIAL DISTRIBUTION LIST

1. Defense Technical Information Center
Ft. Belvoir, Virginia
2. Dudley Knox Library
Naval Postgraduate School
Monterey, California
3. Chairman, Code EC
Department of Electrical and Computer Engineering
Naval Postgraduate School
Monterey, California
4. Professor M. Tummala,
Department of Electrical and Computer Engineering
Naval Postgraduate School
Monterey, California
5. Professor J. C. McEachen
Department of Electrical and Computer Engineering
Naval Postgraduate School
Monterey, California
6. Embassy of Greece,
Office of Naval Attaché
Washington, DC
7. Hellenic Naval Academy,
Hatzikiriakio Piraeus, Greece
8. LTJG Alexopoulos Konstantinos
Hellenic Navy General Staff
Athens, Greece